Role of integrin α11β1 in breast cancer

Hilde Ytre-Hauge Smeland

Thesis for the degree of Philosophiae Doctor (PhD)
University of Bergen, Norway
2021

UNIVERSITY OF BERGEN

Role of integrin α11β1 in breast cancer

Hilde Ytre-Hauge Smeland

Thesis for the degree of Philosophiae Doctor (PhD)
at the University of Bergen

Date of defense: 24.09.2021

Year: 2021
Title: Role of integrin α11β1 in breast cancer

Name: Hilde Ytre-Hauge Smeland
Print: Skipnes Kommunikasjon / University of Bergen

Scientific environment

The research presented in this thesis has been performed in three research groups that are parts of Centre for Cancer Biomarkers (CCBIO) at University of Bergen and headed by Director and Professor Lars A. Akslen. First, the Matrix Biology Group (2015-2018) and the CellNet Group (2018-2020) both at Department of Biomedicine and directed by Professor Donald Gullberg and Professor James C. Lorens, respectively. Second, the Tumor Biology Research Group (2015-2020) directed by Professor Lars A. Akslen at Department of Clinical Medicine. Professor Linda Stuhr has been the main supervisor and Professors Lars A. Akslen, Donald Gullberg and Rolf K. Reed have been co-supervisors. Financial support was received from University of Bergen, The Research Council of Norway and by a Meltzer Fund Research Grant.

Acknowledgements

My dearest Kristian, thank you for your love, friendship and support, for always putting family first, and for our three wonderful children. Magnus, Hanna and lille Erlend, thank you for all the joy, frustrations, and happiness you give me.

Bergen, August 2020   Hilde Ytre-Hauge Smeland

Abbrevations

5FU	5 Fluorouracil
CAF	Cancer-associated fibroblast
CD8	Cluster of differentiation 8
CD10	Cluster of differentiation 10
CFC	Capillary filtration coefficient
COPC	Capillary colloid osmotic pressure
COPIF	Interstitial colloid osmotic pressure
CK14	Cytokeratin 14
CXCL5	CXC motif chemokine ligand 5
DCIS	Ductal carcinoma in situ
ECM	Extracellular matrix
EMT	Epithelial-to-mesenchymal transition
ER	Estrogen receptor
FAP	Fibroblast activation protein
FFPE	Formalin-fixed, paraffin-embedded
FGF	Fibroblast growth factor
FSP-1	Fibroblast specific protein-1
GPR77	G protein-coupled receptor 77
HER2	Human epidermal growth factor receptor 2
HGF	Hepatocyte growth factor
HNSCC	Head and neck squamous cell carcinoma
iCAF	Inflammatory cancer-associated fibroblast
IF	Interstitial fluid
IHC	Immunohistochemistry
IGF1	Insulin-like growth factor 1
IGF2	Insulin-like growth factor 2
Jv	Filtration
KO mice	Knockout mice
LOX	Lysyl oxidase
LOXL1	Lysyl oxidase like 1
METABRIC	Molecular taxonomy of breast cancer international consortium
MMP	Matrix metalloproteinases
MMTV	Mouse mammary tumor virus
mRNA	Messenger ribonucleic acid
myCAF	Myofibroblastic cancer-associated fibroblast

NG2	Neuron glial antigen 2
PAM50	Prediction Analysis of Microarray 50
Pc	Capillary hydrostatic pressure
PDAC	Pancreatic ductal adenocarcinoma
PDGF	Platelet-derived growth factor
PDGFRα	Platelet-derived growth factor receptor alpha
PDGFRβ	Platelet-derived growth factor receptor beta
PIF	Interstitial fluid pressure
PR	Progesterone receptor
PyMT	Polyomavirus middle T antigen
RNA	Ribonucleic acid
SCID	Severe combined immunodeficiency disease
SI	Staining index
TNM	Tumor-nodes-metastasis
TME	Tumor microenvironment
TNBC	Triple-negative breast cancer
TGF-β	Transforming growth factor beta
VEGF	Vascular endothelial growth factor
WT	Wild type
α11-KO	Integrin α11 knockout
αSMA	Alpha smooth muscle actin
σ	Colloid osmotic reflection coefficient

Abstract

Breast cancer cells are strongly influenced by a complex tumor microenvironment comprised of a diversity of stromal cells, including a heterogeneous population of cancer-associated fibroblasts (CAFs), in addition to the extracellular matrix and the interstitial fluid with its solutes. Integrins act as links between the extracellular matrix and the cell cytoskeleton, and integrin α11β1 had previously been shown to be important for fibroblast function in wound healing, fibrosis and in lung cancer. In this thesis, we aimed to achieve a better understanding of the expression and functions of integrin α11β1 in the breast tumor microenvironment.

In the first two papers we explored the effects of stromal integrin α11β1 in triple-negative breast cancer in integrin α11 knockout mice and demonstrated that integrin α11-deficiency reduced tumor interstitial fluid pressure and altered collagen fibril structure in MDA-MB-231 and MDA-MB-468 tumors. In addition, integrin α11-deficiency reduced MDA-MB-231 growth and the same trend was seen in MDA-MB-468 tumors. However, no effects of integrin α11β1 were seen in 4T1 tumors except altered collagen fibril structure. In the third paper, we validated new monoclonal antibodies against the human integrin α11 chain and established conditions for reproducible staining on formalin-fixed, paraffin-embedded (FFPE) human tissues. By investigating the expression of integrin α11 with the 210F4B6A4 monoclonal antibody in a large breast cancer cohort, we reported that integrin α11β1 is expressed in fibroblast-like, stromal cells in the vast majority of invasive breast carcinoma. Strong integrin α11β1 expression was associated with aggressive breast cancer features, although not with breast cancer specific survival. Further, integrin α11β1 co-localized with αSMA in fibroblast-like cells, and αSMA and cytokeratin 14 in a subset of breast myoepithelium.

In summary, this thesis has uncovered a new function of integrin α11β1 in the regulation of tumor interstitial fluid pressure in experimental breast cancer. Integrin α11β1 stimulated

MDA-MB-231 growth *in vivo* and was associated with aggressive cancer phenotypes in human breast cancer, indicating that integrin α11β1 seems to be expressed in a pro-tumorigenic CAF subset. We also detected integrin α11β1 in a subset of breast myoepithelial cells, and the function in these cells is so far not known. Our new monoclonal antibodies against the integrin α11 chain represent new tools for use in further investigation of the expression and function of integrin α11β1.

List of publications

Paper I:

Reigstad I*, **Smeland HYH***, Skogstrand T, Sortland K, Schmid MC, Reed RK, Stuhr L. Stromal Integrin α11β1 Affects RM11 Prostate and 4T1 Breast Xenograft Tumors Differently. *PLoS One* 2016 18;11(3).

* *These authors contributed equally to this work.*

Paper II:

Smeland HYH, Lu N, Karlsen TV, Salvesen G, Reed RK, Stuhr L. Stromal integrin α11-deficiency reduces interstitial fluid pressure and perturbs collagen structure in triple-negative breast xenograft tumors. *BMC Cancer* 2019 15;19(1).

Paper III:

Smeland HYH, Askeland C, Wik E, Knutsvik G, Molven A, Edelmann RJ, Reed RK, Warren DJ, Gullberg D, Stuhr L, Akslen LA. Integrin α11β1 is expressed in breast cancer stroma and associates with aggressive tumor phenotypes. *J Pathol Clin Res* 2020 6(1).

Contents

1. Introduction

1.1 Tumor microenvironment

Cancer remains one of the leading causes of death worldwide despite extensive research in the field, and it surpassed cardiovascular disease as the leading cause of death in Norway in 2017 [1,2]. It is characterized by abnormal cell growth and ability to spread, and cells acquire a malignant phenotype through accumulation of mutations and epigenetic alterations [3,4].

Hanahan and Weinberg proposed ten essential capabilities acquired during the multistep process of cancer development as seen in **Fig 1** [3,4]. Although genetic alterations in the cancer cells, such as activation of oncogenes and inactivation of tumor suppressor genes, are necessary for the acquisition of the hallmark traits, cancer is a complex structure where tumor cells are embedded in an intricate tumor microenvironment (TME) [5,6]. Even though the microenvironment in solid carcinomas mainly consists of the same components as the microenvironment in normal tissue, it can be markedly altered.
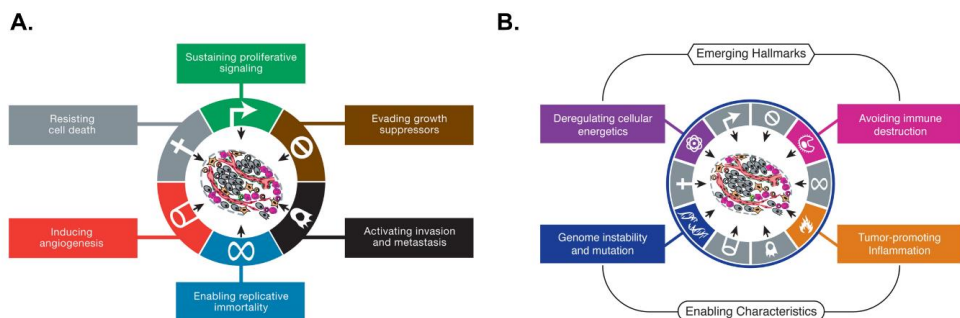
Fig 1. Hallmarks of cancer. A. Hanahan and Weinberg proposed six hallmark capabilities of cancer in 2000. **B.** In 2011, two extra hallmarks and two characteristics that facilitate acquisition of the hallmarks were added. Reprinted from [3], with permission.

Indeed, tumor cells remodel the TME into a milieu supportive of their own growth, and in this way, both cellular and non-cellular components of the TME can contribute to the acquisition of the hallmark traits – increasing the complexity of malignant tumors [5,6].

A better understanding of the complex interplay between the tumor cells and the surrounding TME can hopefully result in more effective cancer treatment. Recent advances in immunotherapy certainly demonstrate that targeting the TME can be a powerful tool in the treatment of cancer. Nonetheless, components of the TME often have multiple and complex functions where some components even have been shown to restrain tumor growth and, with the exception of immunotherapy, targeting the TME in clinical trials has so far not been very successful [7-9]. This underlines the importance of comprehensive knowledge of the different parts of the TME through thorough and broad preclinical and translational research.

The TME has been the framework of the research presented in this thesis; and in particular the role and expression of integrin α11β1 in the breast cancer stroma. Different compartments of the TME will be addressed in the following sections, with special focus on cancer-associated fibroblasts (CAFs), extracellular matrix (ECM), interstitial fluid (IF), and also integrins, particularly integrin α11β1.
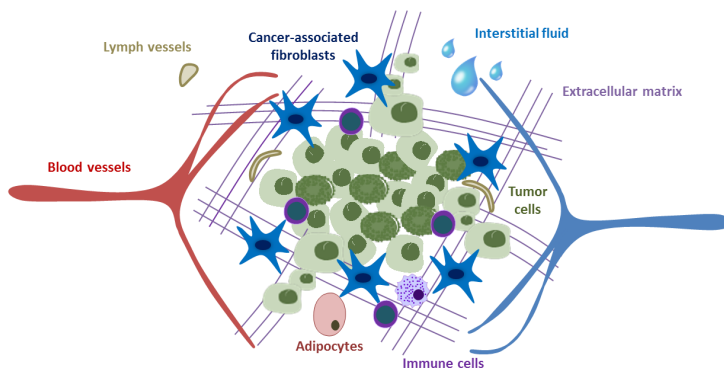
Fig 2. The tumor microenvironment. The tumor cells are embedded in a complex microenvironment.

1.1.1 Cells of the tumor microenvironment

The TME is composed of a variety of non-malignant cells, including CAFs, a heterogeneous population of immune cells, vascular and lymphatic endothelial cells, blood vessel associated smooth muscle cells, pericytes, adipocytes, nerve cells and mesenchymal stem cells **(Fig 2)** [7,8,10,11].

Cancer-associated fibroblasts

Activated fibroblasts in the cancer stroma, often termed CAFs, are an abundant cell type of the TME [12]. CAFs are often identified by their spindle-shaped morphology with indented nuclei compared to resting fibroblasts, in combination with expression of typical markers (such as αSMA, PDGFRα/β, FSP1 and/or FAP, and the absence of epithelial, endothelial and immune cell markers) [10,12,13] .

CAFs make up a heterogeneous population of mesenchymal cells with different origin, expression of markers and function [13-15]. While most studies have shown that CAFs can stimulate tumor growth and progression through particularly paracrine signaling and ECM production and remodeling, some CAF subsets have actually been shown to restrain tumor growth [10,15]. The CAF heterogeneity is manifested by the wide range of markers used to identify the cell type, but there is no consensus on the molecular definition of CAF subtypes [12,16]. Notably, no CAF-specific marker exists, and no marker is expressed by all CAFs, and there is a need to identify markers that can help differentiate between various CAF subtypes to better characterize CAF heterogeneity [12,16]. Therefore, finding ways to distinguish between tumor-supportive and tumor-suppressive CAFs, is probably necessary to identify effective CAF-targeted therapies in cancer treatment [12].

Origin

There is evidence that CAFs originate from different precursor cells [12,13,15]. While activation of tissue resident fibroblasts and recruitment of mesenchymal stem cells are well

documented CAF origins, other probable sources are trans-differentiation from local cells such as pericytes, adipocytes, smooth muscle cells, endothelial cells or tumor cells, and also from recruited fibrocytes [12,13,17-19]. It should be noted that some of these CAF origins are still controversial, for example derivation from tumor cells by epithelial-to-mesenchymal transition (EMT) [13]. Most studies find CAFs to be genetically stable, and the lack of mutations in this cell population questions the existence of a tumor cell-derived CAF subpopulation or indicate that this subpopulation is at least a small minority [20]. However, in a recent work of Bartoschek and colleagues, a subpopulation of CAFs isolated from breast cancer in PyMT mice was found to share gene expression and the PyMT oncogene with the tumor cells, indicating that this small cell population might have epithelial origin [21]. So indeed, the origin of CAFs remains an issue of debate and should be further explored to enlighten the heterogeneity of CAFs.

Activation of fibroblasts

In normal tissue, fibroblasts are usually considered to be quiescent mesenchymal cells embedded within the interstitial ECM, but during tumor initiation and progression the majority of the fibroblasts acquire an activated phenotype [12,16,17]. Activated fibroblasts are typically more contractile, migrative and proliferative, with increased secretion of signaling molecules and ECM components compared to their resting counterparts [12,16,17]. The recruitment and activation of fibroblasts are driven by the release of fibroblast-activating factors like TGF-β, FGFs, PDGFs, but also through other mechanisms such as increased stiffness [12,13,16,17].

Dvorak suggested in 1986 that malignant tumors "invoke the wound healing response to induce the stroma" required for their own survival and growth [22]. This became a seminal paper in the field of TME biology, and now, the similarities between wound healing, fibrosis and tumor stroma generation are well recognized where fibroblasts with an activated phenotype, often called myofibroblasts, share similar functions [10,23].
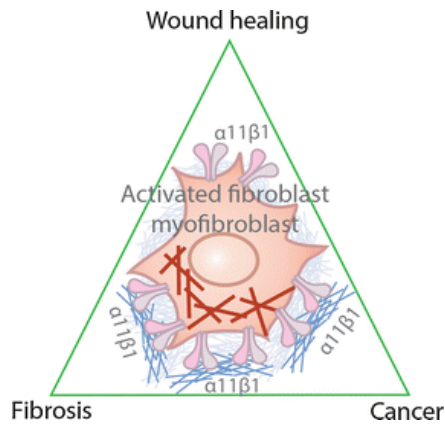
Fig 3. A tumor is a wound that never heals; the wound healing, fibrosis and cancer triad.
Myofibroblasts are responsible for ECM production, remodeling and tissue contraction in wound healing,
fibrosis and in the tumor stroma, and integrin α11β1 has been found to be important for fibroblast function
in all these conditions. The red lines represent αSMA and the blue lines collagen. Reprinted from [24], with
permission.

Myofibroblasts

The terminology used to describe fibroblasts in the cancer stroma is not consistent, and
CAFs are most often used as a "collective term" describing all fibroblast-like cells with an
activated state in the cancer stroma, but names like tumor-associated fibroblasts and
myofibroblasts are also used [10,12]. As different fibroblasts vary in their secretory,
proliferative and contractile abilities, the term myofibroblasts is now often used to describe
CAFs that resemble myofibroblasts seen in the process of wound healing and fibrosis; i.e.
fibroblasts with enhanced contractility due to upregulation of the contractile form of actin,
αSMA [10,16,25]. Further, myofibroblasts are regarded as the cells responsible for
excessive ECM production [16,25,26]. In a healing wound, myofibroblasts will contract the
wound and secrete ECM proteins, thereby generating a mature connective tissue stroma,
and finally when the wound is healed, they will revert to quiescent fibroblasts or undergo
apoptosis [25,27]. On the contrary, the wound healing process is sustained both in fibrosis
and in cancer with persistent inflammation, fibroblast activation and thereby continuous

ECM production and modification, resulting in excessive ECM deposition [25,27]. This is often referred to as the desmoplastic reaction [10]. Integrin α11β1 has emerged as a new myofibroblast marker as it has been found to be upregulated in fibroblasts during their differentiation into myofibroblasts [28-30].

Tumor-supportive functions of CAFs

Extensive experimental data have shown that activated fibroblasts can increase cancer aggressiveness [12,20]. CAFs contribute in different ways to the promotion of tumor growth and invasiveness; they stimulate tumor cell proliferation and survival, promote invasion and metastasis, stimulate maintenance of cancer stemness, and can also increase therapy resistance [12,15,20].

Once activated, CAFs commonly secrete pro-tumorigenic growth factors and cytokines such as HGF and PDGFs. In addition, CAFs also influence tumor cells indirectly through modulation of the TME; by ECM production and modification, by promoting angiogenesis, and the last decade, their interaction with immune cells have been highlighted. Indeed, CAFs can increase the pro-tumorigenic inflammation seen in many carcinomas, and at the same time act immune-suppressive, reducing the anti-tumor immune response, and possibly also reduce the sensitivity to immunotherapy [12,13,15,17,20].

Tumor-suppressive functions of CAFs

Although most data demonstrate a tumor-supportive function of CAFs, some studies have strongly indicated that subsets of CAFs may suppress tumor growth. Two studies published in 2014 indicated a surprising pro-tumorigenic effect of depleting CAFs in PDAC (pancreatic ductal adenocarcinoma) mouse models. First, Ozdemir et al. conditionally depleted proliferating αSMA-expressing cells in a PDAC mouse model, which resulted in more aggressive tumors [31]. Noteworthy, in this study, all αSMA-positive cells were depleted, not only αSMA-positive CAFs. Similarly, Rhim et al. demonstrated with a

different PDAC model, a pro-tumorigenic effect of suppression of Hedgehog signaling in pancreatic epithelial cells and thereby reduction of stromal αSMA-positive cells [32].

Later, other reports have highlighted the heterogeneity of CAFs in the cancer stroma in which different CAF subsets influence the tumor cells differently [19,21,33-35]. Two publications have interestingly highlighted CAF heterogeneity in pancreas and breast cancer. Ohlund and colleagues identified two subsets in PDAC; inflammatory and myofibroblastic CAFs (iCAFs and myCAFs), while Costa and colleagues defined four CAF subtypes in breast cancer. Intriguingly, the subsets seem not to represent fixed cell types, but rather different states of fibroblasts [10,33].

1.1.2 The interstitium

The interstitium fills the space between the cells and the blood and lymph vessels, and consists of the structural molecules comprising the ECM, in addition to the interstitial fluid with its dissolved substances [36].

Extracellular matrix

The structural molecules of the interstitium comprise the ECM [36]. It is a complex network composed of a variety of macromolecules such as collagens, proteoglycans, elastin, fibronectin and laminins, where collagens are the most significant component [37,38]. The ECM acts as an architectural scaffold, provides anchorage for cells, and is a reservoir for various insoluble substances such as growth factors and cytokines [36,37,39,40]. Components of the ECM bind to adhesions receptors such as integrins, which mediate cell-matrix adhesion and signal transduction into the cell, as well as to soluble growth factors, thereby regulating their distribution and activation [36-39]. The ECM composition and structure have a vital role in the regulation of cell behavior, and is dynamic with constant remodeling and modifications – all of which are tightly controlled in normal organ homeostasis [38-41].

Collagen

Collagen is the most abundant protein in the body [37]. In mammals 28 collagen types have been identified, and different tissues have a unique collagen composition [38,39]. Normally, there is a constant production and degradation, and matrix metalloproteinases (MMPs), inhibitors of MMPs and enzymes responsible for modifications such as lysyl oxidases (LOX) are important contributors in this remodeling [39].
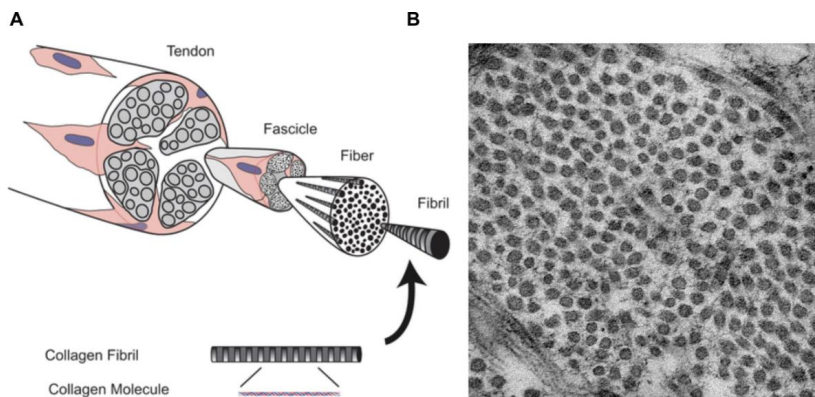
Fig 4. Collagen structure. **A.** Collagen structure in a tendon. Collagen molecules form triple helices which again assemble to form collagen fibrils. Bundles of fibrils are organized as collagen fibers. Reprinted from [42], with permission. **B.** Transmission electron microscopy image from a MDA-MB-468 tumor in an integrin α11 knockout mouse show collagen fibrils.

ECM alterations in cancer

ECM homeostasis, including collagen production, degradation and re-organization, is often perturbed during tumor progression, and this is mainly orchestrated by CAFs [39,41]. Many solid tumors are characterized by excessive collagen deposition, and the collagen is increasingly linearized and crosslinked during tumor progression [39,43]. Moreover, CAFs have been shown to collectively lead invading tumor cells by remodeling the ECM and producing tracks for the invading cells, and this matrix remodeling was dependent of integrin α3β1 and α5β1 in CAFs [44].

In the case of breast cancer, Provenzano et al showed in 2008 that increased stromal collagen density promoted breast cancer initiation, progression and metastasis experimentally [45]. A few years later, they demonstrated that straightened and aligned collagen fibers oriented perpendicular to the tumor boundary were an independent prognostic factor in human breast cancer [46]. Additionally, increased collagen deposition, linearized, thick collagen fibers, and increased tissue stiffness have been found to be most prominent in the aggressive HER2 and TNBC subtypes [47]. Later, elongated, parallel orientated collagen fibers have been demonstrated to correlate with poor survival also in other cancer types [48]. Intriguingly, experimental studies suggest that collagen crosslinking and stiffening of the ECM play a causal role in the promotion of malignant transformation by enhanced integrin signaling [49].

Interstitial fluid pressure and transcapillary fluid exchange

The interstitial fluid is the route of transport of nutrients, signaling molecules and waste products to and from the tissue cells, and the transcapillary fluid flux is therefore vital for normal tissue homeostasis [36,50-52]. Normally, it is formed by transcapillary filtration from blood capillaries into the interstitium and is finally removed by the venous side of the vascular system or lymphatic vessels [36,50-52].

The transcapillary transport of molecules is primarily by diffusion and/or convection [53]. While diffusion is determined by a concentration gradient, convection is transport of molecules by fluid flow, and transcapillary convection is thereby determined by the fluid filtration rate across the capillary membrane [50,53]. While low molecular compounds are transported by both diffusion and convection, high molecular compounds are mainly transported by convection [50].

The pressures that determine the transcapillary fluid filtration rate, i.e. determine the net filtration pressure and thereby transport of molecules by convection, are described by the Starling hypothesis as [51]:

$$J_V = CFC\ [(P_C - P_{IF}) - \sigma\ (COP_C - COP_{IF})]$$

J_V = Filtration
CFC = Capillary filtration coefficient (dependent on the area and permeability of the vessel wall)
P_C = Capillary hydrostatic pressure
P_{IF} = Interstitial fluid pressure,
σ = The colloid osmotic reflection coefficient,
COP_C = Capillary colloid osmotic pressure
COP_{IF} = Interstitial colloid osmotic pressure

In normal tissues, transcapillary fluid filtration is driven by the capillary hydrostatic pressure with additional contribution from the interstitial colloid osmotic pressure and a slightly negative interstitial fluid pressure (PIF) - which all drives fluid flow into the interstitium [50,52]. On the other hand, the capillary colloid osmotic pressure tends to keep fluid within the vessel. The sum of the starling forces is normally a net outward filtration pressure leading to fluid flow from the capillaries into the interstitium, as demonstrated in **Fig 6** [50]. Excessive fluid is finally reabsorbed in the venous section of the capillaries or removed from the interstitium by lymphatic vessels to avoid fluid accumulation [50,54].
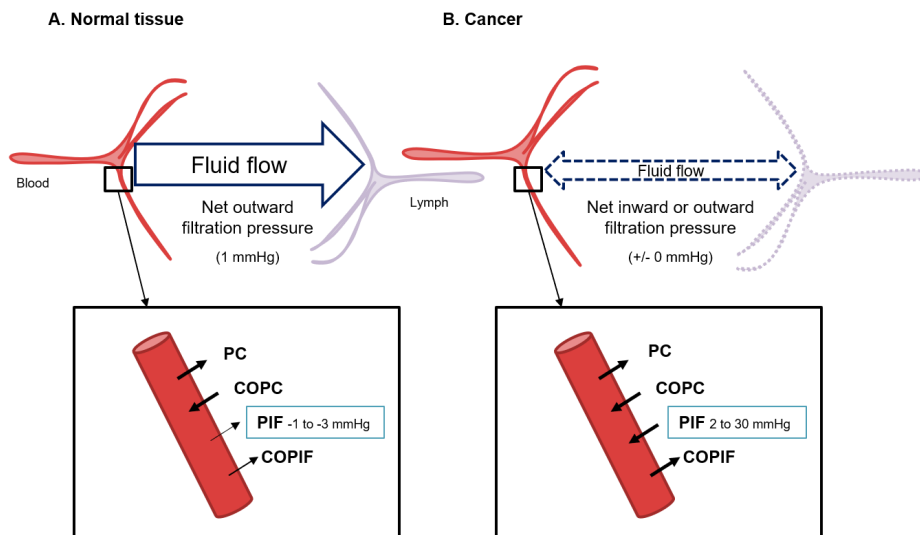
Fig 6. Transcapillary fluid flow. **A.** In normal tissue, there is a net outwards filtration pressure and fluid flows from the capillaries and into the interstitium. **B.** In solid tumors, PIF can be markedly elevated and hinders fluid flow into and within the tumor. PC = Capillary hydrostatic pressure. COPC = Capillary colloid osmotic pressure. PIF = Interstitial fluid pressure. COPIF = Interstitial colloid osmotic pressure.

On the contrary, the vasculature is markedly changed in tumors; the blood vessels are hyperpermeable, and lymphatic vessels are dysfunctional or missing [50,53]. The leaky blood vessels increase the flux of fluid and plasma proteins into the tumor interstitium and at the same time there is reduced lymphatic reabsorption which will lead to fluid accumulation in the tumor interstitium and thereby increased tumor PIF [53,54]. Additional factors that may contribute to increased tumor PIF are a dense ECM which reduce the leakage and escape of fluid, in addition to contractile fibroblasts which are thought to exert a tension on the ECM [50,53].

Drug transport

Cancer therapy must reach the target cells in order to exert their effects, and blood-borne drugs must therefore be transported across the capillary wall and through the tumor interstitium. Since increased tumor PIF decreases fluid transport into and within solid tumors, it may act as a barrier to the delivery of drugs, thereby reducing their efficiency [50,54]. Cancer therapy is mainly transported by convection, especially high-molecular compounds [50], and several studies have shown improved uptake of drugs into the tumor by reducing tumor PIF in some [55-58], but not all models [59,60].

The effects of integrin α11-deficiency on tumor PIF (**paper I and II**), and also on the uptake of ^{3}H-5FU into xenograft breast tumors (**paper II),** are investigated in this thesis.

1.1.3 Integrins

Integrins are cellular adhesion receptors that act as links between the cells and the ECM, and also cell-cell adhesion receptors [61,62]. They regulate diverse cellular functions including cell motility, proliferation and survival, and sense and react to changes in the microenvironment [62-64]. They are crucial for cell migration by coupling the ECM to the cell cytoskeleton, contribute to ECM remodeling, and are also responsible for cell-cell interactions [61,62,65].
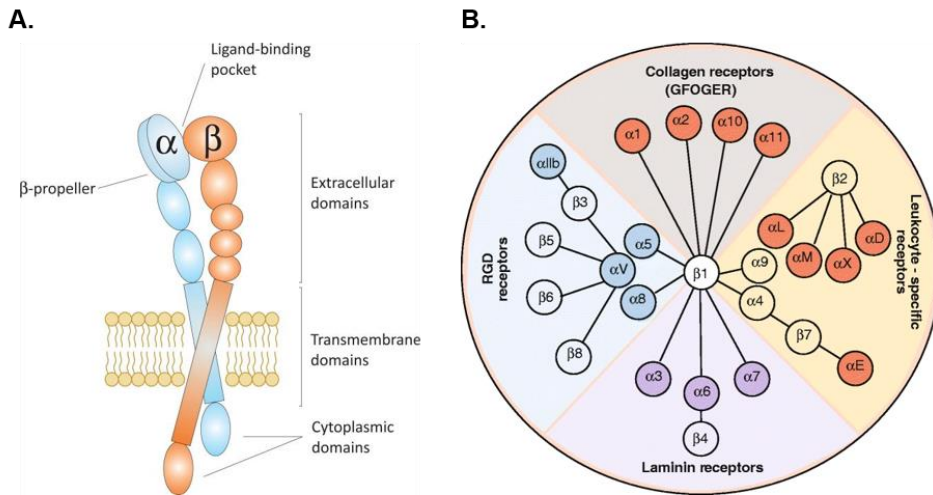
Fig 7. Integrins. A. Integrins are transmembrane heterodimers composed of one α- and one β subunit. The α subunit determines ligand specificity, while the β subunit is mainly responsible for intracellular signaling and is connected to the cytoskeleton. Reprinted from [66], with permission. **B.** The integrin family consists of 18 α and 8 β subunits which can combine to form 24 integrins. Reprinted from [61], with permission.

Integrins are bi-directional signaling molecules with inside-out and outside-in signaling [61]. As they lack intrinsic enzyme activity, integrin signaling is transmitted through intracellular association of soluble kinases and adapter proteins upon activation of the receptor [62,67].

Integrins are expressed on all nucleated cells [68], and the integrin expression pattern and activation state on each cell will determine how a cell responds to its microenvironment and is therefore crucial for cellular responses to microenvironmental changes [62]. However, both the expression pattern of different integrins and their activation state are often transient, making integrin biology and function complex - not only dependent on cell type, but also on tissue type and context [61,63,69].

Collagen-binding integrins

The collagen-binding integrins consist of integrin α1β1, integrin α2β1, integrin α10β1 and integrin α11β1, and mediate cell-collagen interactions by binding to different types of collagens with varying affinity [65]. Although collagen-binding integrins seem to have a limited role in adult connective tissue homeostasis, they are probably important in dynamic connective tissue remodeling such as wound healing, fibrosis and cancer [65].

Integrin α11β1

Integrin α11β1 is the newest and last supplement to the integrin family, and the α11 subunit exclusively forms a heterodimer with the β1 subunit [24].

Distribution

Integrin α11β1 has been shown to be expressed on a subset of fibroblasts and mesenchymal stem cells [65]. In human and mouse embryos [70,71], integrin α11 protein and mRNA are mainly expressed in mesenchymal non-muscle cells in tissues with highly organized collagen, such as fibroblasts around ribs, vertebrae and in intervertebral discs. In human adult tissues, integrin α11 mRNA was in early studies found to be expressed in high levels in uterus and heart [72], but this has not been confirmed at the protein level. Although the expression of integrin α11β1 seems to be restricted to mesenchymal non-muscle cell at sites of highly organized collagen, the characterization of the expression pattern in human adult tissues is so far limited due to lack of specific reagent tools and low expression level in most tissues [24]. In a recent publication, integrin α11β1 was found to be expressed on osteoblasts and to be important in the regulation of osteogenesis and adult skeleton maintenance [73].

The expression of integrin α11β1 seems to be upregulated during myofibroblast differentiation and in CAFs [24]. In 2002, Wang et al. identified integrin α11 mRNA to be overexpressed in non-small cell lung cancer compared to normal lung tissue [74]. Later,

integrin α11 expression has been found to be upregulated in CAFs in lung cancer [75,76] and in oral squamous cell carcinoma [77].

Function in vitro and in vivo

Integrin α11β1 has been shown to bind preferentially to collagen I and is important for attachment and migration of cells on collagen I, and for contraction of collagen gels [70]. It has a role in collagen organization [70] and myofibroblast differentiation *in vitro* [30], and during wound healing [78] and fibrosis [29,79,80] *in vivo*. TGF-β has been shown to upregulate the expression of integrin α11β1 expression in multiple cell lines [81,82].

The integrin α11 knockout (α11-KO) mice have a relatively mild phenotype, but are smaller than their wild type (WT) and heterozygous littermates, especially the first weeks of living, and they display increased mortality [83]. A defect in incisor tooth eruption and altered tooth shape can partly explain this phenotype, but as the α11-KO mice are smaller already at birth, additional factors are likely [24]. They have for example been shown to have reduced serum levels of IGF1 [84].

Experimental studies have indicated that integrin α11β1 can contribute to fibroblast function in both wound healing, fibrosis and in tumorigenesis [24,65]. Regarding wound healing, α11-KO mice have shown reduced granulation tissue formation due to defect in myofibroblast differentiation, and reduced strength of the scar tissue, probably due to reduced collagen remodeling [78]. Further, integrin α11β1 may have a pro-fibrotic role in cardiac fibrosis [28,79,80,85], and α11-KO mice seem to be protected from development of dermal fibrosis *in vivo* [29].

A few studies have indicated that integrin α11β1 may stimulate tumor aggressiveness experimentally. Stromal integrin α11 was shown to stimulate lung cancer growth [75,86] and metastasis [86] *in vivo*, and lung cancer cell proliferation, invasion and migration in a heterospheroid model [87]. The pro-tumorigenic abilities of integrin α11β1 were in these

studies suggested to be related to the production of IGF2 by fibroblasts [75] and CXCL5 by lung tumor cells [87], and also to collagen organization, tissue stiffness and the collagen crosslinking enzyme, LOXL1 [86,88].

Additionally, it should also be noted that a few studies have indicated that integrin α11β1 could have a role in the regulation of dermal PIF *in vivo* [89,90] and PIF in lung cancer heterospheroids [87]. In **paper I and II**, we have investigated the effect of stromal integrin α11 on breast tumor growth, collagen organization and tumor PIF using α11-KO mice. In **paper III**, the expression and prognostic impact of integrin α11 in human breast cancer were investigated.

1.2 Breast cancer

Breast cancer is the most common cancer type among women in Norway [91]. Even if improvements in early detection, breast cancer classification and more tailored treatment have considerably improved the prognosis of breast cancer during the last decades, breast cancer behavior, including metastatic patterns, prognosis, and response to therapy, differ among different breast cancer subgroups [92].

1.2.1 Classification of invasive breast carcinoma

Traditionally, breast cancer has been classified by clinico-pathological assessment and a few molecular markers [93]. The expression of estrogen receptor (ER), progesterone receptor (PR), human epidermal growth factor receptor 2 (HER2) and Ki67 give important prognostic information and directly guide breast cancer treatment [94]. However, breast cancer is a heterogeneous disease, and traditional markers have been shown not to fully reflect the biological heterogeneity of breast cancer [93,95]. With the aim of better individualized therapy, enormous amount of work has been done to further characterize this heterogeneity and to develop better prognostic and predictive markers [93].

Histological classification

Breast carcinomas are classified according to their morphological appearance. The majority of invasive breast carcinomas are classified as invasive carcinoma of no special type (NST) which means that >50% of the tumor does not fit into a defined special subtype [93,96]. Of the special types of invasive breast carcinoma, the most common type is invasive lobular carcinoma [93,96]. Classification of breast cancer by morphology has prognostic value; the special types tubular and mucinous carcinoma are for example associated with good prognosis, while metaplastic carcinoma is associated with poor prognosis [96].

Molecular classification

Great improvements in the molecular classification of breast cancer have been achieved over the last two decades [97]. Microarray-based gene expression profiling studies have demonstrated different subtypes of breast cancer based on the expression of several genes, also called intrinsic breast cancer subtypes (**Fig 8**) [98,99]. Initially, only four subtypes were identified; the luminal, HER2-enriched, basal-like, and normal-like [98,99]. Later, the luminal group has been divided into at least luminal A and luminal B, and the normal-like has been proposed to mainly represent contamination of normal tissue [99,100]. These intrinsic subtypes have shown differences in behavior, prognosis and response to therapy [99-101]. Efforts are ongoing to further sub-classify these subtypes, especially the basal-like subtype that has the least favorable prognosis.

Triple-negative and basal-like breast cancer

Triple-negative breast cancer (TNBC) represents 10-15% of invasive breast carcinomas and is defined by lack of expression of estrogen and progesterone receptors and absence of amplification of HER2 [102]. Patients with TNBC have fewest treatment options and also the least favorable prognosis where a subset of patients have early disease relapse [103,104]. TNBC is diagnosed by exclusion of other breast cancer types, and therefore represents a heterogenous disease regarding biology and clinical behavior. Noteworthy,

TNBC and the basal-like subtype are mostly overlapping, where around 70% of basal-like tumors are TNBC, and 80% of TNBC are basal-like [102]. Gene expression analyses have further subclassified TNBC [105,106], and differentiation by immune-, mesenchymal-, stem cell-, basal and also androgen markers have given important biological information about the molecular differences in TNCB, and have provided frameworks for studies of more targeted therapies in TNBC [102].
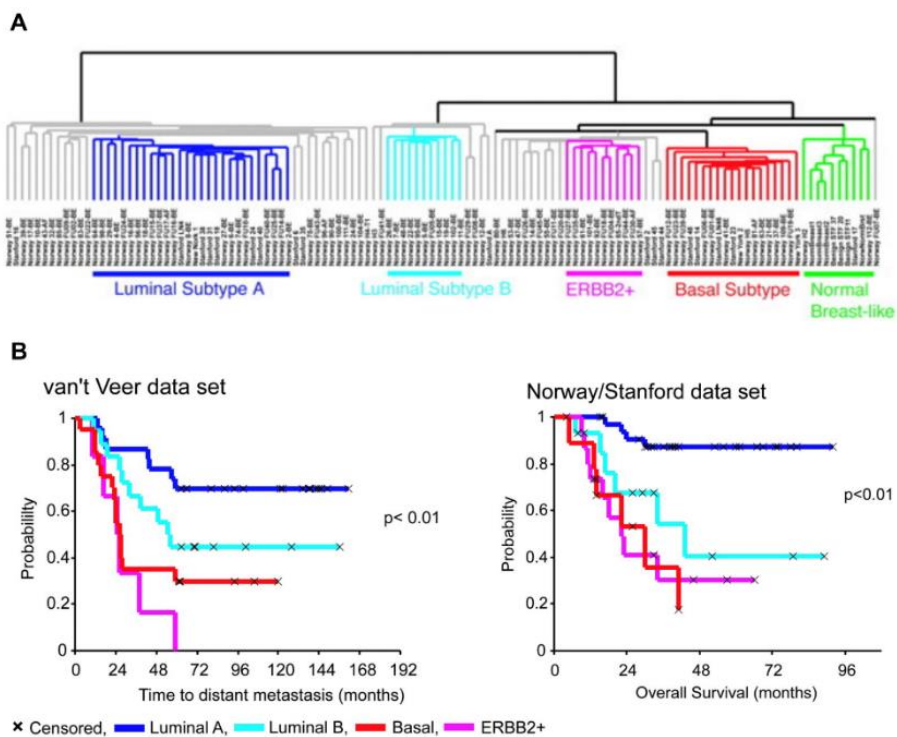
Fig 8. Molecular classification of breast cancer. Pioneer work has identified the existence of distinct molecular subtypes of breast cancer. Modified from **[101]**, with permission. Copyright (2003) National Academy of Sciences, U.S.A.

Prognostic and predictive markers in breast cancer

Several prognostic markers guide breast cancer treatment (and are therefore also predictive markers); TNM stage (tumor size-nodes-metastasis), histologic grade, mitotic count, hormone receptors, HER2-status, and also Ki67, and these markers are routinely reported in pathology reports of invasive breast carcinoma [107].

Based on the studies of molecular classification of breast cancer, gene expression tests such as Oncotype Dx, Mammaprint and Prosigna have been developed and provide prognostic information. These are now being introduced in the clinic, and the Norwegian Breast Cancer Group recommends the test Prosigna for use in some subgroups of breast cancer patients to help guide adjuvant treatment [107].

1.2.2 The tumor microenvironment of breast cancer

Breast cancer consists not only of tumor cells, but as for other solid tumors, of an intricate TME that significantly influences breast cancer development, progression and therapeutic response [108,109]. Altered signaling pathways and molecular changes in stromal cells indeed characterize the breast cancer TME, and many of these alterations or signatures have been shown to predict patient outcome and response to therapy [108,110-112]. Extensive research is now done to find prognostic and predictive stromal markers, and in the development and testing of different stromal therapeutic targets [108].

Breast CAFs as prognostic markers

Breast cancer is often regarded as desmoplastic tumors were CAFs are the main regulator of ECM deposition and remodeling [10]. Extensive experimental data have demonstrated that breast CAFs can stimulate breast cancer growth and progression [113]. Further, the heterogeneity of breast CAFs has recently been highlighted [19,21,34,35], and several studies have aimed to identify tumor-supportive CAF subtypes with prognostic value.

αSMA-positive fibroblasts are more abundant in invasive breast carcinomas compared to normal breast tissue and benign lesions [114,115]. High stromal αSMA expression has been associated with aggressive breast cancer phenotypes and has been shown to predict poor prognosis in some studies [114,116-120]. However, αSMA-positive fibroblasts, often referred to as myofibroblastic CAFs (myCAFs), surprisingly seem to represent a CAF subset with tumor-suppressive functions in PDAC [121], and future experimental research should investigate if these findings are transferable to breast cancer. High PDGFRβ expression has also been associated with aggressive breast cancer phenotypes and can predict poor prognosis and therapy response [122,123]. Furthermore, several studies of FAP expression in various cancers have given conflicting results, where FAP's prognostic value varies from study to study which has been suggested to reflect the lack of specificity of several commercial antibodies [124].

Costa and colleagues identified one breast CAF subset (CAF-S1) expressing high levels of αSMA and FAP which was localized in close proximity to the tumor cells. This subtype was found to attract T-cells and to contribute to immunosuppression. However, none of the four CAF subsets identified in this study could predict patient survival although both CAF-S1 and CAF-S4 were associated with the TNBC subtype [34]. In another study, Su et al. characterized a CAF subtype positive for both CD10 and GPR77 that promoted tumor formation and chemoresistance, and also reflected patient outcome and treatment response in several breast cancer cohorts [35].

Nevertheless, even if several studies have implicated that at least some CAF subsets can have prognostic and predictive value in breast cancer, for several markers the results are partly conflicting, and more research is highly warranted.

Tumor microenvironment in TNBC

Also, regarding the TME, TNBC seems to be markedly heterogenous, and indeed, features of the TME have shown to predict outcome [125]. Number of tumor-infiltrating

lymphocytes seen by immunohistochemistry (IHC) are a well-known predictor of good prognosis of TNBC, but lately, more complex and deeper characterization of the TME in TNBC seems to provide additional prognostic information [125]. For example, a recent study demonstrated that not only the frequency, but also the location of tumor-infiltrating lymphocytes correlated with gene signatures and clinical outcome [126]. In the future, more detailed characterization of the TME will hopefully contribute to the identification of distinct TNBC phenotypes, with the aim of more personalized therapy in this aggressive breast cancer subtype.

Breast myoepithelium

The epithelium of the mammary gland consists of an inner luminal and a surrounding myoepithelial cell layer [127]. The myoepithelial cells are important for normal mammary gland development by influencing the polarization of the luminal epithelium and branching of the mammary ducts, and also milk production [128,129]. The myoepithelial cells are contractile, which is important for their function in milk ejection during lactation [128].

The presence of malignant cells outside the myoepithelium and basement membrane discriminates *in situ* lesions from invasive carcinoma [130]. As visualization of the basement membrane is challenging in tissue sections, identification of a myoepithelial cell layer is therefore a surrogate marker of an intact basement membrane and is of huge importance in the diagnosis of invasive breast carcinomas [130]. The myoepithelial layer can most often be easily identified with markers such as αSMA and cytokeratin 14 (CK14), but there can sometimes be challenges in the histological interpretation; the myoepithelial layer may be interrupted and/or express an altered immunoprofile, and in some non-malignant lesions, such as in microglandular adenosis, the myoepithelial layer is absent [130].

Myoepithelial cells are thought to play a part in the early stages of breast cancer tumorigenesis [131]. Normally, they act as a physical barrier that together with the

basement membrane separate the stroma from the epithelial cells, and can also be active tumor suppressors [130,131]. Sirka et al. demonstrated that myoepithelial cells can actually restrain and recapture invasive breast cancer cells [131]. Recent data have shown that DCIS-associated myoepithelial cells are altered compared to myoepithelial cells in normal breast tissue [130,132]. Further, the tumor-suppressive functions of myoepithelium may be lost with DCIS progression, and loss of this suppression has been suggested as at least a contribution to the transition from preinvasive to invasive cancer [129]. In pre-invasive breast lesion, these differences have been suggested as possible markers for risk-stratification or targets for prevention of invasive breast cancer.

Integrin expression in breast myoepithelial cells

Myoepithelial cells express integrins that are important for attachment of the cells to the basement membrane, which is mainly formed of collagen IV and laminins [133]. The collagen-binding integrins α1β1 and α2β1 have collagen IV as a known ligand and are expressed in myoepithelial cells [65]. Integrin α11β1 binds to collagen IV with low affinity and has not been shown to bind to other components of the basement membrane [65,70]. The expression of integrin α11β1 expression in breast myoepithelial cells is discussed in **paper III**.

2. Aims of the study

Overall aim:

To investigate the role of integrin α11β1 in breast cancer.

Specific aims:

1: Examine the role of stromal integrin α11β1 in experimental breast tumor growth, collagen organization and interstitial fluid pressure regulation using different integrin α11-deficient mouse models (**paper I and II**).

2: Establish conditions for reproducible staining of integrin α11 in formalin-fixed, paraffin-embedded human tumor material using new antibodies against the integrin α11 subunit (**paper III**).

3: Investigate the expression pattern of integrin α11 in human breast cancer, and based on this, examine the association of stromal integrin α11 expression with aggressive breast cancer phenotypes and potential prognostic impact in human breast cancer (**paper III**).

3. Methodological considerations

The methods used in **paper I-III** are described in detail in the respective manuscripts, but some essential methodological aspects are discussed in the following sections.

3.1 Mouse models for studying the tumor microenvironment

Mice play an essential role in breast cancer research, and mouse models represent an important step between *in vitro* experiments and clinical studies [134]. They are easy to handle, breed effectively, have molecular and physiological resemblances to humans, and provide us with research opportunities like standardized study populations and the possibility of genetic modifications [135,136]. The last decades, there has been enormous growth in the number and sophistication of mouse models for cancer research [136]. Since all mouse systems have their strengths and limitations, and different models give complementary information, various mouse models should be investigated to maximize what can be learned from them [136]. However, animal welfare should be central when working with mice, with special focus on replacing animal experiments if possible, reducing the number of animals, and refining the experiments i.e. make sure the animals suffer as little as possible (the 3Rs).

Mice have been essential for the work presented in **paper I and II** and have also enabled the generation of new anti-human integrin α11 antibodies used in **paper III**.

Engraftment of cancer cell lines

In **paper I and II**, murine (**I**) and human (**II**) cancer cell lines were injected into severe immunodeficient (SCID) WT and SCID α11-KO mice. SCID mice have a severe deficiency in mature B and T lymphocytes [137]. The engraftment of cancer cell lines in mice has provided enormous knowledge about breast cancer biology, and is the most commonly used mouse cancer model, as it is simple and relatively rapid to establish, and also homogenous

and therefore requires reduced number of animals compared to other models [134]. Further, there are numerous, diverse and well-characterized cell lines that represent different cancer types and also different cancer subtypes. Nevertheless, engraftment of cancer cell lines does not reflect the intratumor heterogeneity of human carcinomas, represents late stages of primary tumor evolution since the cancer cells are derived from highly aggressive tumors, and probably most important for the investigation of integrin α11β1, the stromal infiltration is often scarce and highly homogenous compared to human cancers [134,136,138]. Indeed, as many of the cancer cell lines are highly aggressive, they may not be that dependent of stromal interactions to grow, invade and spread. Additionally, when using immunodeficient mice, this model does not incorporate the impact of the immune system on the tumor response [136], which is a concern also when investigating CAFs. Indeed, different components of the tumor interact with each other, and CAFs have been shown to influence tumor cells through immunomodulation [17,77]. Therefore, even if the engraftment of cell lines to WT and α11-KO mice (**paper I and II**) does provide important information about integrin α11's role in breast cancer, these projects should be complemented with other *in vivo* and *in vitro* systems.

When engrafting mouse cancer cell lines to mice, syngeneic models offers the "advantage of studying cancer biology within the context of an intact immune system and species-specific TME" [136]. However, mouse cancer cells were injected into immunodeficient mice in **paper I**, and although we would have preferred to use syngeneic mouse cells in immunocompetent mice, the SCID α11-KO mice were the only strain available for our purpose. Further, we used the extremely rapidly growing tumors 4T1 and RM11 in **paper I**, and in **paper II** we choose cell lines growing more slowly and thus possibly more stromal-dependent.

Ideally, different cell lines and different models should be investigated to reflect the complexity of breast cancer including all breast cancer subtypes. In **paper II**, we initially tried to use other cell lines (MCF7 and BT474). However, mice in these pilots showed

severe side effects of supplemented hormone treatment despite low dosage 17β-estradiol (0.18 mg/pellet and custom-made 0.1 mg/pellet), and the pilots were thus terminated due to animal welfare. Therefore, only TNBC cell lines were used in **paper I and II**.

The cell lines in **paper I and II** were injected orthotopically and/or ectopically. Orthotopic implantation is regarded to be superior to ectopic implantation in engraftment models [138], as discussed in **paper I.** Nevertheless, it should be noted that the architecture of the murine mammary tissue is substantially different compared to the mammary tissue in humans especially in regards to stromal components as seen in **Fig 9** [113,127,139].
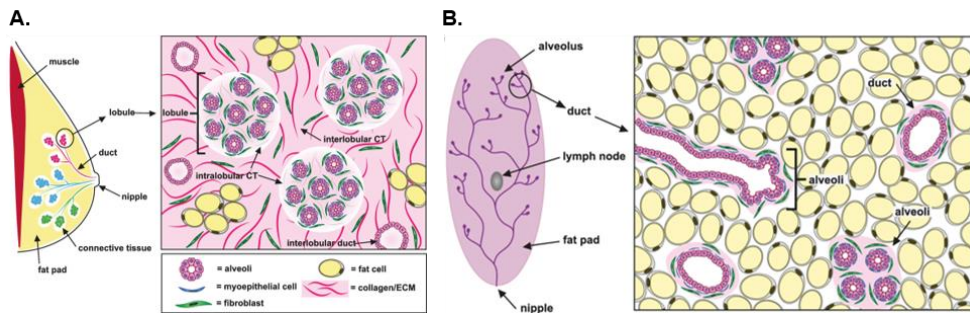
Fig 9. **Human and murine mammary tissue.** There are notable differences between human and murine mammary tissue architecture including differences in the stromal components surrounding the mammary epithelium. In humans, the ducts and lobules are embedded in loose connective tissue (**A**), while the murine stroma is mainly composed of adipose tissue and markedly less fibroblasts and ECM (therefore often referred to as mammary fat pad) (**B**). Reprinted from [113], with permission.

Knockout mice

In conventional genetically modified KO-mice, such as the α11-KO mice, a functional gene has permanently been deleted or inactivated within the whole mouse [140]. This model provides a valuable tool for studying the function of a specific gene, but several complicating factors can influence the results from such studies. When comparing differences between tumors in WT and KO-mice, the study groups should ideally be identical beyond the function of the gene in the investigated tissue. In regard to integrin

α11β1, the α11-KO mice have a fairly mild phenotype, but are significantly smaller than their WT littermates at young age. They have reduced capability to eat food of solid material because of tooth defects, and both WT and α11-KO mice were therefore given powder food. Additionally, compensatory mechanisms may take over a gene's function when it is inactivated, and there have been conflicting results regarding compensatory mechanisms as a result of integrin α11 deletion [71,75,89]. Consequently, the above-mentioned factors contribute to study groups that are not completely identical representing a bias in **paper I and II**. Production of a conditional α11-KO mouse model, in which the gene knockout can be spatially and temporally regulated [140] would be highly valuable.

Other mouse models relevant in the study of TME

In genetically engineered mouse models where oncogenes or tumor suppressor genes have been manipulated, the tumor develops through different stages of epithelial transformation and evolves within the context of a TME that more accurately reflect human disease, including a well-functioning immune system, stromal remodeling, angiogenesis and inflammation [136]. Therefore, these models are especially relevant for the study of the stepwise breast cancer progression and also to investigate features of the TME. The MMTV-PyMT breast cancer mouse model has been recognized for its relevance in the study of breast CAFs since the carcinomas in this model consist of a fibroblasts-rich, fibrotic stroma resembling human carcinomas, and the expression of different CAF markers is remarkable similar as in human carcinomas [141]. Interestingly, a collaborating group has crossed the MMTV-PyMT mice with α11-KO mice to investigate the role of integrin α11 in breast cancer [142]. This model resembles human breast cancer of the luminal B subgroup (ER and HER2-positive) [141], and thus, additional models are needed to investigate different subtypes of breast cancer.

CAF heterogeneity in experimental breast cancer models

A very recent study of breast CAF heterogeneity demonstrates that CAFs show obvious heterogeneity across different murine TNBC tumors, indicating that cancer cell intrinsic factors may strongly affect the CAF subpopulations [143]. Further, the expression of different CAF markers changes during tumor progression even in the same tumor model [143], and integrin α11 expression in PyMT tumors indeed seem to display temporal heterogeneity [142]. Therefore, CAF heterogeneity in relation to different tumor models, and also to temporal intratumoral heterogeneity, may explain conflicting results when investigating CAFs experimentally. Of note, most measurements in **paper I and II** were done at end point day and investigations during different time spans in these models could give additional information.

3.2 Collagen analyses

In **paper I and II**, different methods were used to study collagen. Picrosirius red staining is a simple and sensitive method to identify fibrillar collagen in tissue sections [144], and was used to investigate the amount of collagen in the engrafted tumors. While some reports indicate that it can distinguish between collagen I and III according to their colors under polarized light, this has been an issue for debate [145], and this approach was not used. However, we additionally performed IHC staining of collagen III in **paper II**.

Electron microscopy offers high magnification images and was therefore used to investigate collagen fibril structure and organization. However, due to the limited field of view, it provides minimal information about collagen fiber organization.

3.3 Measurement of intersititial fluid pressure

In **paper I and II**, the wick-in-needle and micropuncture technique were used to measure PIF in engrafted tumors and in heterosperoids, respectively. Both methods are well-

established in our group. The micropuncture technique gives highly reproducible PIF, induces little tissue trauma and should be chosen whenever applicable [52]. However, it can only record PIF down to 1 mm below the surface and is therefore not suitable for measurements of PIF in tumors, but is usually chosen to measure PIF in heterospheroids due to their small size [52], as we did in **paper II**.

The wick-in-needle technique has the great advantage that it can record deep in tissues and is regarded as standard method for measuring PIF in engrafted tumors [50,52]. Although tissue trauma usually always will occur to some degree, comparison between micropuncture and wick-in-needle technique has shown similar pressures [50,52]. In **paper I and II**, tumors with evident bleeding during the PIF measurement, seen as a continuous fall in PIF or blood stain on the wick upon removal from the tumor, were excluded.

3.4 Breast cancer series

The breast cancer cohort used in **Paper III** is a retrospective, population-based patient series, including women aged 50-69 years when diagnosed with primary breast cancer in Hordaland County during 1996-2003. Patients with distant metastatic disease at time of diagnosis were excluded. Follow-up data (survival status, survival time and cause of death) were collected from the Norwegian Cause of Death Registry of Norway, the Cancer Register of Norway and also patient records. No patients were lost to follow-up. Treatment and response to treatment were not registered, but the patients received treatment according to standard treatment protocols at that time.

Population-based series reduce the risk of sampling bias which can increase the applicability of the generated results to the general breast cancer patient population. An additional advantage of this patient series is long and complete follow-up data on both incidence and outcome. However, only women with primary breast cancer aged 50-69 years old were included, and results generated from this cohort may not be generalizable to patients younger than 50 years and older than 69 years. Additionally, anti-HER2 treatment

was not standard as adjuvant treatment of primary breast cancer in the period of 1996-2003, and therefore, patients diagnosed with HER2-positive breast cancer receiving standard treatment today have a markedly improved prognosis compared to HER2-positive breast cancer patients enrolled in this study.

3.5 Immunohistochemistry

IHC visualizes antigens within tissue sections by binding of a labelled antibody to its antigen [146]. It enables determination of the spatial distribution of one or more proteins in tissues and semi-quantitative quantification of the target protein [146,147]. IHC was used in all papers in this thesis.

Although IHC analyses are easy, inexpensive and widely used both in routine pathology and in research, the technique has several pitfalls that can cause both false positive and false negative staining results and thereby lead to incorrect conclusions [146,148,149]. Indeed, variations in both the pre-analytic, analytic and post-analytic phase can contribute to bias in the IHC results [146,147].

The impact of different variables on the IHC results is antigen-, antibody- and also tissue- and preparation-dependent [146,147]. Therefore, before introducing a new IHC protocol, the protocol should be properly validated and optimized using tissues with the same pre-analytic, analytic and post-analytic treatment as the tissue to be tested. Validation of an IHC protocol is important when using new antibodies or "old" antibodies in a new setting, and to enable inter-laboratory comparison and standardization. In **paper I and II**, already well-established IHC protocols were used. In **paper III**, efforts were made to properly validate new monoclonal antibodies and establish the IHC protocol.

Pre-analytical varibles

Pre-analytical variables can significantly impact the IHC staining result [146,147]. As the sections for the cohort in **paper III** were assembled prior to the current study, variables such as time to fixation, fixation time and paraffin impregnation were not available to adjustment. Therefore, we cannot exclude influences on antigenicity of the integrin α11 epitope by these variables.

Antibody validation and IHC controls

Lack of proper antibody validation and appropriate IHC controls contribute to the difficulties seen in reproducing IHC-derived data; and even more seriously, improper validated IHC protocols can generate reproducible, but incorrect conclusions [148]. To ensure correct and consistent results, optimized and standardized tissue protocols are required [147,148]. This includes proper validation of the primary antibody and careful selection of positive and negative controls [148].

Appropriate controls are crucial to ensure that the obtained IHC result is a consequence of binding of the primary antibody to the correct antigen in tissue sections [148]. The controls should confirm that the primary antibody only binds to the correct antigen, that the labelling observed is due solely to binding of the secondary antibody to the primary antibody and that the labelling is not a result of endogenous fluorescence or enzyme reactivity (for example endogenous peroxidase) [148]. An overview over recommended controls in IHC is summarized in **Table 1**.

In regard to fibroblasts markers, investigations of FAP in human material have shown different, often contradicting results [124]. As reported by Pure and Blomberg, several commercially available anti-FAP antibodies lack specificity, and studies using immune-based assays with antibodies against FAP should be interpreted based on inclusion of appropriate controls [124]. Similarly, to our experience, most commercially available

antibodies against integrin α11 do not show specific binding in FFPE tissue. As an example, a previous study investigating the expression and prognostic impact of integrin α11 in a series of 80 FFPE invasive human breast carcinomas obtained contrasting results to our study. They reported that integrin α11 was strongly expressed in the tumor cells and no staining of the stromal compartment was described [150]. The anti-integrin α11 antibody

Reagent controls	Biological controls
Positive reagent control A different antibody against the same protein.	**Positive tissue control** Tissue known to express the protein. The protein should ideally be expressed in stable levels, with different intensity (low to high). **Types of positive tissue controls** a. External tissue control b. Internal tissue control c. Cell pellet control: cell line with known expression or transfected with the target protein
Negative reagent control **a. Isotype control** Isotype-specific immunoglobulin at the same concentration as the primary antibody. Control for non-specific interaction of the antibody with the tissue and the detection system. **b. Antibody diluent control** Omitting the primary antibody. Only a control for the detection system beyond the primary antibody.	**Negative tissue control** Tissue known to not express the protein. **Types of negative tissue controls** a. External tissue control b. Internal tissue control c. Cell pellet control: cell line known to not express the target protein/non-transfected cell or knock down of the expression of the target protein Ideally biological controls should be fixed, processed and analyzed in the exact same manner as the test sample.

Table 1. **IHC controls**. An overview over recommended IHC controls. In addition, absorption control/competitive blocking is often used to verify the primary antibody specificity [147,148,151].

used in this study has been shown to lack specificity in our laboratory and no IHC controls were reported in their study, and we believe that conclusions from studies using anti-integrin α11 antibodies should be interpreted with caution if proper controls are not reported.

Controls in paper I and II

For the IHC experiments in **paper I and II**, an isotype control has been used whenever applicable. Internal controls have been used for αSMA and PDGFRβ and a positive tissue control for integrin α11-expressing mouse tissue.

Antibody validation and controls in paper III

In the initial screening of different clones, clones reactive to integrin α11 were included, and clones with cross-reactivity to other proteins of human and mouse origin, especially against other integrins, were excluded [81]. The clones were then investigated by western blotting and immunofluorescence staining of cells.
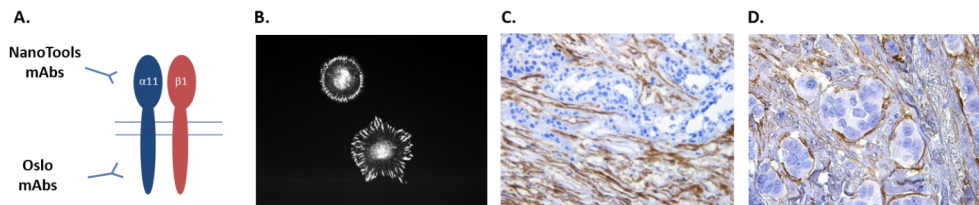
Fig 10. Anti-human integrin α11 antibodies. Monoclonal mouse anti-human integrin α11 antibodies were produced against the extracellular (by NanoTools) and the intracellular (by Oslo University Hospital) domain of the integrin α11 chain (**A**). The antibodies were tested with different methods including western blotting (not shown) and immunostaining of cells and tissue sections. Immunofluorescence staining of C2C12-α11 cells with D120.4 (**B**). Immunostaining of a PDAC cryosection with 203E3 (NanoTools) (**C**) and a FFPE section of invasive breast carcinoma with 210F4B6A4 (NanoTools) (**D**). Own unpublished data.

Reagent controls

A positive reagent control is preferable when testing new antibodies. During the production and characterization of the new monoclonal antibodies, supernatants from numerous hybridomas were screened and tested in different conditions. Although several clones showed the same staining pattern on FFPE material, clone 210F4B6A4 used in **paper III** was clearly superior in this condition, and a positive reagent control was not available for FFPE material.

Another clone, 203E3, has recently been shown to be superior in immunostaining of cryosections [81], and was therefore used as a positive reagent control for immunostaining of cryosections in **paper III** in addition to a previously validated polyclonal antibody [72,75,152].

IgG2b in same concentration as 210F4B6A4 was used as negative reagent control (isotype control).

Biological controls

Since antibodies should be validated in the condition where it is applied, we made different FFPE cell pellets to show the specificity and sensitivity of the antibodies on FFPE material. The following cells were used:

- C2C12-α11 (positive control); mouse myoblast cell line that lacks endogenous collagen-binding integrins overexpressing human integrin α11β1 – to identify clones reactive to human integrin α11.

- C2C12- α2 (negative control); mouse myoblast cell line that lacks endogenous collagen-binding integrins overexpressing human integrin α2β1 – to exclude clones with cross-reactivity to human integrin α2.

- U2OS (positive control); human osteosarcoma cell line expressing low levels of integrin α11. Ideally, biological controls should express the protein of interest in different intensity levels [148]. Since transfected cell lines like the C2C12-α11 tend to display only high expression levels, addition of a low expressing cell line was valuable when calibrating the IHC protocol.

- HEK293 (negative control); human embryonic kidney cell line not expressing human integrin α11 – to identify clones with cross-reactivity against other human integrins/proteins.

Tissue sections were also used when validating the antibodies and calibrating the IHC protocol. As other anti-integrin α11 antibodies only are reliable on cryosections, we used corresponding cryo- and FFPE sections from the same tumors where the polyclonal integrin α11 antibody and 203E3 were used as controls for the cryosections. Unfortunately, we did not have corresponding cryo- and FFPE sections from invasive breast carcinoma, and we therefore used PDAC sections where integrin α11 recently has been shown to be highly expressed [81]. After optimizing the IHC protocol on FFPE sections from cell pellets, PDAC and invasive breast carcinomas, similar expression and intensity levels of integrin α11 staining were seen in corresponding cryo- and FFPE PDAC sections. These sections were then used as positive biological controls.

To conclude, when staining the breast cancer series, the following controls were included in each run:

- Serial sections of one invasive breast carcinoma; one section applied with IgG2b in same concentration as 210F4B6A4 (negative reagent control), another with 210F4B6A4 (positive biological control).
- Positive and negative cell pellet controls (positive and negative biological controls).

The antibody validity was also strengthened by the fact that clones against extracellular (NanoTools clones) and intracellular epitopes (Oslo clones and polyclonal antibody) showed similar results in western blotting and immunostaining. Furthermore, correspondence between mRNA and protein expression provided additional support for antibody specificity and sensitivity.

In our laboratory, several commercial antibodies were shown to lack specificity and were therefore not used in this thesis.

Optimizing the IHC protocol in paper III

The staining protocol was optimized by testing different clones and different retrieval systems, such as microwave oven and pressure cooker with different retrieval buffers, and also enzymatic retrieval. Optimal titration of the primary antibodies was obtained through testing of different concentrations of the antibody.

As demonstrated in **Fig 11**, we were not able to visualize integrin α11 in FFPE material with the use of "standard" antigen retrieval protocols, resulting in false negative results, and high temperature was crucial to unmask the epitope. Extensive testing of different protocols was done to find the most gentle antigen retrieval that was able to unmask the epitope with high sensitivity, but also the final protocol was hard on the tumor tissue, resulting in a high degree of loss of sections. In the breast cancer series used in **paper III**, 25% of the cases were excluded because of insufficient remaining tissue after the antigen retrieval protocol, and these "drop-out" cases were not equally distributed across molecular subtypes of breast cancer. This is of course a clear bias, and efforts were made to reduce the loss of tissue, such as baking of the sections, use of poly-lysine coated glasses and freshly cut sections.
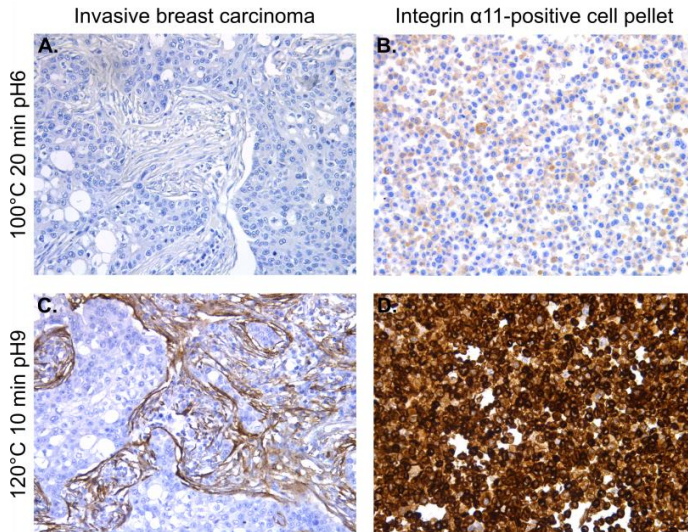
Fig 11. Integrin α11 expression in human invasive breast carcinoma (**A** and **C**) and C2C12- α11 cell pellets (**B** and **D**) by IHC with different antigen retrieval protocols. Note that pressure cooker 120° for 10 min (**C** and **D**) was clearly superior to microwave 20 min (**A** and **B**). Own unpublished data.

Muliplex IHC

When doing multiplex IHC, the antigen retrieval protocol used for integrin α11 single staining was used for the sections to be used in mulitiplex IHC. In advance, serial sections of different invasive breast carcinomas were stained, comparing the expression pattern and intensity of staining obtained by using pressure cooker 120° 10 min pH9 with the standard antigen retrieval protocols for the specific antibodies (αSMA, CK14 and FVIII). This was to ensure that with a different antigen retrieval protocol, similar expression was obtained as with the standard antigen retrieval protocol.

One should be aware that with chromogenic IHC that aims to demonstrate co-localization with the result of a mixture of colours, spectral differentiation of the colour used may be challenging to the visual eye. Therefore, we choose colours that should be easy to define separately, and also contrast well with the mixed colours. However, the colour mixture is

often most visible with even intensity levels of the proteins, and if one of the proteins is more abundant, it will tend to dominate the other colours and it can be difficult to identify the low expressing antigen. However, this is avoided with the use of immunofluorescence staining where you can investigate each antibody reaction in different channels and afterwards merge the colours. We used triple chromogenic IHC with integrin α11, αSMA and FVIII, and concluded that integrin α11 and αSMA co-localized, but not completely. In addition, we also performed double immunofluorescence staining with integrin α11 and αSMA to verify this finding (not shown in **paper III**).

Evaluation of IHC results

There is no consensus on how to best analyze IHC results in research. Intra- and interobserver variability, different scoring methods and systems, and different cut-off values contribute to the challenge in reproducing IHC results.

Manual examination by a pathologist in light microscope is so far the most used method, but digital examination and quantification are now being increasingly used.

Paper I and II

Image J was used to measure the percentage of αSMA, PDGFRβ, collagen III and Sirius red-positive pixels in pictures taken from the tumor periphery (5-6 pictures/tumor) to investigate different expression levels tumors in WT and α11-KO mice, and the average expression level was then calculated for each tumor. The area with highest expression was also quantified (i.e. hot spot method) for all the markers and showed similar results as the average expression level and was not reported in the publications. Alternatively, the whole section could have been scanned for analyses of the whole tumor.

Paper III

Published literature investigating markers of breast CAFs shows a huge variation in the evaluation of IHC staining, which makes it challenging to compare results from different studies. Staining index (SI) was used to quantify the expression of integrin α11 in **paper III**. This is a well-established scoring system in our research group where the observer combines the score of intensity of staining with area stained, resulting in totally seven SI values (SI 0, 1, 2, 3, 4, 6 and 9). The number of severity levels may have an effect on the results; high levels of severities tend to reduce the repeatability, while few levels may reduce the sensitivity of the scoring system [147], therefore it has been suggested that 4-5 levels may be "the optimal number to maximize detection and repeatability" [147] which is in line with the use of SI scoring system used in our group.

Nevertheless, one should have in mind that semi-quantitative, manual scoring systems like SI is subjective and are therefore susceptible to observer variation and may therefore contribute to reduced reproducibility [147,153]. Indeed, consistency in tissue scoring can be difficult to maintain, especially when investigating a large cohort of samples, batches of samples are scored over a prolonged period of time, and also when multiple pathologists score different samples/cohorts [147,153]. Clearly defined scoring systems can reduce the inconsistency to some degree [153]. The SI scoring system has previously shown good intra- and inter observer agreement for other markers [154-156], but the variability of the integrin α11 scoring system used in **paper III** should ideally be examined to investigate if it can be consistently repeated at different times and by other observers.

In **paper III**, we have reported the percentage of fibrous stroma stained for integrin α11 and did not take into consideration the amount of stroma in each tumor. When investigating published literature using IHC to quantify breast CAFs, evaluation of the amount of stained CAFs in relation to the stromal compartment and not in relation to the total tumor area, seems to be the most common method [116,118,122,123,157]. This is in line with our evaluation in **paper III**. Also, quantification of the total amount of stroma compared to

tumor cells in the breast cancer series used in **paper III** is an ongoing project in the group, and will give additional information about the total amount of integrin α11 protein expression in the breast cancer sections, not only percentage of integrin α11-positive fibrotic stroma.

The use of whole tissue sections is time consuming in both the analytical and post-analytical phase, but might give more accurate and reproducible IHC results, especially for markers with excessive intratumor heterogeneity. Since the expression of integrin α11 was indeed markedly heterogeneous (**Fig S3 paper III**), whole tissue sections of breast cancer samples were therefore used in **paper III**. However, sections of invasive breast carcinomas often contain benign-looking and pre-malignant tissue in addition to the invasive cancer cells, and therefore, the evaluation of whole sections can be challenging for non-pathologist since it is crucial to only score the invasive parts of the sections. The scoring in **paper III** was guided by a senior breast cancer pathologist and this issue was therefore avoided.

3.6 RNA datasets

Publicly available gene expression datasets, METABRIC discovery and METABRIC validation cohorts, were investigated for the expression of *ITGA11*. This is mRNA microarray-based gene expression data from invasive breast cancer and includes both mRNA data from the tumor cells and the stromal compartment. While we have reported percentage of fibrous stroma positive for integrin α11 in our protein data, the METABRIC datasets report the amount of integrin α11 mRNA in the sample investigated. Therefore, these datasets are not directly comparable to our SI scoring.

Based on our IHC observations that integrin α11-positivity in invasive breast carcinomas is predominantly expressed in fibroblast-like cells, it is probably acceptable to assume that integrin *ITGA11* expression in the METABRIC datasets, represents integrin α11 positivity in fibroblast-like cells. However, small contribution from myoepithelial remnants could

account for a minority of the integrin α11 mRNA expression seen in the METABRIC datasets.

3.7 Statistical considerations

Both Student's t-test and Mann-Whitney U test were applied on the *in vivo* data in **paper I** and **II**; the Student's t-test was used if the data fulfilled the criteria of normal distribution and, if not, the Mann-Whitney U test was performed.

In **paper III**, the values for integrin α11 SI were dichotomized, and there was no pre-established cut-off value for integrin α11 expression. To avoid bias by multiple testing and therefore over-fitting of the cut-off level to our breast cancer series, the frequency histograms for SI were evaluated prior to statistical analyses. Since the histograms demonstrated a clear binary distribution, the cases in the breast cancer series were dichotomized by this distribution corresponding to a cut-off value at the lower tertile. Pearson's chi-square test was used to compare two categorical variables, Kruskal-Wallis test was used to compare integrin α11 expression across molecular subgroups, and the Kaplan-Meier method was used to analyze survival data with death from breast cancer as end-point and significance determined by the log-rank test.

4. Summary of results

4.1 Paper I

Stromal integrin α11β1 affects RM11 prostate and 4T1 breast xenograft tumors differently

In this paper, we investigated the effect of stromal integrin α11-deficiency on tumor growth, collagen organization and interstitial fluid pressure (PIF) regulation in 4T1 mammary and RM11 prostate murine tumors using SCID mice deficient of integrin α11 (α11-KO mice). We reported reduced RM11 prostate tumor growth in the α11-KO mice compared to wild type (WT), but no effect of integrin α11-deficiency on tumor growth in the 4T1 mammary tumors. Further, lack of integrin α11 lead to a decrease in collagen fibril diameter in the 4T1 tumors. No differences in the amount of activated fibroblasts, collagen content, collagen organization or PIF were found.

4.2 Paper II

Stromal integrin α11-deficiency reduces interstitial fluid pressure and perturbs collagen structure in triple-negative breast xenograft tumors

Here, we investigated the effect of stromal integrin α11-deficiency in triple-negative breast cancer using the human breast cancer cell lines MDA-MB-231 and MDA-MB-468 (orthotopic and ectopic tumors) and SCID α11-KO mice. Integrin α11-deficiency impeded MDA-MB-231 orthotopic tumor growth, and decreased tumor PIF and perturbed collagen structure with fewer aligned and thinner collagen fibrils in both orthotopic models. Despite decreased PIF in the orthotopic MDA-MB-231 tumors in α11-KO mice, integrin α11-deficiency had no effect on tumor uptake of the chemotherapeutic drug ^{3}H-5FU. No effects of integrin α11-deficiency were observed in the ectopic MDA-MB-231 model. Correspondingly, a decrease in PIF was found in spheroids composed of MDA-MB-231

cells and α11-KO fibroblasts compared to spheroids composed of MDA-MB-231 cells and WT fibroblasts.

4.3 Paper III

Integrin α11β1 is expressed in breast cancer stroma and associates with aggressive tumor phenotypes

After testing and validating several new monoclonal antibodies against the human integrin α11 chain, clone 210F4B6A4 was selected as the best for immunostaining of human breast cancer FFPE samples. We observed that integrin α11 was expressed in stromal spindle-shaped, fibroblast-like cells where it co-localized with αSMA. Additionally, integrin α11 was expressed in a subgroup of breast myoepithelium in predominantly premalignant lesions where it co-localized with αSMA and cytokeratin 14. By investigating the immunohistochemical expression of integrin α11 in 392 whole sections of human breast cancer, integrin α11 was found to be expressed in fibroblast-like cells in the stroma in 99% of the cases. Further, strong stromal integrin α11 protein expression (66% of cases) was associated with aggressive breast cancer phenotypes such as high histologic grade, increased tumor cell proliferation (Ki67 and mitotic count), ER negativity, HER2 positivity, and triple-negative phenotype, but was not associated with breast cancer specific survival. Additionally, in the METABRIC discovery and validation cohorts (n=1782), integrin α11 mRNA expression was not found to be associated with breast cancer specific survival.

5. General discussion

Altered integrin expression is often detected in cancer, and in accordance with the essential roles of integrins in various aspects of tissue homeostasis, several integrins have been found to play a role in tumorigenesis [62,63]. In cancers, individual integrins can be expressed on a diversity of cells, commonly both on tumor and stromal cells, and can have different, sometimes even antagonistic functions on each cell type. This makes it difficult to predict the net effect of the individual integrins [63]. Inhibition of integrin function in cancer has been broadly studied the last decades, but unfortunately, only a few clinical trials with anti-integrin therapies have been successful in the treatment of cancer despite promising preclinical studies, underlining the complexity of integrin biology [62,63,68]. Integrin α11β1 is the last member to be identified in the integrin family and thorough investigation of the expression pattern and function in different cell types and in different tissues are necessary to understand the role of integrin α11β1 in pathological conditions such as cancer and fibrosis.

Integrin α11β1 has been linked to collagen organization and tissue contraction and is upregulated during activation of fibroblasts. In the breast TME, fibroblasts represent a diverse cell type which can display both pro- and anti-tumorigenic effects, making a strong rationale for better characterization of CAF heterogeneity. In this setting, integrin α11β1 could represent a functionally important receptor on breast CAFs. We have therefore investigated the role of stromal integrin α11β1 in experimental TNBC (**paper I and II**), and also the expression and potential prognostic impact of integrin α11β1 in human breast cancer (**paper III**) in this thesis.

Integrin α11β1 is expressed in fibroblasts-like cells in the breast TME

We report that integrin α11β1 is mainly expressed in stromal, spindle-shaped cells in implanted TNBC xenografts (**paper II**) and in human invasive breast carcinoma (**paper**

III). Further, integrin α11β1 co-localizes with αSMA, and therefore our data strongly indicate that integrin α11β1 is expressed on breast CAFs both in mouse models and in human breast cancer. This is consistent with other recent studies supporting that integrin α11β1 is mainly restricted to CAFs in breast cancer [142] and also in other tumor types such as pancreas [81], lung [75] and HNSCC [152]. However, by the methods used in **paper II and III**, it is not possible to exclude that at least some of the spindle-shaped cells expressing integrin α11β1 could additionally represent other cell types, such as mesenchymal stem cells, pericytes or cancer cells that have undergone EMT. Therefore, we used the terminology fibroblast-like cells in **paper III**. In future research, it will be of importance to further characterize the fibroblast-like cells positive for integrin α11β1 in the breast TME, and to investigate if these cells are solely CAFs or if integrin α11β1 additionally is expressed on other cell types, although biomarkers that clearly distinguishes these cells types are presently not available [10].

Integrin α11 is expressed on a pro-tumorigenic CAF subset

In **paper II**, stromal integrin α11-deficiency led to reduced MDA-MB-231 tumor growth, and there was a trend towards reduced MDA-MB-468 tumor growth, while no effect on TNBC growth was observed in the 4T1 model in **paper I**. In agreement with the result in **Paper II**, a collaborative group recently demonstrated that stromal integrin α11-deficiency in MMTV-PyMT mice reduced breast cancer growth and metastasis. They also observed that the pro-tumorigenic abilities of integrin α11β1 relied on crosstalk with PDGFRβ and production of tenascin-C [142]. As previously mentioned, integrin α11β1 was found to be expressed on a subset of breast CAFs (**paper II and III**, [142]), and data from pre-clinical models therefore indicate that this CAF subset has pro-tumorigenic abilities in breast cancer, although this has not been consistent in all models so far.

We further demonstrated that integrin α11β1 is associated with aggressive breast cancer features by investigating the immunohistochemical expression of stromal integrin α11 in a

large human breast cancer cohort (**paper III**), which is in line with the aforementioned pre-clinical data. However, high integrin α11 expression was not correlated to breast cancer specific survival either at the protein or mRNA level (**paper III**). Of interest, Primac et al. have demonstrated that high ITGA11 mRNA correlated with poor prognosis in the Kaplan-Meier plotter in human breast cancer [142]. However, they used automatic best cut off value in this article, which is a less robust statistical approach, and with no validation cohorts for this cut-off value. They further demonstrated by IHC that double α11/PDGFRβ positivity was associated with aggressive breast cancer features, and also to metastasis and mortality. Taken together, integrin α11β1 seems to be expressed on a pro-tumorigenic CAF subset, but does not seem to have potential as a prognostic marker alone (no significant effect in our study and possible weak effect in [142]). However, this should be confirmed also in other breast cancer cohorts.

Integrin α11β1 as a new CAF marker

Few markers have been validated to give predictive or prognostic information of value for clinical handling of cancer patients. Although some studies have identified single CAF markers that can predict patient outcome in breast cancer, recent studies indicate that combinations of different markers should probably be used to identify functionally distinct CAF subsets [21,34,35]. Only a few studies up till now have investigated the co-expression pattern of integrin α11 with other CAF markers. Both in human breast cancer (**paper III**), and also in implanted murine TNBC (**paper II**), integrin α11 co-localized with αSMA, but some subsets were only positive for one of the markers. The number of cases investigated was, however, limited. In another breast cancer cohort, integrin α11 strongly associated with PDGFRβ and Tenascin C, which are both expressed on CAFs in human breast cancer [142]. In PyMT tumors, integrin α11 co-localized strongly with PDGFRβ, and surprisingly, poorly with αSMA, PDGFRα, NG2, FAP, and FSP1 [142]. The link between PDGFRβ and integrin α11 described by Primac et al. is indeed intriguing, but unexpectedly, integrin α11-deficiency did not influence the amount of PDGFRβ in the TNBC xenografts in **paper II**.

Noteworthy, the lack of co-expression of integrin α11 with NG2 in breast cancer [142], has also been found in PDAC [81], and indicates that integrin α11 is not expressed on pericytes in those experimental systems.

Fibroblasts with a myofibroblastic phenotype share similar functions in fibrosis and in the TME, and so far αSMA has been the most commonly used myofibroblast marker. However, αSMA is an inconsistent myofibroblast marker in fibrosis [158], and integrin α11β1 has emerged as a new receptor that can identify at least a subset of myofibroblasts in wound healing [78], fibrosis [79,159] and in the TME (**paper II and III**, [75,81,86,142,152]). In the TME, myofibroblastic CAFs (myCAFs) are poorly defined and their function compared to other CAFs is still not fully understood. Surprisingly, seminal papers in the field of CAF heterogeneity have demonstrated that myCAFs expressing high αSMA and located peritumorally seem to be associated with tumor-suppressive functions in PDAC [31-33]. Costa et al. identified two αSMA-positive subsets in human breast cancer, where one of these subsets (CAFS1) showed similar characteristics to myCAFs in PDAC as they expressed both αSMA and FAP and had predominantly peritumoral localization [34]. However, in contrast to myCAFs in PDAC, this CAF subset was demonstrated to be immunosuppressive and a potential candidate for CAF-targeted therapy. Of note, integrin α11 was found to be strongly expressed in the peritumoral area (**paper III**, [142]) and co-localized with αSMA (**paper II and III**), and it would be of high interest to investigate the expression of integrin α11 in relation to the CAF subsets defined by Costa et al. In another study of breast CAF heterogeneity, four different CAF subsets have been identified in late stage of murine PyMT tumors; matrix CAFs, vascular CAFs, cell cycle CAFs and developmental CAFs [21]. Here, αSMA and FAP were expressed in all subsets, and not surprisingly, integrin α11 was mostly expressed in matrix CAFs, but also to some degree in dCAFs and vCAFs (personal communication, Kristian Pietras, Lund University, Sweden). Thus, also among myCAFs the heterogeneity seems so be substantial, not only between PDAC and breast cancer, but also within different breast cancer stages and subtypes.

Given the contrasting reports regarding CAF function in breast cancer, it will be of interest to further explore different functional subtypes of CAFs. First, to investigate if these can be identified by a more detailed characterization by simultaneous staining of integrin α11 with other markers. Second, to investigate the impact of their spatial localization within the tissue sections. With this in mind, inclusion of anti-integrin α11 antibody in multitiplexed immunostaining or imaging mass cytometry will allow simultaneous comparison of the expression of integrin α11 with multiple other CAF markers.

Stromal integrin α11-deficiency reduces interstitial fluid pressure and alters collagen structure

The progressive changes in the TME during tumor development lead to markedly increased PIF in most solid tumors [53,54]. Abnormal blood and lymphatic vessels are well-recognized features and contribute to elevated tumor PIF, but also contractile fibroblasts and a dense ECM have been proposed to modify PIF [50]. Interestingly, in **paper II**, we demonstrated that stromal integrin α11-deficiency decreased PIF in two different implanted TNBC xenografts, suggesting a role for integrin α11β1 in the regulation of breast tumor PIF. In spheroids composed of only fibroblasts and breast cancer cells, we further showed that this effect was mediated, at least partly, by integrin α11-positive fibroblasts. The role of integrin α11β1 in regulation of tumor PIF has later also been demonstrated in implanted murine E0771 breast tumors (Reed/Stuhr et al., in preparation). These results are in agreement with the model for dynamic control of transcapillary fluid flow and PIF proposed by Reed et al. [160]. Here, fibroblasts exert a tension on the collagen network through collagen-binding integrins which limits swelling of underhydrated ECM. Increased fluid flux caused by dysfunctional vasculature may therefore result in increased PIF in solid tumors. In support of this, previous studies have shown that transcapillary fluid flow is dependent on collagen-binding integrins [87,89,90,161-163]. Integrin α11β1 overexpressed in the breast TME may therefore contribute to the regulation of tumor PIF through binding to and promoting contraction of the complex collagen network.

Structural and physical properties of the ECM have been shown to be essential in breast tumorigenesis, where abundance and linearization of fibrillar collagen, and also increased tissue stiffness, promote breast tumor progression and are associated with poor outcome [45,47,49,164]. Integrin α11β1 has been proposed to influence tumor progression through altered regulation and organization of the ECM since ablation of integrin α11 has reduced the amount of collagen and collagen fiber organization [86,142]. We found that integrin α11-deficiency led to thinner (**paper I and II**) and more disorganized (**paper II**) collagen fibrils, and several studies have demonstrated an association between collagen fibril diameter and PIF. Thinner collagen fibrils seem to be linked to a decrease in tumor PIF (**paper II**, [165,166]), while thicker collagen fibrils associate with increased tumor PIF [167,168]. Structural changes in the ECM are likely to influence the fluid transport through the TME and thereby PIF, but further studies are needed to show if there are causative effects of collagen fibril structure on tumor PIF. Of note, other possible roles of integrin α11β1 in the regulation of tumor PIF, such as influence on tumor vasculature, capillary permeability, and lymphatic vessels, are not investigated in this thesis, and could indeed be explored in future studies. Furthermore, collagen fiber structure beyond what we can see from electron microscopy has not been investigated in this thesis.

Increased tumor PIF reduces convection-driven transport of fluid into and within the tumor and can therefore cause insufficient penetration and distribution of anti-neoplastic drugs [169]. However, in **paper II**, reduced tumor PIF by integrin α11-deficiency did not affect the uptake of the low-molecular weight drug, ^{3}H-5FU, into MDA-MB-231 tumors. Of note, measurements of drug uptake with microdialysis can be technically difficult as it can lead to decreased recovery, inflammation, and bleeding. Therefore, it could be of interest to repeat and extend these studies using other methods and other drugs.

Integrin α11 is expressed in a subset of breast myoepithelial cells

Intriguingly, integrin α11 was also found to be expressed in a subset of breast myoepithelium, predominantly in DCIS-associated myoepithelial cells where it co-localized with αSMA and CK14 (**paper III**). Myoepithelial cells, separated from the stroma by the basement membrane, are in normal circumstances not in contact with collagen I, which is the known ligand for integrin α11β1. The expression of integrin α11β1 in myoepithelium is therefore surprising, and one central issue concerns the ligand for integrin α11β1 in breast myoepithelium. Further studies should elucidate if myoepithelial integrin α11β1 binds to components of the basement membrane such as collagen IV. If not, upregulation of integrin α11β1 expression in breast myoepithelium could be an early sign of myoepithelial contact with collagen in the tumor stroma (which would indicate dissociation of the basement membrane). The myoepithelium observed was DCIS-associated myoepithelium or myoepithelium in relation to benign ducts at the border of the breast cancer samples (**paper III)**. In other studies, integrin α11β1 expression seems to be low or absent in normal tissues, including normal breast tissue, although a limited number of sections have been investigated [81,142]. The expression and function of integrin α11β1 in myoepithelium in normal breast tissue, in DCIS and in the transition to invasive breast cancer should indeed be further explored. Of note, engraftment of breast cancer cell lines into mice, which has been performed in **paper I and II**, represents late stage of primary tumor growth. This model bypasses the early stages of breast cancer development where myoepithelium has been shown to play a part and is therefore not optimal for investigation of breast myoepitheilium.

Heterogeneity across different models

Although integrin α11-positive CAFs in experimental breast cancer seem to exert a tumor-promoting function and to contribute to an increased tumor PIF and collagen organization (**paper II**, [142]), such effects of integrin α11β1 have not been found in all pre-clinical

models, and in the 4T1 model (**paper I**) only minor effects of integrin α11-deficiency was seen. As previously mentioned, CAFs seems to display significant heterogeneity across different murine TNBC tumors, and to display temporal heterogeneity during tumor progression, which may lead to different results when studying CAFs in different pre-clinical models. As such, the discrepancies in the pre-clinical studies regarding integrin α11β1 (**paper I and II**, [142]) are most likely linked to differences in methodology, such as different breast cancer cell lines and different species, in addition to breast cancer subtypes and stages. Further studies are therefore needed to elucidate integrin α11β1's role in different breast cancer subtypes and stages using different pre-clinical models.

Furthermore, the effect of genetic ablation of integrins in mouse models has shown conflicting results. For example, integrin αvβ3 has in some, but not all, pre-clinical models been shown to increase tumor PIF and collagen fibril diameter, increase tumor angiogenesis and stimulate tumorigenesis [170,171]. Compensatory mechanisms and overlapping functions are common features for integrins [171]. As recently reported, the effect of integrin α11 inhibition on collagen contraction and CAF migration is greater in the absence of other collagen receptors, and smaller than the effect of inhibition of β1 integrin, indicating that not only other collagen-binding integrins, but also other β1 integrins, partly overlap with integrin α11β1's function [81]. Especially, integrin α11β1 shows functional resemblances to the collagen-binding integrin α2β1 as both integrins are responsible for fibroblast-collagen interactions [65]. However, the role of integrin α2β1 in tumorigenesis has been difficult to dissect because of its wide expression [65]. In breast cancer, integrin α2β1 is actually downregulated and ablation in mice seems to increase breast cancer metastasis [10,172]. With this in mind, studies should aim to not only explore the co-expression and function of integrin α11β1 in relation to other CAF markers, but also in relation to other integrins.

6.   Main conclusions

1: Using integrin α11-KO mice, we found that integrin α11-deficiency lead to reduced tumor PIF with two of three breast cancer cell lines tested. Further, changes in collagen fibril structure were observed in all orthotopic breast cancer models and growth of MDA-MB-231 breast cancer cells was inhibited in α11-KO compared to WT mice. Thus, stromal integrin α11β1 seems to contribute to high tumor PIF, collagen fibril organization and may also stimulate experimental breast cancer growth *in vivo* although this was not consistent in all pre-clinical models.

2: We have established conditions for reproducible and specific staining of integrin α11 in FFPE human tumor material using a new antibody against the integrin α11 subunit.

3: Integrin α11 was found to be expressed in stromal spindle-shaped cells compatible with CAFs in the breast TME. Additionally, integrin α11 was expressed on a subset of breast myoepithelial cells. Further, strong stromal integrin α11 expression was associated with aggressive breast cancer features, but not with breast cancer specific survival.

7. Future perspectives

We and others have over the last decade demonstrated that integrin α11β1 is highly expressed in the breast cancer stroma, and that it seems to be involved in breast tumor PIF regulation, collagen organization and have a promoting role in breast cancer progression. However, many questions remain regarding the role of integrin α11β1 in breast cancer. Further investigation of integrin α11-positive cells in the breast TME should continue in different breast cancer subtypes and stages.

First, integrin α11β1 should be included in studies aiming to further characterize functionally distinct CAF subsets. Second, it will be intriguing to dissect the spindle-shaped cell population positive for integrin α11β1 in the breast TME and to investigate if integrin α11β1 additionally is expressed on other cell types than merely CAFs. With this in mind, investigation of the expression of integrin α11β1 in regard to other markers and their spatial localization will be of importance, and this will be possible by including anti-integrin α11 antibodies in multiplexed IHC or imaging mass cytometry. Our new antibodies against human integrin α11 will also enable cell sorting and thereby closer characterization of integrin α11-expressing cells with for example single cell sequencing. Furthermore, isolation of integrin α11-positive cells and functional studies are necessary to gain further mechanistic insight into the role of integrin α11β1 in breast cancer.

Although integrin α11β1 currently does not seem to have a clear role as a prognostic marker alone based on the results on breast cancer in this thesis, these data should be confirmed in other breast cancer cohorts, and the prognostic value of integrin α11β1 in combination with other markers should be investigated.

In the future, sophisticated mouse models will hopefully be valuable tools used to further investigate integrin α11β1's role in breast cancer. Especially, conditional α11-KO mice, in which the knockout of integrin α11 can be spatially and temporally regulated, would

provide important information of the isolated effect of integrin α11β1 in different cell types and at different times.

Also, further investigation of the mechanism behind how integrin α11β1 contribute to the regulation of tumor PIF is needed, and other models for drug uptake should be performed.

Finally, both *in vitro* and *in vivo* experiments should aim to investigate the function of integrin α11β1 in breast myoepithelium, in addition to careful characterization of the expression of integrin α11β1 in breast myoepithelium in normal and pathological human breast tissue.

8. Source of data

1.   Norwegian Institute of Public Health N. Dødsårsaksregisterets statistikkbank. http://statistikkbank.fhi.no/dar/. Accessed 17.08.20. 2020.
2.   WHO. World Health Organization https://www.who.int/health-topics/cancer Accessed 17.08.20.
3.   Hanahan D, Weinberg RA. Hallmarks of cancer: the next generation. *Cell* 2011; **144**: 646-674.
4.   Hanahan D, Weinberg RA. The hallmarks of cancer. *Cell* 2000; **100**: 57-70.
5.   Maman S, Witz IP. A history of exploring cancer in context. *Nature reviews Cancer* 2018; **18**: 359-376.
6.   Hanahan D, Coussens LM. Accessories to the crime: functions of cells recruited to the tumor microenvironment. *Cancer Cell* 2012; **21**: 309-322.
7.   Valkenburg KC, de Groot AE, Pienta KJ. Targeting the tumour stroma to improve cancer therapy. *Nature reviews Clinical oncology* 2018; **15**: 366-381.
8.   Belli C, Trapani D, Viale G, *et al.* Targeting the microenvironment in solid tumors. *Cancer treatment reviews* 2018; **65**: 22-32.
9.   Hegde PS, Chen DS. Top 10 Challenges in Cancer Immunotherapy. *Immunity* 2020; **52**: 17-35.
10.   Zeltz C, Primac I, Erusappan P, *et al.* Cancer-associated fibroblasts in desmoplastic tumors: emerging role of integrins. *Seminars in cancer biology* 2020; **62**: 166-181.
11.   Arese M, Bussolino F, Pergolizzi M, *et al.* Tumor progression: the neuronal input. *Ann Transl Med* 2018; **6**: 14.
12.   Chen XM, Song EW. Turning foes to friends: targeting cancer-associated fibroblasts. *Nat Rev Drug Discov* 2019; **18**: 99-115.
13.   Barbazan J, Vignjevic DM. Cancer associated fibroblasts: is the force the path to the dark side? *Current opinion in cell biology* 2019; **56**: 71-79.
14.   Sugimoto H, Mundel TM, Kieran MW, *et al.* Identification of fibroblast heterogeneity in the tumor microenvironment. *Cancer Biol Ther* 2006; **5**: 1640-1646.
15.   LeBleu VS, Kalluri R. A peek into cancer-associated fibroblasts: origins, functions and translational impact. *Disease models & mechanisms* 2018; **11**.
16.   Ohlund D, Elyada E, Tuveson D. Fibroblast heterogeneity in the cancer wound. *Journal of Experimental Medicine* 2014; **211**: 1503-1523.
17.   Ziani L, Chouaib S, Thiery J. Alteration of the Antitumor Immune Response by Cancer-Associated Fibroblasts. *Front Immunol* 2018; **9**: 414.
18.   Barth PJ, Ebrahimsade S, Ramaswamy A, *et al.* CD34(+) fibrocytes in invasive ductal carcinoma, ductal carcinoma in situ, and benign breast lesions. *Virchows Arch* 2002; **440**: 298-303.

19. Raz Y, Cohen N, Shani O, *et al.* Bone marrow-derived fibroblasts are a functionally distinct stromal cell population in breast cancer. *The Journal of experimental medicine* 2018; **215**: 3075-3093.

20. Kwa MQ, Herum KM, Brakebusch C. Cancer-associated fibroblasts: how do they contribute to metastasis? *Clinical & experimental metastasis* 2019; **36**: 71-86.

21. Bartoschek M, Oskolkov N, Bocci M, *et al.* Spatially and functionally distinct subclasses of breast cancer-associated fibroblasts revealed by single cell RNA sequencing. *Nature communications* 2018; **9**: 5150.

22. Dvorak HF. Tumors: wounds that do not heal. Similarities between tumor stroma generation and wound healing. *N Engl J Med* 1986; **315**: 1650-1659.

23. Dvorak HF. Tumors: wounds that do not heal-redux. *Cancer Immunol Res* 2015; **3**: 1-11.

24. Zeltz C, Gullberg D. Integrin Alpha11 (ITGA11). In: Encyclopedia of Signaling Molecules. Choi S, (ed)^(eds). Springer New York: New York, NY, 2016; 1-8.

25. Pakshir P, Hinz B. The big five in fibrosis: Macrophages, myofibroblasts, matrix, mechanics, and miscommunication. *Matrix Biol* 2018; **68-69**: 81-93.

26. Darby IA, Zakuan N, Billet F, *et al.* The myofibroblast, a key cell in normal and pathological tissue repair. *Cell Mol Life Sci* 2016; **73**: 1145-1157.

27. Yazdani S, Bansal R, Prakash J. Drug targeting to myofibroblasts: Implications for fibrosis and cancer. *Adv Drug Deliv Rev* 2017; **121**: 101-116.

28. Talior-Volodarsky I, Connelly KA, Arora PD, *et al.* alpha11 integrin stimulates myofibroblast differentiation in diabetic cardiomyopathy. *Cardiovasc Res* 2012; **96**: 265-275.

29. Schulz JN, Plomann M, Sengle G, *et al.* New developments on skin fibrosis - Essential signals emanating from the extracellular matrix for the control of myofibroblasts. *Matrix biology : journal of the International Society for Matrix Biology* 2018; **68-69**: 522-532.

30. Carracedo S, Lu N, Popova SN, *et al.* The fibroblast integrin alpha11beta1 is induced in a mechanosensitive manner involving activin A and regulates myofibroblast differentiation. *The Journal of biological chemistry* 2010; **285**: 10434-10445.

31. Ozdemir BC, Pentcheva-Hoang T, Carstens JL, *et al.* Depletion of carcinoma-associated fibroblasts and fibrosis induces immunosuppression and accelerates pancreas cancer with reduced survival. *Cancer Cell* 2014; **25**: 719-734.

32. Rhim AD, Oberstein PE, Thomas DH, *et al.* Stromal elements act to restrain, rather than support, pancreatic ductal adenocarcinoma. *Cancer Cell* 2014; **25**: 735-747.

33. Ohlund D, Handly-Santana A, Biffi G, *et al.* Distinct populations of inflammatory fibroblasts and myofibroblasts in pancreatic cancer. *The Journal of experimental medicine* 2017; **214**: 579-596.

34. Costa A, Kieffer Y, Scholer-Dahirel A, *et al.* Fibroblast Heterogeneity and Immunosuppressive Environment in Human Breast Cancer. *Cancer Cell* 2018; **33**: 463-479.e410.

35. Su SC, Chen JN, Yao HR, *et al.* CD10(+) GPR77(+) Cancer-Associated Fibroblasts Promote Cancer Formation and Chemoresistance by Sustaining Cancer Stemness. *Cell* 2018; **172**: 841-+.

36. Wagnerand M, Wiig H. Tumor interstitial fluid formation, characterization, and clinical implications. *Frontiers in oncology* 2015; **5**: 12.

37. Walker C, Mojares E, Hernandez AD. Role of Extracellular Matrix in Development and Cancer Progression. *International journal of molecular sciences* 2018; **19**: 31.

38. Mouw JK, Ou G, Weaver VM. Extracellular matrix assembly: a multiscale deconstruction. *Nature reviews Molecular cell biology* 2014; **15**: 771-785.

39. Nissen NI, Karsdal M, Willumsen N. Collagens and Cancer associated fibroblasts in the reactive stroma and its relation to Cancer biology. *J Exp Clin Cancer Res* 2019; **38**: 12.

40. Frantz C, Stewart KM, Weaver VM. The extracellular matrix at a glance. *Journal of cell science* 2010; **123**: 4195-4200.

41. Lu P, Weaver VM, Werb Z. The extracellular matrix: a dynamic niche in cancer progression. *The Journal of cell biology* 2012; **196**: 395-406.

42. Mienaltowski MJ, Birk DE. Structure, physiology, and biochemistry of collagens. *Advances in experimental medicine and biology* 2014; **802**: 5-29.

43. Kaushik S, Pickup MW, Weaver VM. From transformation to metastasis: deconstructing the extracellular matrix in breast cancer. *Cancer Metastasis Rev* 2016; **35**: 655-667.

44. Gaggioli C, Hooper S, Hidalgo-Carcedo C, *et al.* Fibroblast-led collective invasion of carcinoma cells with differing roles for RhoGTPases in leading and following cells. *Nature cell biology* 2007; **9**: 1392-1400.

45. Provenzano PP, Inman DR, Eliceiri KW, *et al.* Collagen density promotes mammary tumor initiation and progression. *BMC medicine* 2008; **6**: 11.

46. Conklin MW, Eickhoff JC, Riching KM, *et al.* Aligned collagen is a prognostic signature for survival in human breast carcinoma. *Am J Pathol* 2011; **178**: 1221-1232.

47. Acerbi I, Cassereau L, Dean I, *et al.* Human breast cancer invasion and aggression correlates with ECM stiffening and immune cell infiltration. *Integrative biology : quantitative biosciences from nano to macro* 2015; **7**: 1120-1134.

48. Hanley CJ, Noble F, Ward M, *et al.* A subset of myofibroblastic cancer-associated fibroblasts regulate collagen fiber elongation, which is prognostic in multiple cancers. *Oncotarget* 2016; **7**: 6159-6174.

49. Levental KR, Yu H, Kass L, *et al.* Matrix crosslinking forces tumor progression by enhancing integrin signaling. *Cell* 2009; **139**: 891-906.

50. Heldin CH, Rubin K, Pietras K, *et al.* High interstitial fluid pressure - an obstacle in cancer therapy. *Nature reviews Cancer* 2004; **4**: 806-813.

51. Reed RK, Rubin K. Transcapillary exchange: role and importance of the interstitial fluid pressure and the extracellular matrix. *Cardiovasc Res* 2010; **87**: 211-217.

52. Wiig H, Swartz MA. Interstitial fluid and lymph formation and transport: physiological regulation and roles in inflammation and cancer. *Physiol Rev* 2012; **92**: 1005-1060.

53. Stylianopoulos T, Munn LL, Jain RK. Reengineering the Physical Microenvironment of Tumors to Improve Drug Delivery and Efficacy: From Mathematical Modeling to Bench to Bedside. *Trends in cancer* 2018; **4**: 292-319.

54. Samatov TR, Galatenko VV, Block A*, et al.* Novel biomarkers in cancer: The whole is greater than the sum of its parts. *Seminars in cancer biology* 2017; **45**: 50-57.

55. Salnikov AV, Iversen VV, Koisti M*, et al.* Lowering of tumor interstitial fluid pressure specifically augments efficacy of chemotherapy. *Faseb j* 2003; **17**: 1756-1758.

56. Rubin K, Sjoquist M, Gustafsson AM*, et al.* Lowering of tumoral interstitial fluid pressure by prostaglandin E(1) is paralleled by an increased uptake of (51)Cr-EDTA. *Int J Cancer* 2000; **86**: 636-643.

57. Stuhr LE, Salnikov AV, Iversen VV*, et al.* High-dose, short-term, anti-inflammatory treatment with dexamethasone reduces growth and augments the effects of 5-fluorouracil on dimethyl-alpha-benzanthracene-induced mammary tumors in rats. *Scand J Clin Lab Invest* 2006; **66**: 477-486.

58. Pietras K, Ostman A, Sjoquist M*, et al.* Inhibition of platelet-derived growth factor receptors reduces interstitial hypertension and increases transcapillary transport in tumors. *Cancer research* 2001; **61**: 2929-2934.

59. Jevne C, Moen I, Salvesen G*, et al.* A reduction in the interstitial fluid pressure per se, does not enhance the uptake of the small molecule weigh compound 5-fluoruracil into 4T1 mammary tumors. *Drugs and therapy studies* 2011; **1**: e5.

60. Moen I, Tronstad KJ, Kolmannskog O*, et al.* Hyperoxia increases the uptake of 5-fluorouracil in mammary tumors independently of changes in interstitial fluid pressure and tumor stroma. *BMC cancer* 2009; **9**: 446.

61. Barczyk M, Carracedo S, Gullberg D. Integrins. *Cell and tissue research* 2010; **339**: 269-280.

62. Hamidi H, Pietila M, Ivaska J. The complexity of integrins in cancer and new scopes for therapeutic targeting. *British journal of cancer* 2016; **115**: 1017-1023.

63. Hamidi H, Ivaska J. Every step of the way: integrins in cancer progression and metastasis. *Nat Rev Cancer* 2018; **18**: 532-547.

64. Kechagia JZ, Ivaska J, Roca-Cusachs P. Integrins as biomechanical sensors of the microenvironment. *Nature reviews Molecular cell biology* 2019; **20**: 457-473.

65. Zeltz C, Gullberg D. The integrin-collagen connection--a glue for tissue repair? *Journal of cell science* 2016; **129**: 653-664.

66. Mas-Moruno C, Rechenmacher F, Kessler H. Cilengitide: the first anti-angiogenic small molecule drug candidate design, synthesis and clinical evaluation. *Anticancer Agents Med Chem* 2010; **10**: 753-768.

67. Kim C, Ye F, Ginsberg MH. Regulation of integrin activation. *Annu Rev Cell Dev Biol* 2011; **27**: 321-345.

68. Raab-Westphal S, Marshall JF, Goodman SL. Integrins as Therapeutic Targets: Successes and Cancers. *Cancers (Basel)* 2017; **9**.

69. Desgrosellier JS, Cheresh DA. Integrins in cancer: biological implications and therapeutic opportunities. *Nature reviews Cancer* 2010; **10**: 9-22.

70. Tiger CF, Fougerousse F, Grundstrom G*, et al.* alpha11beta1 integrin is a receptor for interstitial collagens involved in cell migration and collagen reorganization on mesenchymal nonmuscle cells. *Developmental biology* 2001; **237**: 116-129.

71. Popova SN, Rodriguez-Sanchez B, Liden A*, et al.* The mesenchymal alpha11beta1 integrin attenuates PDGF-BB-stimulated chemotaxis of embryonic fibroblasts on collagens. *Developmental biology* 2004; **270**: 427-442.

72. Velling T, Kusche-Gullberg M, Sejersen T*, et al.* cDNA cloning and chromosomal localization of human alpha(11) integrin. A collagen-binding, I domain-containing, beta(1)-associated integrin alpha-chain present in muscle tissues. *The Journal of biological chemistry* 1999; **274**: 25735-25742.

73. Shen B, Vardy K, Hughes P*, et al.* Integrin alpha11 is an Osteolectin receptor and is required for the maintenance of adult skeletal bone mass. *eLife* 2019; **8**: 31.

74. Wang KK, Liu N, Radulovich N*, et al.* Novel candidate tumor marker genes for lung adenocarcinoma. *Oncogene* 2002; **21**: 7598-7604.

75. Zhu CQ, Popova SN, Brown ER*, et al.* Integrin alpha 11 regulates IGF2 expression in fibroblasts to enhance tumorigenicity of human non-small-cell lung cancer cells. *Proceedings of the National Academy of Sciences of the United States of America* 2007; **104**: 11754-11759.

76. Navab R, Strumpf D, Bandarchi B*, et al.* Prognostic gene-expression signature of carcinoma-associated fibroblasts in non-small cell lung cancer. *Proceedings of the National Academy of Sciences of the United States of America* 2011; **108**: 7160-7165.

77. Costea DE, Hills A, Osman AH*, et al.* Identification of two distinct carcinoma-associated fibroblast subtypes with differential tumor-promoting abilities in oral squamous cell carcinoma. *Cancer research* 2013; **73**: 3888-3901.

78. Schulz JN, Zeltz C, Sorensen IW*, et al.* Reduced Granulation Tissue and Wound Strength in the Absence of alpha11beta1 Integrin. *The Journal of investigative dermatology* 2015.

79. Civitarese RA, Talior-Volodarsky I, Desjardins JF*, et al.* The alpha 11 integrin mediates fibroblast-extracellular matrix-cardiomyocyte interactions in health and disease. *Am J Physiol-Heart Circul Physiol* 2016; **311**: H96-H106.

80. Romaine A, Sorensen IW, Zeltz C*, et al.* Overexpression of integrin alpha 11 induces cardiac fibrosis in mice. *Acta Physiologica* 2018; **222**.

81. Zeltz C, Alam J, Liu H*, et al.* alpha11beta1 Integrin is Induced in a Subset of Cancer-Associated Fibroblasts in Desmoplastic Tumor Stroma and Mediates In Vitro Cell Migration. *Cancers (Basel)* 2019; **11**.

82. Zeltz C, Lu N, Gullberg D. Integrin alpha11beta1: A Major Collagen Receptor on Fibroblastic Cells. *Advances in experimental medicine and biology* 2014; **819**: 73-83.

83. Popova SN, Barczyk M, Tiger CF, *et al.* Alpha11 beta1 integrin-dependent regulation of periodontal ligament function in the erupting mouse incisor. *Molecular and cellular biology* 2007; **27**: 4306-4316.

84. Blumbach K, Niehoff A, Belgardt BF, *et al.* Dwarfism in mice lacking collagen-binding integrins alpha2beta1 and alpha11beta1 is caused by severely diminished IGF-1 levels. *The Journal of biological chemistry* 2012; **287**: 6431-6440.

85. Talior-Volodarsky I, Arora PD, Wang Y, *et al.* Glycated collagen induces alpha11 integrin expression through TGF-beta2 and Smad3. *Journal of cellular physiology* 2014.

86. Navab R, Strumpf D, To C, *et al.* Integrin alpha11beta1 regulates cancer stromal stiffness and promotes tumorigenicity and metastasis in non-small cell lung cancer. *Oncogene* 2016; **35**: 1899-1908.

87. Lu N, Karlsen TV, Reed RK, *et al.* Fibroblast alpha11beta1 Integrin Regulates Tensional Homeostasis in Fibroblast/A549 Carcinoma Heterospheroids. *PloS one* 2014; **9**: e103173.

88. Zeltz C, Pasko E, Cox TR, *et al.* LOXL1 Is Regulated by Integrin α11 and Promotes Non-Small Cell Lung Cancer Tumorigenicity. *Cancers* 2019; **11**: 705.

89. Svendsen OS, Barczyk MM, Popova SN, *et al.* The alpha11beta1 integrin has a mechanistic role in control of interstitial fluid pressure and edema formation in inflammation. *Arteriosclerosis, thrombosis, and vascular biology* 2009; **29**: 1864-1870.

90. Liden A, Karlsen TV, Guss B, *et al.* Integrin alphaV beta3 can substitute for collagen-binding beta1 -integrins in vivo to maintain a homeostatic interstitial fluid pressure. *Exp Physiol* 2018.

91. Norway CRo. Cancer in Norway 2018 - Cancer incidence, mortality, survival and prevalence in Norway. 2019.

92. Tang Y, Wang Y, Kiani MF, *et al.* Classification, Treatment Strategy, and Associated Drug Resistance in Breast Cancer. *Clinical breast cancer* 2016; **16**: 335-343.

93. Rakha EA, Green AR. Molecular classification of breast cancer: what the pathologist needs to know. *Pathology* 2017; **49**: 111-119.

94. Goldhirsch A, Winer EP, Coates AS, *et al.* Personalizing the treatment of women with early breast cancer: highlights of the St Gallen International Expert Consensus on the Primary Therapy of Early Breast Cancer 2013. *Ann Oncol* 2013; **24**: 2206-2223.

95. Harbeck N, Gnant M. Breast cancer. *Lancet (London, England)* 2017; **389**: 1134-1150.

96. Board WCoTE. Breast Tumours. ed). World Health Organization, 2019 5th edition.

97. Dahlstrom JE, Rakha EA, Lakhani SR, *et al.* Current topics in breast pathology: expert perspectives. *Pathology* 2017; **49**: 109-110.

98. Perou CM, Sorlie T, Eisen MB, *et al.* Molecular portraits of human breast tumours. *Nature* 2000; **406**: 747-752.

99. Sorlie T, Perou CM, Tibshirani R, *et al.* Gene expression patterns of breast carcinomas distinguish tumor subclasses with clinical implications. *Proceedings of the National Academy of Sciences of the United States of America* 2001; **98**: 10869-10874.

100. Parker JS, Mullins M, Cheang MCU, *et al.* Supervised Risk Predictor of Breast Cancer Based on Intrinsic Subtypes. *J Clin Oncol* 2009; **27**: 1160-1167.

101. Sorlie T, Tibshirani R, Parker J, *et al.* Repeated observation of breast tumor subtypes in independent gene expression data sets. *Proceedings of the National Academy of Sciences of the United States of America* 2003; **100**: 8418-8423.

102. Denkert C, Liedtke C, Tutt A, *et al.* Molecular alterations in triple-negative breast cancer-the road to new treatment strategies. *Lancet (London, England)* 2017; **389**: 2430-2442.

103. Hwang SY, Park S, Kwon Y. Recent therapeutic trends and promising targets in triple negative breast cancer. *Pharmacology & therapeutics* 2019; **199**: 30-57.

104. Dent R, Trudeau M, Pritchard KI, *et al.* Triple-negative breast cancer: clinical features and patterns of recurrence. *Clinical cancer research : an official journal of the American Association for Cancer Research* 2007; **13**: 4429-4434.

105. Lehmann BD, Bauer JA, Chen X, *et al.* Identification of human triple-negative breast cancer subtypes and preclinical models for selection of targeted therapies. *The Journal of clinical investigation* 2011; **121**: 2750-2767.

106. Lehmann BD, Jovanović B, Chen X, *et al.* Refinement of Triple-Negative Breast Cancer Molecular Subtypes: Implications for Neoadjuvant Chemotherapy Selection. *PloS one* 2016; **11**: e0157368.

107. Helsedirektoratet. Nasjonalt handlingsprogram med retningslinjer for diagnostikk, behandling og oppfølging av pasienter med brystkreft1Nasjonalt handlingsprogram med retningslinjer for diagnostikk, behandling ogoppfølging av pasienter medbrystkreft. 05/2020.

108. Soysal SD, Tzankov A, Muenst SE. Role of the Tumor Microenvironment in Breast Cancer. *Pathobiology* 2015; **82**: 142-152.

109. Mittal S, Brown NJ, Holen I. The breast tumor microenvironment: role in cancer development, progression and response to therapy. *Expert Rev Mol Diagn* 2018; **18**: 227-243.

110. Farmer P, Bonnefoi H, Anderle P, *et al.* A stroma-related gene signature predicts resistance to neoadjuvant chemotherapy in breast cancer. *Nature medicine* 2009; **15**: 68-74.

111. Winslow S, Leandersson K, Edsjo A, *et al.* Prognostic stromal gene signatures in breast cancer. *Breast cancer research : BCR* 2015; **17**: 23.

112. Finak G, Bertos N, Pepin F, *et al.* Stromal gene expression predicts clinical outcome in breast cancer. *Nature medicine* 2008; **14**: 518-527.

113. Houthuijzen JM, Jonkers J. Cancer-associated fibroblasts as key regulators of the breast cancer tumor microenvironment. *Cancer Metastasis Rev* 2018; **37**: 577-597.

114. Yazhou C, Wenlv S, Weidong Z, *et al.* Clinicopathological significance of stromal myofibroblasts in invasive ductal carcinoma of the breast. *Tumour biology : the*

journal of the International Society for Oncodevelopmental Biology and Medicine 2004; **25**: 290-295.

115.   Sappino AP, Skalli O, Jackson B*, et al.* Smooth-muscle differentiation in stromal cells of malignant and non-malignant breast tissues. *Int J Cancer* 1988; **41**: 707-712.

116.   Surowiak P, Murawa D, Materna V*, et al.* Occurence of stromal myofibroblasts in the invasive ductal breast cancer tissue is an unfavourable prognostic factor. *Anticancer research* 2007; **27**: 2917-2924.

117.   Toullec A, Gerald D, Despouy G*, et al.* Oxidative stress promotes myofibroblast differentiation and tumour spreading. *EMBO Mol Med* 2010; **2**: 211-230.

118.   Catteau X, Simon P, Noel JC. Myofibroblastic stromal reaction and lymph node status in invasive breast carcinoma: possible role of the TGF-beta1/TGF-betaR1 pathway. *BMC cancer* 2014; **14**: 499.

119.   Yamashita M, Ogawa T, Zhang X*, et al.* Role of stromal myofibroblasts in invasive breast cancer: stromal expression of alpha-smooth muscle actin correlates with worse clinical outcome. *Breast cancer (Tokyo, Japan)* 2012; **19**: 170-176.

120.   Amornsupak K, Jamjuntra P, Warnnissorn M*, et al.* High ASMA(+) Fibroblasts and Low Cytoplasmic HMGB1(+) Breast Cancer Cells Predict Poor Prognosis. *Clinical breast cancer* 2017; **17**: 441-452.e442.

121.   Pereira BA, Vennin C, Papanicolaou M*, et al.* CAF Subpopulations: A New Reservoir of Stromal Targets in Pancreatic Cancer. *Trends in cancer* 2019; **5**: 724-741.

122.   Paulsson J, Ryden L, Strell C*, et al.* High expression of stromal PDGFRbeta is associated with reduced benefit of tamoxifen in breast cancer. *The journal of pathology Clinical research* 2017; **3**: 38-43.

123.   Paulsson J, Sjoblom T, Micke P*, et al.* Prognostic significance of stromal platelet-derived growth factor beta-receptor expression in human breast cancer. *Am J Pathol* 2009; **175**: 334-341.

124.   Pure E, Blomberg R. Pro-tumorigenic roles of fibroblast activation protein in cancer: back to the basics. *Oncogene* 2018; **37**: 4343-4357.

125.   Marra A, Viale G, Curigliano G. Recent advances in triple negative breast cancer: the immunotherapy era. *BMC medicine* 2019; **17**: 90.

126.   Gruosso T, Gigoux M, Manem VSK*, et al.* Spatially distinct tumor immune microenvironments stratify triple-negative breast cancers. *The Journal of clinical investigation* 2019; **129**: 1785-1800.

127.   Adriance MC, Inman JL, Petersen OW*, et al.* Myoepithelial cells: good fences make good neighbors. *Breast Cancer Research* 2005; **7**: 190-197.

128.   Moumen M, Chiche A, Cagnet S*, et al.* The mammary myoepithelial cell. *Int J Dev Biol* 2011; **55**: 763-771.

129.   Russell TD, Jindal S, Agunbiade S*, et al.* Myoepithelial cell differentiation markers in ductal carcinoma in situ progression. *Am J Pathol* 2015; **185**: 3076-3089.

130. Rakha EA, Miligy IM, Gorringe KL*, et al.* Invasion in breast lesions: the role of the epithelial-stroma barrier. *Histopathology* 2018; **72**: 1075-1083.

131. Sirka OK, Shamir ER, Ewald AJ. Myoepithelial cells are a dynamic barrier to epithelial dissemination. *The Journal of cell biology* 2018; **217**: 3368-3381.

132. Mardekian SK, Bombonati A, Palazzo JP. Ductal carcinoma in situ of the breast: the importance of morphologic and molecular interactions. *Human pathology* 2016; **49**: 114-123.

133. Bonnans C, Chou J, Werb Z. Remodelling the extracellular matrix in development and disease. *Nature reviews Molecular cell biology* 2014; **15**: 786-801.

134. Holen I, Speirs V, Morrissey B*, et al.* In vivo models in breast cancer research: progress, challenges and future directions. *Disease models & mechanisms* 2017; **10**: 359-371.

135. Frese KK, Tuveson DA. Maximizing mouse cancer models. *Nature reviews Cancer* 2007; **7**: 645-658.

136. Manning HC, Buck JR, Cook RS. Mouse Models of Breast Cancer: Platforms for Discovering Precision Imaging Diagnostics and Future Cancer Medicine. *Journal of nuclear medicine : official publication, Society of Nuclear Medicine* 2016; **57 Suppl 1**: 60s-68s.

137. Bosma MJ, Carroll AM. THE SCID MOUSE MUTANT - DEFINITION, CHARACTERIZATION, AND POTENTIAL USES. *Annual Review of Immunology* 1991; **9**: 323-350.

138. Gengenbacher N, Singhal M, Augustin HG. Preclinical mouse solid tumour models: status quo, challenges and perspectives. *Nature reviews Cancer* 2017; **17**: 751-765.

139. Ingthorsson S, Briem E, Bergthorsson JT*, et al.* Epithelial Plasticity During Human Breast Morphogenesis and Cancer Progression. *J Mammary Gland Biol Neoplasia* 2016; **21**: 139-148.

140. Tratar UL, Horvat S, Cemazar M. Transgenic Mouse Models in Cancer Research. *Frontiers in oncology* 2018; **8**: 18.

141. Roswall P, Pietras K. Of mice and men: a comparative study of cancer-associated fibroblasts in mammary carcinoma. *Upsala journal of medical sciences* 2012; **117**: 196-201.

142. Primac I, Maquoi E, Blacher S*, et al.* Stromal integrin alpha11 regulates PDGFR-beta signaling and promotes breast cancer progression. *The Journal of clinical investigation* 2019; **130**: 4609-4628.

143. Venning F, Zornhagen K, Wullkopf L*, et al.* Deciphering the temporal heterogeneity of cancer-associated fibroblast subpopulations in breast cancer. *bioRxivpreprint* 2020.

144. Junqueira LC, Bignolas G, Brentani RR. Picrosirius staining plus polarization microscopy, a specific method for collagen detection in tissue sections. *The Histochemical journal* 1979; **11**: 447-455.

145. Lattouf R, Younes R, Lutomski D*, et al.* Picrosirius red staining: a useful tool to appraise collagen networks in normal and pathological tissues. *The journal of*

histochemistry and cytochemistry : official journal of the Histochemistry Society 2014; **62**: 751-758.

146. Ramos-Vara JA, Miller MA. When tissue antigens and antibodies get along: revisiting the technical aspects of immunohistochemistry--the red, brown, and blue technique. *Vet Pathol* 2014; **51**: 42-87.

147. Meyerholz DK, Beck AP. Principles and approaches for reproducible scoring of tissue stains in research. *Lab Invest* 2018; **98**: 844-855.

148. Hewitt SM, Baskin DG, Frevert CW*, et al.* Controls for immunohistochemistry: the Histochemical Society's standards of practice for validation of immunohistochemical assays. *The journal of histochemistry and cytochemistry : official journal of the Histochemistry Society* 2014; **62**: 693-697.

149. Yaziji H, Barry T. Diagnostic Immunohistochemistry: what can go wrong? *Adv Anat Pathol* 2006; **13**: 238-246.

150. Pan Y, Liu G, Yuan Y*, et al.* Analysis of differential gene expression profile identifies novel biomarkers for breast cancer. *Oncotarget* 2017; **8**: 114613-114625.

151. Torlakovic EE, Nielsen S, Vyberg M*, et al.* Getting controls under control: the time is now for immunohistochemistry. *Journal of clinical pathology* 2015; **68**: 879-882.

152. Parajuli H, Teh MT, Abrahamsen S*, et al.* Integrin alpha11 is overexpressed by tumour stroma of head and neck squamous cell carcinoma and correlates positively with alpha smooth muscle actin expression. *Journal of oral pathology & medicine : official publication of the International Association of Oral Pathologists and the American Academy of Oral Pathology* 2017; **46**: 267-275.

153. La Perle KMD. Comparative Pathologists: Ultimate Control Freaks Seeking Validation! *Vet Pathol* 2019; **56**: 19-23.

154. Collett K, Stefansson IM, Eide J*, et al.* A basal epithelial phenotype is more frequent in interval breast cancers compared with screen detected tumors. *Cancer Epidemiology Biomarkers & Prevention* 2005; **14**: 1108-1112.

155. Collett K, Eide GE, Arnes J*, et al.* Expression of enhancer of zeste homologue 2 is significantly associated with increased tumor cell proliferation and is a marker of aggressive breast cancer. *Clin Cancer Res* 2006; **12**: 1168-1174.

156. Bachmann IM, Halvorsen OJ, Collett K*, et al.* EZH2 expression is associated with high proliferation rate and aggressive tumor subgroups in cutaneous melanoma and cancers of the endometrium, prostate, and breast. *J Clin Oncol* 2006; **24**: 268-273.

157. Yang Z, Ni W, Cui C*, et al.* Tenascin C is a prognostic determinant and potential cancer-associated fibroblasts marker for breast ductal carcinoma. *Experimental and molecular pathology* 2017; **102**: 262-267.

158. Sun KH, Chang Y, Reed NI*, et al.* alpha-Smooth muscle actin is an inconsistent marker of fibroblasts responsible for force-dependent TGFbeta activation or collagen production across multiple models of organ fibrosis. *Am J Physiol Lung Cell Mol Physiol* 2016; **310**: L824-836.

159. Martin K, Pritchett J, Llewellyn J*, et al.* PAK proteins and YAP-1 signalling downstream of integrin beta-1 in myofibroblasts promote liver fibrosis. *Nature communications* 2016; **7**: 12502.

160. Reed RK, Liden A, Rubin K. Edema and fluid dynamics in connective tissue remodelling. *Journal of molecular and cellular cardiology* 2010; **48**: 518-523.

161. Reed RK, Rubin K, Wiig H*, et al.* Blockade of beta 1-integrins in skin causes edema through lowering of interstitial fluid pressure. *Circulation research* 1992; **71**: 978-983.

162. Reed RK, Berg A, Gjerde EA*, et al.* Control of interstitial fluid pressure: role of beta1-integrins. *Semin Nephrol* 2001; **21**: 222-230.

163. Wiig H, Rubin K, Reed RK. New and active role of the interstitium in control of interstitial fluid pressure: potential therapeutic consequences. *Acta Anaesthesiol Scand* 2003; **47**: 111-121.

164. Piersma B, Hayward MK, Weaver VM. Fibrosis and cancer: A strained relationship. *Biochim Biophys Acta Rev Cancer* 2020; **1873**: 188356.

165. Olof Olsson P, Gustafsson R, Salnikov AV*, et al.* Inhibition of integrin alphaVbeta6 changes fibril thickness of stromal collagen in experimental carcinomas. *Cell communication and signaling : CCS* 2018; **16**: 36.

166. Olsson PO, Gustafsson R, In 't Zandt R*, et al.* The Tyrosine Kinase Inhibitor Imatinib Augments Extracellular Fluid Exchange and Reduces Average Collagen Fibril Diameter in Experimental Carcinoma. *Molecular cancer therapeutics* 2016; **15**: 2455-2464.

167. Reigstad I, Sortland K, Skogstrand T*, et al.* The Effect of Stromal Integrin beta 3-Deficiency on Two Different Tumors in Mice. *Cancers* 2016; **8**: 14.

168. Friman T, Gustafsson R, Stuhr LB*, et al.* Increased fibrosis and interstitial fluid pressure in two different types of syngeneic murine carcinoma grown in integrin beta3-subunit deficient mice. *PloS one* 2012; **7**: e34082.

169. Bockelmann LC, Schumacher U. Targeting tumor interstitial fluid pressure: will it yield novel successful therapies for solid tumors? *Expert opinion on therapeutic targets*: 10.

170. Reigstad I, Sortland K, Skogstrand T*, et al.* The Effect of Stromal Integrin β3-Deficiency on Two Different Tumors in Mice. *Cancers (Basel)* 2016; **8**.

171. Alday-Parejo B, Stupp R, Rüegg C. Are Integrins Still Practicable Targets for Anti-Cancer Therapy? *Cancers (Basel)* 2019; **11**.

172. Ramirez NE, Zhang Z, Madamanchi A*, et al.* The $\alpha_2\beta_1$ integrin is a metastasis suppressor in mouse models and human cancer. *The Journal of clinical investigation* 2011; **121**: 226-237.

RESEARCH ARTICLE

Stromal Integrin α11β1 Affects RM11 Prostate and 4T1 Breast Xenograft Tumors Differently

Inga Reigstad[1,2]☯ *, Hilde Y. H. Smeland[1,3]☯, Trude Skogstrand[1,2], Kristina Sortland[1,2], Marei Caroline Schmid[1,3], Rolf K. Reed[1,3], Linda Stuhr[1]

1 Department of Biomedicine, University of Bergen, Bergen, Norway, **2** Matrix biology group, Haukeland University Hospital, Bergen, Norway, **3** Center of Cancer Biomarkers, University of Bergen, Bergen, Norway

☯ These authors contributed equally to this work.
* inga.reigstad@uib.no

Competing Interests: The authors have declared that no competing interests exist.

Abstract

Purpose

It has been implied that the collagen binding integrin α11β1 plays a role in carcinogenesis. As still relatively little is known about how the stromal integrin α11β1 affects different aspects of tumor development, we wanted to examine the direct effects on primary tumor growth, fibrosis, tumor interstitial fluid pressure (PIF) and metastasis in murine 4T1 mammary and RM11 prostate tumors, using an *in vivo* SCID integrin α11-deficient mouse model.

Methods

Tumor growth was measured using a caliper, PIF by the wick-in-needle technique, activated fibroblasts by α-SMA immunofluorescence staining and fibrosis by transmission electron microscopy and picrosirius-red staining. Metastases were evaluated using hematoxylin and eosin stained sections.

Results

RM11 tumor growth was significantly reduced in the SCID integrin α11-deficient (α11-KO) compared to in SCID integrin α11 wild type (WT) mice, whereas there was no similar effect in the 4T1 tumor model. The 4T1 model demonstrated an alteration in collagen fibril diameter in the integrin α11-KO mice compared to WT, which was not found in the RM11 model. There were no significant differences in the amount of activated fibroblasts, total collagen content, collagen organization or PIF in the tumors in integrin α11-deficient mice compared to WT mice. There was also no difference in lung metastases between the two groups.

Conclusion

Deficiency of stromal integrin α11β1 showed different effects on tumor growth and collagen fibril diameter depending on tumor type, but no effect on tumor PIF or development of lung metastasis.

Introduction

Carcinomas consist of both malignant cells and stroma, the latter being composed of extracellular matrix (ECM) molecules and associated cells [1]. The main focus of cancer research has traditionally been on tumor cell alterations, but in the last decade ECM has been identified as an important contributor to tumor development and progression [2, 3]. Tumor cells release growth factors and proteolytic enzymes that modulate the stroma [4, 5], and the stromal components interact with the tumor cells in a reciprocal manner to regulate different aspects of tumor development [1].

Integrins belong to a family of major cell surface receptors that mainly bind ECM proteins. Twenty-four different integrins, forming heterodimers by combining 18 α- and 8 β-subunits, have been identified. The integrins mediate cell-cell and cell-matrix adhesion and are capable of cell inside-out and outside-in signaling [6, 7]. Their role on the surface of tumor cells has been extensively studied, and integrins contribute to proliferation, migration and survival of malignant cells, and have thus been suggested to play an important role in tumor progression [8]. Altered integrin expression in several stromal cells, including the cancer associated fibroblasts, may also influence tumor growth and progression [8–10], and the present study focuses on the effect of the collagen binding integrin α11β1 in the tumor stroma.

The integrin subunit α11 forms a heterodimer with integrin subunit β1 and is one of four collagen-binding integrins [11]. In mouse embryos, integrin α11β1 is a major collagen receptor on a subset of fibroblasts [12], but characterization of its expression in adult and human tissue is still insufficient [13]. Integrin α11β1 has high affinity for collagen type I, and has been indicated to be involved in cell migration and collagen reorganization [10, 14, 15], but other than this, there is limited knowledge about α11β1's normal physiological role.

Integrin α11 has also been implicated to play a role in carcinogenesis. Integrin α11 is expressed in metastases from human malignant melanoma [16], and in stromal fibroblasts in human non-small-cell lung cancer (NSCLC) [9, 17]. It has also been shown, both *in vitro* and *in vivo*, that α11 integrin expressed on fibroblasts may stimulate the growth of tumor cells [9, 10, 18]. Earlier findings have indicated that stromal integrin α11 has a role in both primary tumor growth and in the metastatic process [9, 10], and this has raised the question if integrin α11 could be used as a biomarker, or if targeting integrin α11 could prove to be a novel approach in cancer treatment.

Since still relatively little is known about how the stromal integrin α11β1 in tumors affects different aspects of tumor development, we decided to examine the direct effects of integrin α11β1 on primary tumor growth, fibrosis, tumor interstitial fluid pressure and metastasis in a 4T1 mammary tumor- and a RM11 prostate tumor model.

Methods

Cell Lines

The murine mammary carcinoma cell line 4T1 was obtained from the American Type Culture Collection (Manassas, VA., USA). The prostate cell line RM11 was a gift from Associate professor Thomas S. Griffith (University of Minnesota, Minneapolis, MN., USA). This cell line was originally derived from a ras/myc reconstituted tumor in a Balb/c mouse [19]. The cells were grown in RPMI-1640 medium (HEPES solution for RM11 cells) supplemented with 10% Foetal Bovine Serum (Sigma-Aldrich, Steinheim, Germany), 100 units/ml penicillin, 100 μg/ml streptomycin, 1–2% L-glutamine (all from Sigma-Aldrich, Steinheim, Germany), with an addition of 1% sodium pyruvate for the RM11 cells. All cells were grown as single monolayers in a humidified incubator at 37°C in 5% CO_2 and they were seeded and used at log phase in all

experiments. SV40 transformed wild type MEF cell line [12] was cultured in DMEM (Sigma-Aldrich, Steinheim, Germany), 10% Foetal Bovine Serum and 100 units/ml penicillin, 100 μg/ml streptomycin as previosly described.

Animal Model

The integrin α11-deficient heterozygous SCID mouse strain was generated as described [10]. The mice were bred heterozygously, and SCID integrin α11 wild type (WT) and SCID integrin α11-deficient (α11-KO) offsprings were used in the experiments. PCR-genotyping was performed on DNA extracted from ear biopsies as previously described [20]. Female mice were used for the mammary 4T1 tumor model and male mice for the prostate RM11 tumor model. The animals were kept in individually ventilated cages and cared for regularly. Efforts were made to age- and weight match the animals. The animal experiments were approved by the local ethical committee at The Laboratory Animal Facility, the Department of Clinical Medicine, the Faculty of Medicine and Dentistry, University of Bergen (Permit Number 20135571). All experiments were performed in accordance with the regulations of the Norwegian Animal Research Authority.

Establishing Tumors

A total of 1×10^6 4T1 tumor cells in 0.15 ml PBS were injected into the fourth mammary fat pads on each side. 3×10^5 RM11 cells were injected subcutaneously on both sides of the mouse flank. The 4T1 tumors were measured using a caliper on days 7, 10, 13, 16 and endpoint 18 post injection, but some were ended day 17 due to rapid tumor growth. The RM11 tumors were measured using a caliper on days 9, 11 and endpoint day 13 post injection. All experiments were performed blinded to genotype. The tumor volume was calculated using the formula; *tumor volume (mm³) = (π/6) x a^2 x b*, where *a* represents the shortest diameter and *b* represents the longest diameter of the tumor. All animals were anesthetized using Isofluran (Isoba®vet. 100%, Schering-Plough A/S, Farum, Denmark) and were sacrificed by cervical dislocation under anesthesia.

Measurement of Interstitial Fluid Pressure

The tumor interstitial fluid pressure (PIF) was measured using the wick-in-needle technique [21]. Briefly, a standard 23-gauge needle with a side hole filled with nylon floss and saline was inserted into the central part of the tumor after calibration and connected to a PE-50 catheter, a pressure transducer and a computer for pressure registrations, using the software Powerlab chart (version 5, PowerLAb/ssp ADinstruments, Dunedin, New Zealand). After a period of stable pressure measurements, the fluid communication was tested by clamping the catheter which shall cause a transient rise and fall in pressure. Measurements were accepted if the pre- to post-clamping value was within ± 1 mmHg.

Electron Microscopy of Collagen Fibrils in the Tumor

A JEM-1230 Transmission Electron Microscope (TEM) (Jeol, Tokyo, Japan) was used to measure the diameter of the collagen fibrils. The tissue samples were cut into approximately 1x1x1 mm samples and fixed in 2.5% glutaraldehyde in 0.1 M phosphate buffer, and then washed in PBS. The samples were post-fixed in 1% OsO_4 in PBS and dehydrated in increasing concentrations of ethanol (70%, 95% and 100%), and then propylenoxide, before being embedded in Agar 100 Resin and sectioned at 60 nm. Four to five images from different areas of the tissue were captured at x100 000 magnification and analyzed using Image J 1.46 (National Institute

of Health, Beteshda, MD., USA). Because of uneven distribution of collagen in the tissue, the images were taken from the areas of the tissue where collagen was found.

A Jeol JSM-7400F Scanning Electron microscope (SEM) was used to study the tumor collagen scaffold architecture. The tumors were cut in 1x1x1 mm samples and fixed in 2.5% glutaraldehyde in 0.1 M phosphate buffer, before being placed in 10% NaOH for 7 days with replacement every day. The samples were thereafter placed in tap-water for 2–4 days and then dehydrated in increasing concentrations of ethanol (70%, 95% and 100%), and dried in a "critical point-dryer". The tumor tissue was mounted on an Au-stub and coated with a 10 nm layer of gold and palladium using a Jeol JFC-2300HR High Resolution fine coater. Five images from different areas of the tumor were captured from each tumor at x10 000 magnification.

Protein Extraction and Western Blot Analysis

The protein expression of integrin α11 in tumors lysates and cultured tumor cell lines was investigated. Tumor samples and cultured cell lines were lysed in buffer containing 50 mM Tris-HCl, pH 7.4, 150 mM NaCl and 1% Triton X supplemented with one tablet of protease inhibitor cocktail (complete EDTA-free; Roche Diagnostics GMBh, Mannheim, Germany) per 10 ml buffer. After homogenization, tumor samples were centrifuged for 10 min at 12 000 rpm and protein concentration was measured using Pierce[TM] BCA Protein Assay Kit (Life Technologies, Thermo Fisher Scientific, Waltham, MA., USA) according to the manufacturer's protocol. For western blot analysis cell lines were grown to confluency in 6 well plates washed with cold PBS, lysed and scraped with cell scraper on ice. Cell lysates were centifuged at 13 000 rpm for 30 min at +4° C, and supernatant harvested. Protein lysates were loaded in XT Sample Buffer, 4X (Bio-Rad Laboratories, Inc, Hercules, CA., USA) containing 50 mM DL-Dithiothreitol (dTT) (Sigma-Aldrich, Steinheim, Germany), and run through a 10% Precise[TM] Protein Gel (Life Technologies, Thermo Fisher Scientific). The proteins were then transferred to a nitrocellulose membrane using Invitrogen[TM] iBlot® Dry Blotting System (Life Technologies, Thermo Fisher Scientific) and an iBlot® Transfer Stack (Life Technologies, Thermo Fisher Scientific). After blocking in I-block (Life Technologies, Thermo Fisher Scientific) for 1 hour at room temperature, the membranes were incubated over-night with rabbit polyclonal anti-mouse α11 antiserum [22] 1:500 in I-block at +4°C. The anti-mouse α11 antiserum is produced against the peptide CRREPGLDPTPKVLE from the integrin α11 cytoplasmic domain (Innovagen AB, Lund, Sweden) [22]. This was followed by incubation with a HRP-coupled secondary antibody (goat anti-rabbit; AB97051, Abcam, Cambridge, UK; 1:5000 in TBS-T). The bands were visualized by the ECL system Pierce[TM] ECL Western Blotting Substrate (Life Technologies, Thermo Fisher Scientific). The membrane was then re-probed with β-actin antibody (AB8227, Abcam; 1:5000 in I-block) and HRP-coupled secondary antibody (goat anti-rabbit; AB97051, Abcam; 1:5000 in TBS-T). Membranes were visualized using the Gel ChemiDoc system and Quantity One 4.6.6 imaging software (Bio-Rad Laboratories, Inc, Hercules, CA., USA).

Picrosirius-Red and Immunofluorescence Staining

For a semi-quantitative measurement of collagen type I and III, picrosirius-red stain (Polysciences inc, Warrington, FL., USA) was used. Five paraffin embedded tumor sections with a thickness of 5μ from each group were deparaffinized, stained in picrosirius-red for one hour, dehydrated and mounted. Five to six images from each tumor were captured with x10 magnification (Nikon Digital Sight, Nikon Corporation, Tokyo, Japan).

For α-SMA staining, FITC-conjugated monoclonal anti-actin α-smooth muscle antibody (F3777, dilution 1:200, Sigma Aldrich, Steinheim, Germany) was used. Five paraffin embedded

tumor sections with a thickness of 10μ from each group were stained. Prior to staining, the sections were first deparaffinized, and then placed in citrate buffer for 25 minutes in 95°C. Non-specific background staining was reduced by adding 0.3% hydrogen peroxide in methanol to the sections. Five images from each tumor were captured with x20 magnification with an Axioscope fluorescence microscope and a digital Axiocam MRm camera (Zeiss, Oberkochen, Germany).

To identify the amount of pixels positive for picrosirius-red staining and α-SMA, the software Image J (National Institute of Health, Beteshda, MD., USA) was used. Individual threshold values were set for each image to adjust for differences in intensity and background. For both stainings, images were taken in an organized pattern in the tumor periphery in order to avoid the necrotic central area.

Metastasis

To allow development of metastasis, female animals were injected with 3×10^5 4T1 cells in their right, fifth mammary fat pad. The experiment was ended on day 21 due to animal welfare. The lungs were fixed using approximately 1 ml of Bouin's solution (Gurr BDH Chemicals Ltd, Poole, UK) injected into the trachea. Then the lungs were dissected out, fixed in new Bouin's solution and washed in 70% ethanol before dehydration. Immediately following this procedure, the liver and brain were harvested and fixed in formalin. All tissues were embedded in paraffin using standard procedures, sectioned, and stained with hematoxylin and eosin (H & E). To quantify lung metastasis, three coronal sections, 600 μm apart and covering both lungs, were examined for each animal. The number of metastases per section was counted and total area covered by metastases was measured (Nikon Digital Sight, Nikon Corporation, Tokyo, Japan).

Statistical Analysis

For statistical analysis, Sigmaplot 12.5 (Systat Software Inc., Chicago, IL., USA) and Graph Pad Prism 6 (GraphPad Software, Inc., La Jolla, CA., USA) were used. Either the unpaired two-tailed t-test or the Mann U Whitney t-test, were used to analyze statistical differences between the two groups. For analysis of tumor growth, t-test with Welch correction was used. The mice injected with 4T1 cells were sacrificed at either day 17 or day 18, and the tumors harvested on the same day were tested against each other. Results were accepted as statistically different when $p < 0.05$. Graph Pad Prism 6 was used to create all figures. Data is given as mean ± SD, and number of measurements (n) refers to number of tumors unless otherwise specified.

Results

Integrin α11 Expression

Using western blotting, integrin α11 was found to be expressed in tumor lysates from both 4T1 and RM11 tumors grown in WT mice, whereas no integrin α11 was detected in the tumors grown in α11-KO mice (Fig 1). No integrin α11 expression was detected in lysates from cultured 4T1 and RM11 tumor cells (Fig 1).

Tumor Growth

The tumor volume of RM11 prostate tumors grown subcutaneously were significantly impeded ($p < 0.04$ and 0.02) in tumors grown in α11-KO mice compared to tumors grown in WT mice during their 13 day growth period, whereas 4T1 mammary tumors did not show any difference in tumor growth between α11-KO mice and WT mice when comparing tumors that were
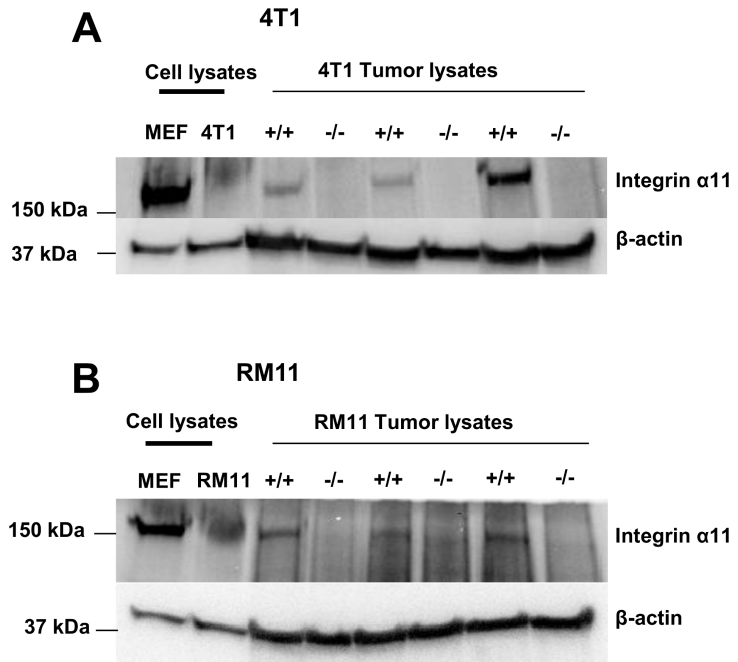
Fig 1. The integrin α11 expression in 4T1 (A) and RM11 (B) cultured tumor cells and tumor lysates from tumors in SCID integrin α11 wild type (+/+) and SCID integrin α11-deficient (-/-) mice. Positive control is a SV40 transformed wildtype mouse embryonic fibroblast cell line (MEF).

doi:10.1371/journal.pone.0151663.g001

harvested on the same day (17 or 18) (Fig 2). All end-point measurements in the 4T1 tumor model are summarized at day 17 in Fig 2.

α-Smooth Muscle Actin (α-SMA) Expression

α-SMA immunofluorescent stained tumor sections were used to quantify the relative amount of activated fibroblasts in the tumors (represented by pixels). There was no significant difference in the level of α-SMA expression in the 4T1 or the RM11 tumors grown in α11-KO mice compared to that in WT mice (Fig 3).

Tumor Collagen Structure

In the present study collagen structure in the α11-KO versus WT tumors was compared by measuring the collagen fibril diameters using transmission electron microsopy (TEM) analyses. An uneven distribution of fibril diameter was found, leading to a shift towards thinner collagen fibrils in 4T1 carcinomas grown in α11-KO mice compared to WT (Fig 4A). The average collagen diameter in the 4T1 tumors grown in α11-KO mice (37.2 ± 1.5 nm) was significantly smaller ($p < 0.006$) than in WT mice (50.4 ± 3.0 nm) (Fig 4B). In the RM11 tumors there was no such difference in the collagen diameter between the tumors grown in α11-KO and WT mice (Fig 4D). To evaluate whether the decreased collagen fibril diameter was a more general feature in the α11-KO mice and not only tumor specific, collagen fibril diameter in dermis
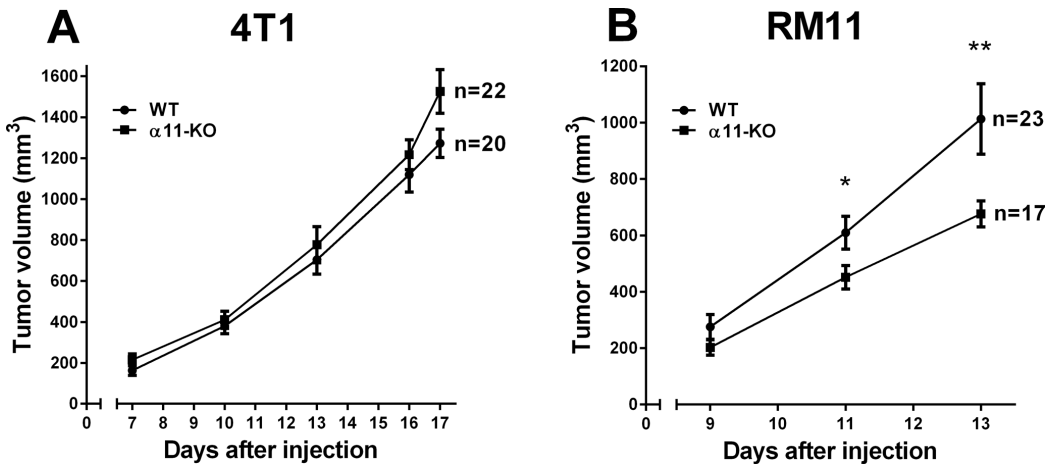
Fig 2. The growth of 4T1 (A) and RM11 (B) tumors in SCID integrin α11 wild type (WT) and SCID integrin α11-deficient (α11-KO) mice. A total of 1 x 10⁶ 4T1 and 3 x 10⁵ RM11 cells were injected into the mammary fat pad and subcutaneously in the mouse flank, respectively. Endpoint values in the 4T1 model include tumors that were harvested on days 17 and 18. Mean ± SEM. * p < 0.04, ** p < 0.02.

doi:10.1371/journal.pone.0151663.g002

from healthy male mice was evaluated. In dermis, no difference in the collagen diameter between α11-KO and WT mice was found.

Scanning electron microscopy (SEM) did not show any difference in collagen architecture between the α11-KO and WT neither in the 4T1 tumors nor the RM11 tumors (Fig 5).

Tumor Collagen Amount

Picrosirius-red staining was used to quantify the most abundant collagens; type I and III, in the tumor sections. No significant difference in the amount of collagen was seen in the 4T1 and the RM11 tumors grown in α11-KO compared to those grown in WT mice (Fig 6).

Tumor Interstitial Fluid Pressure (PIF)

Tumor PIF was determined using the wick-in-needle technique. There was no significant difference in PIF in either 4T1 or RM11 tumors grown in α11-KO versus WT mice (Fig 7).

Tumor Metastases

To evaluate whether stromal integrin α11 has an effect on metastatic potential, H & E stained sections from the 4T1 metastatic model were used. The 4T1 breasts cancer cell line is known to metastasize to lungs, liver, bone and brain [23]. Excessive macroscopic surface metastases were observed in all lungs. There was no difference in the 4T1 tumor cells ability to metastasize to the lungs in the α11-KO mice compared to the WT mice investigated at day 21 post injection (Fig 8). Metastases were also observed in the livers. In addition, the livers were significantly infiltrated by isles of extramedullary hematopoiesis, thereby making it difficult to quantify these metastases. Hence, the liver metastases were not further evaluated. No metastases were found in the brain of any of the animals at endpoint day 21.
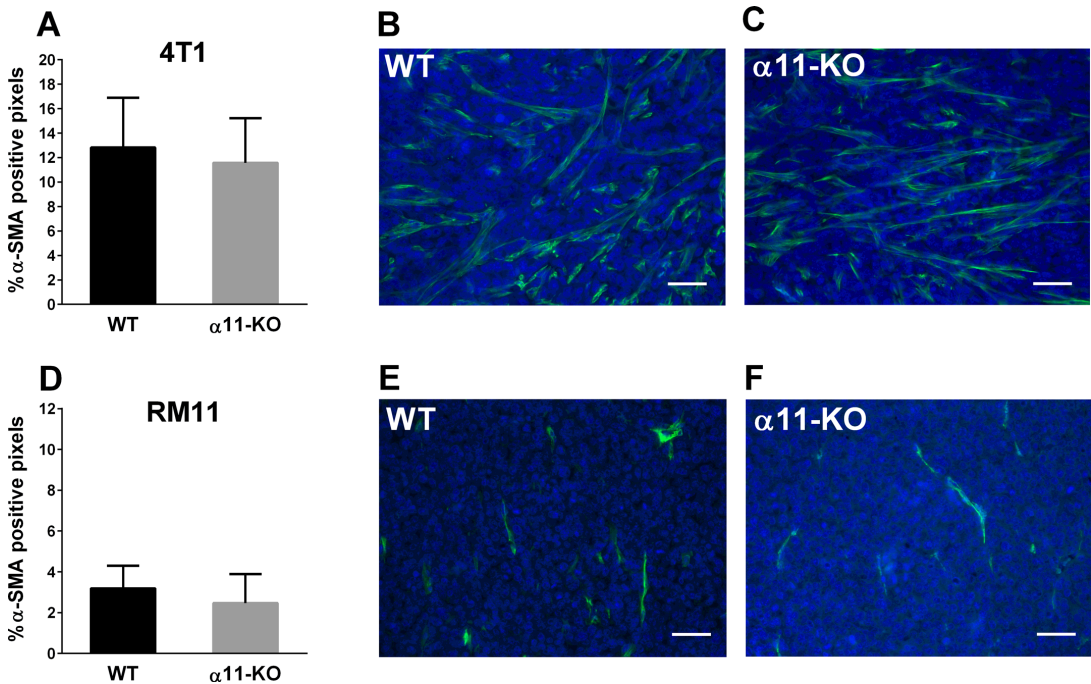
Fig 3. Percentage of pixels positive for α-SMA in 4T1 (n = 5) and RM11 (n = 5) tumors from SCID integrin α11 wild type (WT) and SCID integrin α11-deficient (α11-KO) mice were calculated from immunofluorescent images (A, D). No statistical differences in 4T1 (p = 0.62) or RM11 (p = 0.40) tumors were found using unpaired two-tailed t-test. Mean ± SD. Representative images of α-SMA-staining (green) from both genotypes in 4T1 (B, C) and RM11 (E, F) tumors are shown. Scale bars indicate 50 μm.

doi:10.1371/journal.pone.0151663.g003

Discussion

Stromal integrin α11β1 has been implicated to play a role in experimental non-small-cell lung cancer (NSCLC) carcinogenesis [9, 10], and is expressed in human lung cancer [9, 17, 24] and in metastasis from human malignant melanoma [16]. However, the role of integrin α11β1 in other cancer types remains to be elucidated.

The present study showed that the primary tumor growth of RM11 prostate tumors was reduced in α11-deficient mice compared with WT mice, however, this was not the case in 4T1 mammary tumors. Furthermore, there was a shift towards thinner collagen fibrils in the 4T1 tumors grown in α11-deficient mice. In spite of altered collagen fibrils, there were no differences in the amount of activated fibroblasts, total collagen content, collagen organization or PIF in the tumors. In addition, the metastatic potential to the lung of 4T1 tumors was not affected by stromal α11-deficiency.

In this study we examined the role of integrin α11 in tumor stroma. Following injection of tumor cells in both WT and α11-KO mice, the implanted tumor cells derive their stroma from the host animal, and hence the tumors in α11-KO mice will have stroma that is deficient in integrin α11. Differences in tumor development can be presumed to be due to differences in tumor stroma between the two groups since the tumor cells injected are the same. As seen in
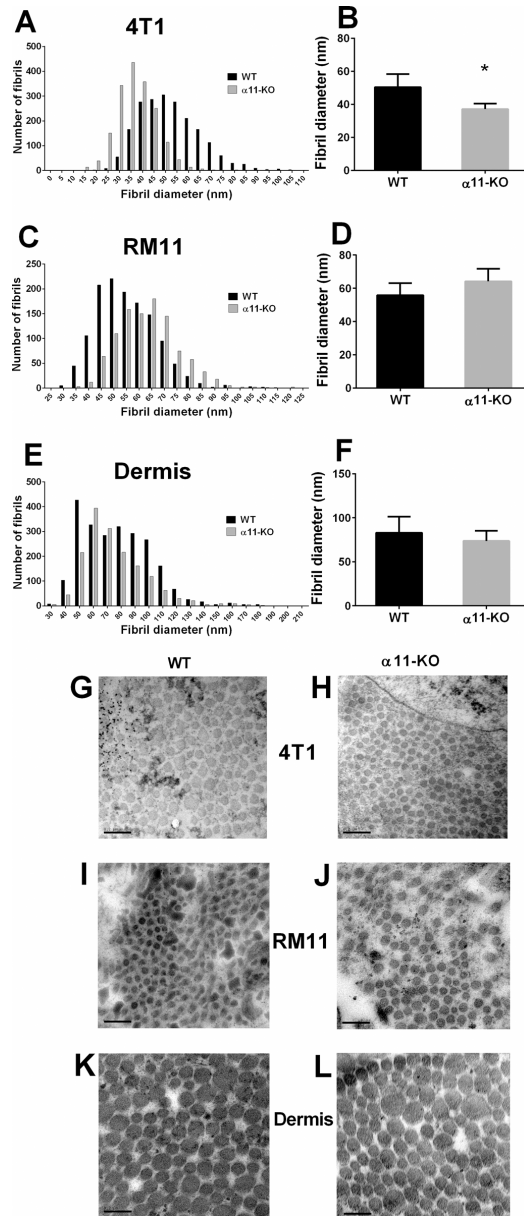
Fig 4. Collagen fibrils were analyzed using transmission electron microscopy (TEM). Collagen fibril diameter distribution and average fibril diameter per tumor in 4T1 (n = 7 and n = 5) tumors (A, B), showed a shift towards thinner fibrils in SCID integrin α11-deficient (α11-KO) mice. RM11 tumors (n = 4 and n = 3) (C, D) and dermis (n = 4 and n = 3) (E, F) showed no significant differences in average collagen fibril diameter in SCID integrin α11 wild type (WT) and SCID integrin α11-deficient (α11-KO) mice (RM11 p = 0.20, dermis

p = 0.47) using unpaired two-tailed t-test. Mean ± SD. * p < 0.006. Representative TEM images of collagen fibrils from both genotypes in 4T1 tumors (G, H), RM11 tumors (I, J) and dermis (K, L) are shown. Scale bars indicate 0.2 μm.

doi:10.1371/journal.pone.0151663.g004

Fig 1, we find that integrin α11 is expressed in tumors grown in WT mice, but not in the tumors grown in α11-KO mice.

There are only two previous *in vivo* studies concerning tumor growth and stromal integrin α11-deficiency, and they both showed a stimulatory effect of integrin α11 on tumor growth [9, 10]. First, wildtype mouse embryonic fibroblasts (MEFs) were found to have a greater stimulating effect on the growth of human NSCLC cells than MEFs lacking integrin α11 when co-
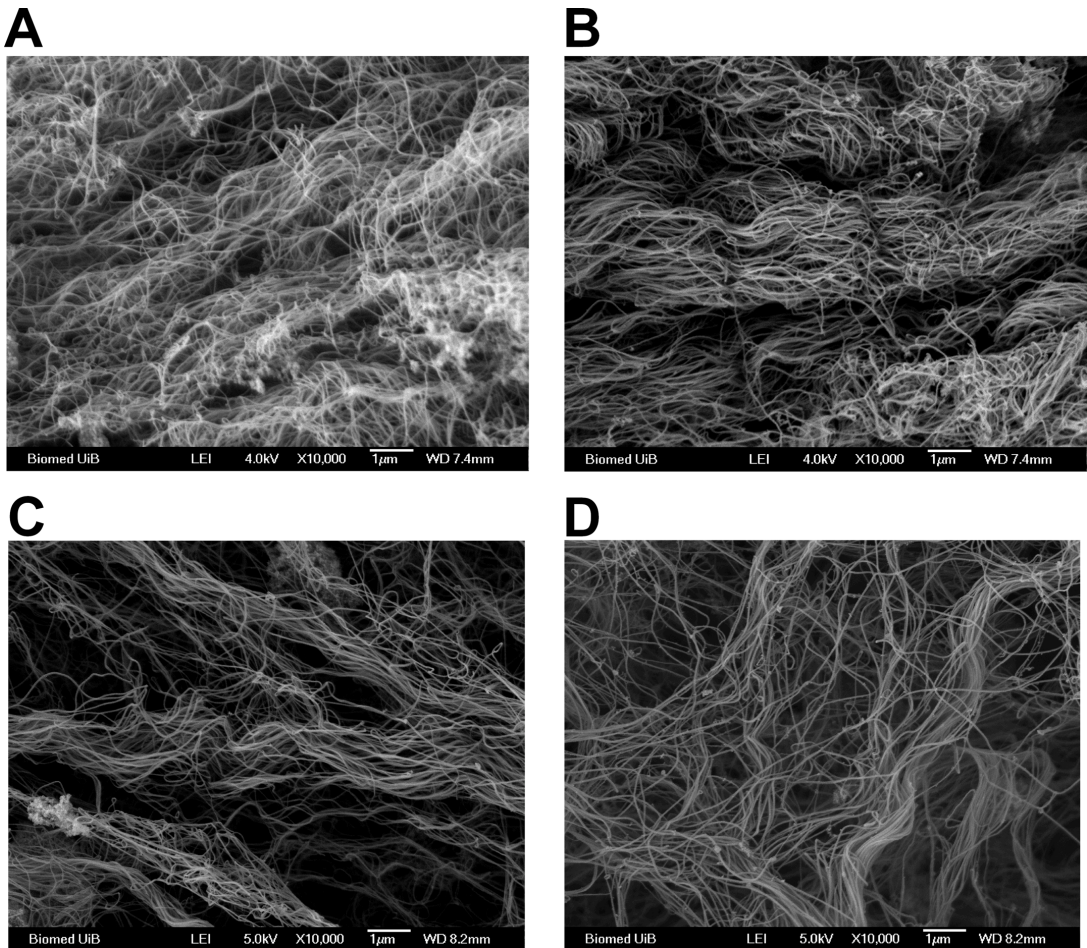
Fig 5. A representative scanning electron micrograph of collagen in 4T1 tumors (n = 3) from SCID integrin α11 wild type (WT) (A) and SCID integrin α11-deficient (α11-KO) (B) and RM11 tumors (n = 3) from WT (C) and α11-KO mice (D), respectively. Scale bars indicate 1 μm.

doi:10.1371/journal.pone.0151663.g005
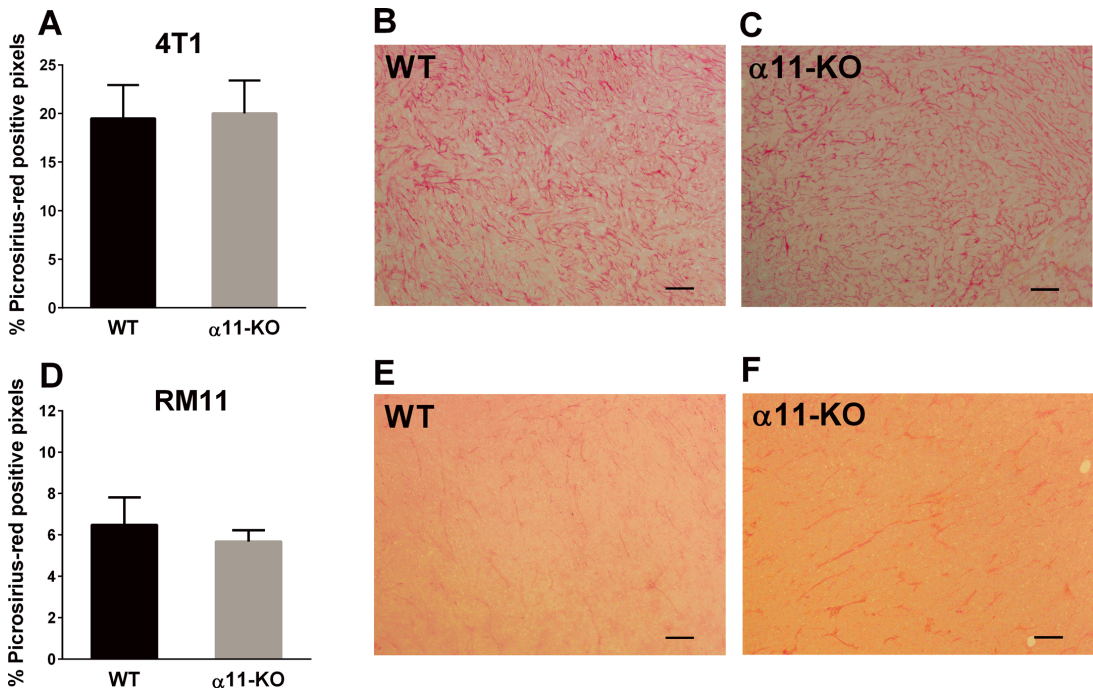
Fig 6. The total fraction of picrosirius-red staining quantified in 4T1 (n = 5) and RM11 (n = 5 and n = 3) tumors in SCID integrin α11 wild type (WT) and SCID integrin α11-deficient (α11-KO) (A, D). No statistical differences in 4T1 (p = 0.82) or RM11 (p = 0.37) tumors were found using unpaired two-tailed t-test. Mean ± SD. Representative images of picrosirius-red staining from both genotypes in 4T1 (B, C) and RM11 (E, F) tumors are shown. Scale bars indicate 100 μm.

injected in mice together with tumor cells [9]. Second, in a recent study by Navab *et al.*, reduced tumor growth in α11-KO mice was described using subcutaneously implanted NSCLC xenografts [10]. In addition, in an *in vitro* heterospheroid model, Lu *et al.* showed that human lung cancer cells grown with WT fibroblasts had a higher tendency to proliferate and migrate compared to tumor cells grown with fibroblasts deficient in integrin α11 [18]. Taken together, these studies indicate that α11 integrin on fibroblasts interact with tumor cells and can play a role in regulating tumor growth. Nevertheless, in the present study we only found an effect on tumor growth in the subcutaneously implanted RM11 tumor model, and not in the orthotopically implanted 4T1 tumor model. It is not known whether these effects are tumor-type specific, or if other factors such as the location of tumor implantation, is of importance.

Integrin α11 is a collagen-binding integrin, and has previously been shown to play a role in collagen reorganization both *in vitro* and *in vivo* [10, 14, 15]. In this study we found that the collagen fibrils in the 4T1 tumors grown in integrin α11-deficient mice were thinner than those in tumors grown in WT mice. However, this finding was not universal, since the RM11 tumors showed no difference in collagen fibril diameter. A recent study on wound healing also found an increase in thinner collagen fibrils in the granulation tissue from integrin α11-deficient mice [25]. Furthermore, the study demonstrated that α11-deficiency resulted in reduced
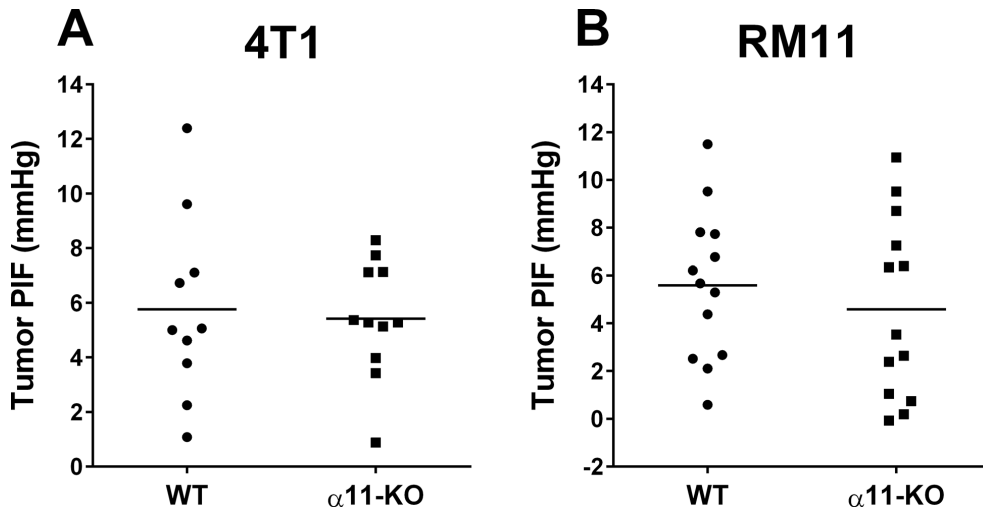
Fig 7. The individual interstitial fluid pressures (PIF) in 4T1 (A) and RM11 (B) tumors in SCID integrin α11 wild type (WT) and SCID integrin α11-deficient (α11-KO) mice. The horizontal lines indicate the mean values. No statistical differences in 4T1 (p = 0.78) or RM11 (p = 0.47) tumors were found using unpaired two-tailed t-test.

formation of granulation tissue and impaired wound contraction [25]. As tumors can be looked upon as "wounds that do not heal" and involve many of the same processes [26], this could represent an interesting parallel to the present study. It is somewhat surprising that in the current study the shift towards thinner collagen fibrils only was seen in the 4T1 model, in which there was no effect of integrin α11 deficiency on tumor growth, whereas no alteration in collagen fibrils was seen in the RM11 tumor model.

Activated fibroblasts play a crucial role in synthesis and remodeling of collagen in tumors [27, 28]. We found here that the amount of activated fibroblasts, identified by the marker α-SMA, was the same in tumors grown in α11-deficient mice when compared with WT mice. This does not correspond to the findings in the study on NSCLC where a decrease in α-SMA expression in α11-KO xenograft tumors was found compared to in WT xenograft tumors [10]. Moreover, reduced α-SMA expression was found in granulation tissue in integrin α11-deficient mice compared to WT mice [25]. In addition, also two earlier studies have suggested that integrin α11 stimulates fibroblast differentiation under different conditions [29, 30]. Thus, available data suggest that integrin α11 may play a role in activation of fibroblasts, although in this study we did not observe any difference in α-SMA expression in tumors grown in α11-deficient mice compared to WT mice.

Regarding the amount of collagen in the tumors, there was no significant difference in the amount of picrosirus-red staining in the 4T1 or the RM11 tumors in the present study. This does not correspond with the recent study on NSCLC where the amount of fibrillar collagen was reduced in xenografts in α11-KO compared to WT mice [10].

While we did not observe any difference in collagen organization in 4T1 or RM11 tumors, neither with SEM nor with picrosirus-red staining, Navab et al [10] found that collagen had a more non-linearized pattern in NSCLC tumors in α11-KO mice using different approaches, namely picrosirus-red staining, second harmonic generation imaging and atomic force
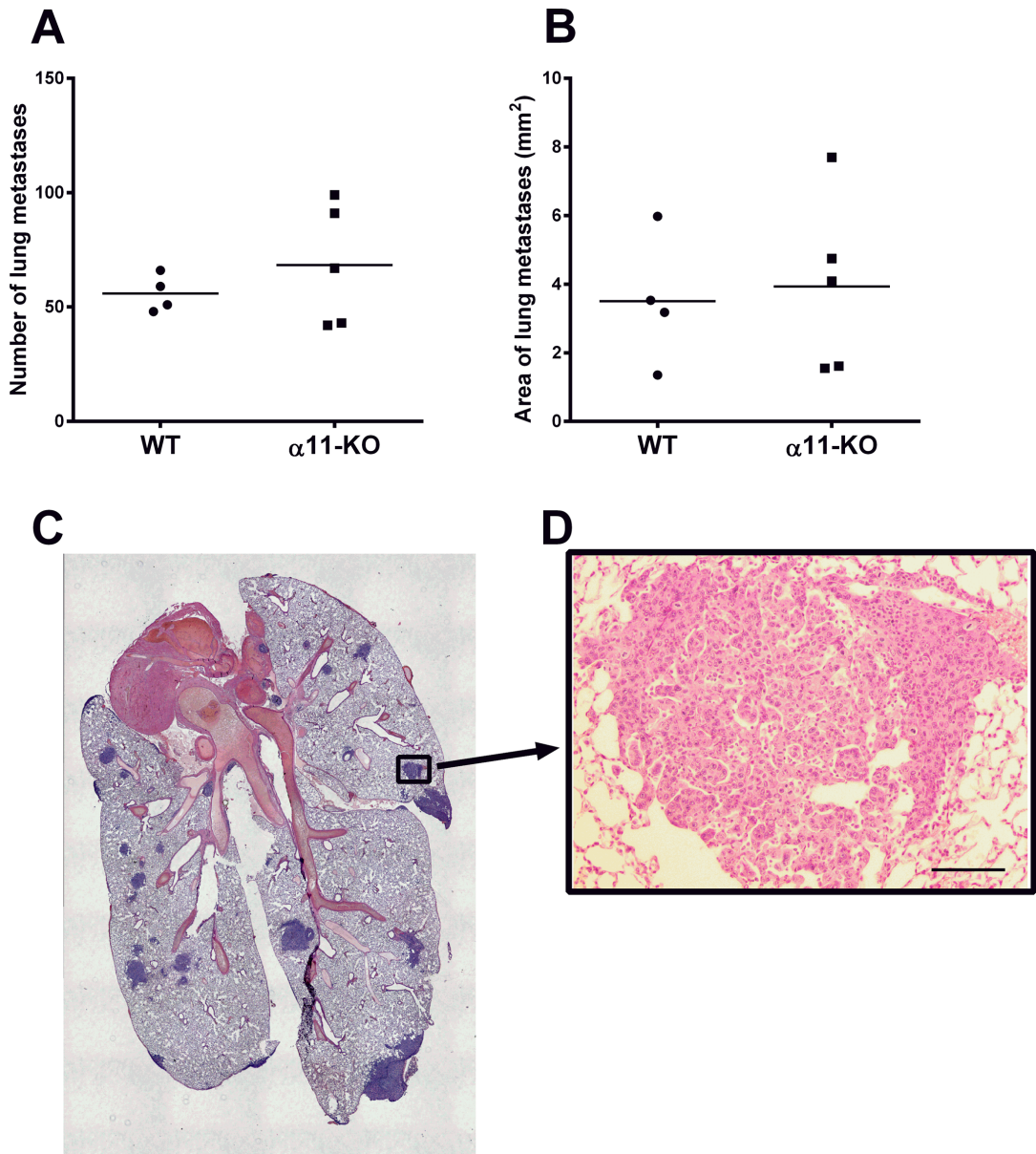
Fig 8. Histomorphometric quantification of H & E -stained lungs from the 4T1 model from SCID integrin α11 wild type (WT) (n = 4) and SCID integrin α11-deficient (α11-KO) (n = 5) mice. Average number of metastasis per section (A) and average area per section (B) is shown. The horizontal lines indicate the mean values. No significant differences were observed (p = 0.73 and p = 0.79) using Mann U Whitney t-test and unpaired two-tailed t-test, respectively. A representative lung with metastasis from a WT mouse is shown (C, D). Scale bar indicates 100 μm.

doi:10.1371/journal.pone.0151663.g008

microscopy. It is therefore likely that the role of integrin α11 in collagen organization differs in the NSCLC tumor model compared to the tumor models that were used in the present study.

Taken together, reduced tumor growth in α11-KO mice, has in an earlier study, been shown to be concomitant with reduced α-SMA and altered collagen structure in the tumors [10]. The findings in the present study, however, are different. Stromal α11-deficiency caused reduced RM11 tumor growth, despite no differences in collagen fibril diameter, collagen amount or α-SMA expression. In addition, there is a smaller proportion of activated fibroblasts (a-SMA staining) and collagen in the RM11 tumors than the 4T1 tumors (Figs 3 and 6), and one could therefore suggest that these stromal factors seem less relevant for RM11 tumor pathogenesis. Hence, in this study, the difference in tumor growth cannot be associated to changes in fibroblast activation or collagen alterations, and the pathogenesis behind the reduced tumor growth in the present study remains unknown. One can conclude, however, that the present findings indicate that different tumors seem to show different responses to stromal integrin α11-deficiency, although the mechanisms responsible are at this point not yet known.

One of the common features in the tumor microenvironment is the high interstitial fluid pressure (PIF), which can hinder efficient delivery of cytostatic drugs across the capillary barrier and into the tumor [31, 32]. Therefore, pharmacologically lowering of PIF can improve transport of cytostatic drugs [32]. Collagen in tumors has been recognized to be one of the factors important for tumor PIF [32–34]. Furthermore, two previous studies have shown that integrin α11 may have a role in regulating PIF in different conditions [15, 18]. It was of interest for us, therefore, to investigate the effect of stromal α11 deficiency on tumor PIF. In this study we did not find any difference in PIF between tumors grown in integrin α11-deficient mice compared to WT mice, indicating that α11 may not be important for PIF regulation in these tumors. Since collagen content is one of the factors that have been shown to be important for PIF [32–34], and the present study did not reveal any effect of stromal integrin α11 deficiency on amount of collagen in the tumors, an unchanged PIF was probably to be expected.

Little is known about how integrin α11 affects tumor metastasis, although there are some findings that indicate that it may play a role in the metastatic process. Integrin α11 mRNA has been found to be expressed in human metastases from malignant melanoma and high mRNA levels of the collagen binding integrins α1, α2 and α11 correlated with poor patient outcome [16].

In the *in vivo* study by Navab *et al.*, NCI-H460SM lung carcinoma cells formed significantly less spontaneous metastases in SCID integrin α11-deficient mice compared to SCID WT mice [10]. Furthermore, in a heterospheroid *in vitro* model it was found that human lung cancer cells had reduced migratory and invasive capacity when cultured together with integrin α11-KO fibroblasts compared with WT fibroblasts [18]. Some studies have also indicated that integrin α11 on *cancer cells* may be important in the metastatic process, such as the study by Westcott *et al* where integrin α11 was among the genes highly expressed in a subpopulation of breast cancer cells with enhanced invasiveness [35]. Furthermore, two separate tumor studies indicate that integrin α11 RNA is upregulated during epithelial to mesenchymal transition (EMT) [36, 37].

However, in spite of earlier findings, in the present study we found no indication that there was a difference in lung metastases of 4T1 tumors grown in the integrin α11-deficient mice compared to those grown in WT mice, again demonstrating that integrin α11`s role in cancer development may vary in different tumor models.

Conclusion

The present study showed reduced tumor growth in the α11-deficient mice in the RM11 model, but no effect in the 4T1 model, only partially confirming the suggested role of integrin

α11 in promoting tumor growth. Even though the present study demonstrated an alteration in collagen fibril diameter in 4T1 mammary tumors in the α11-deficient mice, it did not confirm previously shown alterations in collagen amount and organization, or in α-SMA expression. These discrepancies may be due to differences in tumor model, tumor type, location and aggressiveness of the tumor type. Our findings clearly show that further investigations regarding the role of integrin α11β1 in different tumor types are needed.

Acknowledgments

Author Contributions

Conceived and designed the experiments: LS RKR. Performed the experiments: IR HYHS KS TS MCS. Analyzed the data: IR HYHS LS RKR. Wrote the paper: IR HYHS LS RKR KS TS MCS.

References

1. Hanahan D, Weinberg RA. Hallmarks of cancer: the next generation. Cell. 2011; 144(5):646–74. Epub 2011/03/08. doi: S0092-8674(11)00127-9 [pii] doi: 10.1016/j.cell.2011.02.013 PMID: 21376230.

2. van Dijk M, Goransson SA, Stromblad S. Cell to extracellular matrix interactions and their reciprocal nature in cancer. Experimental cell research. 2013; 319(11):1663–70. Epub 2013/02/20. doi: 10.1016/j.yexcr.2013.02.006 PMID: 23419246.

3. Lu P, Weaver VM, Werb Z. The extracellular matrix: a dynamic niche in cancer progression. The Journal of cell biology. 2012; 196(4):395–406. Epub 2012/02/22. doi: 10.1083/jcb.201102147 PMID: 22351925; PubMed Central PMCID: PMCPmc3283993.

4. Mueller MM, Fusenig NE. Friends or foes—bipolar effects of the tumour stroma in cancer. Nature reviews Cancer. 2004; 4(11):839–49. Epub 2004/11/02. doi: 10.1038/nrc1477 PMID: 15516957.

5. Kalluri R, Zeisberg M. Fibroblasts in cancer. Nature reviews Cancer. 2006; 6(5):392–401. Epub 2006/03/31. doi: 10.1038/nrc1877 PMID: 16572188.

6. van der Flier A, Sonnenberg A. Function and interactions of integrins. Cell Tissue Res. 2001; 305(3):285–98. Epub 2001/09/27. PMID: 11572082.

7. Barczyk M, Carracedo S, Gullberg D. Integrins. Cell Tissue Res. 2010; 339(1):269–80. Epub 2009/08/21. doi: 10.1007/s00441-009-0834-6 PMID: 19693543; PubMed Central PMCID: PMCPMC2784866.

8. Desgrosellier JS, Cheresh DA. Integrins in cancer: biological implications and therapeutic opportunities. Nature reviews Cancer. 2010; 10(1):9–22. Epub 2009/12/24. doi: nrc2748 [pii] doi: 10.1038/nrc2748 PMID: 20029421.

9. Zhu CQ, Popova SN, Brown ER, Barsyte-Lovejoy D, Navab R, Shih W, et al. Integrin alpha 11 regulates IGF2 expression in fibroblasts to enhance tumorigenicity of human non-small-cell lung cancer cells. Proceedings of the National Academy of Sciences of the United States of America. 2007; 104(28):11754–9. Epub 2007/06/30. doi: 10.1073/pnas.0703040104 PMID: 17600088; PubMed Central PMCID: PMCPmc1913903.

10. Navab R, Strumpf D, To C, Pasko E, Kim KS, Park CJ, et al. Integrin alpha11beta1 regulates cancer stromal stiffness and promotes tumorigenicity and metastasis in non-small cell lung cancer. Oncogene. 2015. Epub 2015/07/07. doi: 10.1038/onc.2015.254 PMID: 26148229.

11. Popova SN, Lundgren-Akerlund E, Wiig H, Gullberg D. Physiology and pathology of collagen receptors. Acta physiologica (Oxford, England). 2007; 190(3):179–87. Epub 2007/06/22. doi: 10.1111/j.1748-1716.2007.01718.x PMID: 17581134.

12. Popova SN, Rodriguez-Sanchez B, Liden A, Betsholtz C, Van Den Bos T, Gullberg D. The mesenchymal alpha11beta1 integrin attenuates PDGF-BB-stimulated chemotaxis of embryonic fibroblasts on collagens. Developmental biology. 2004; 270(2):427–42. Epub 2004/06/09. doi: 10.1016/j.ydbio.2004.03.006 PMID: 15183724.

13. Zeltz C, Lu N, Gullberg D. Integrin alpha11beta1: a major collagen receptor on fibroblastic cells. Advances in experimental medicine and biology. 2014; 819:73–83. Epub 2014/07/16. doi: 10.1007/978-94-017-9153-3_5 PMID: 25023168.

14. Tiger CF, Fougerousse F, Grundstrom G, Velling T, Gullberg D. alpha11beta1 integrin is a receptor for interstitial collagens involved in cell migration and collagen reorganization on mesenchymal nonmuscle cells. Developmental biology. 2001; 237(1):116–29. Epub 2001/08/24. doi: 10.1006/dbio.2001.0363 PMID: 11518510.

15. Svendsen OS, Barczyk MM, Popova SN, Liden A, Gullberg D, Wiig H. The alpha11beta1 integrin has a mechanistic role in control of interstitial fluid pressure and edema formation in inflammation. Arteriosclerosis, thrombosis, and vascular biology. 2009; 29(11):1864–70. Epub 2009/09/05. doi: 10.1161/atvbaha.109.194308 PMID: 19729609.

16. Vuoristo M, Vihinen P, Vlaykova T, Nylund C, Heino J, Pyrhonen S. Increased gene expression levels of collagen receptor integrins are associated with decreased survival parameters in patients with advanced melanoma. Melanoma research. 2007; 17(4):215–23. Epub 2007/07/13. doi: 10.1097/CMR.0b013e328270b935 PMID: 17625451.

17. Navab R, Strumpf D, Bandarchi B, Zhu CQ, Pintilie M, Ramnarine VR, et al. Prognostic gene-expression signature of carcinoma-associated fibroblasts in non-small cell lung cancer. Proceedings of the National Academy of Sciences of the United States of America. 2011; 108(17):7160–5. Epub 2011/04/09. doi: 10.1073/pnas.1014506108 PMID: 21474781; PubMed Central PMCID: PMCPMC3084093.

18. Lu N, Karlsen TV, Reed RK, Kusche-Gullberg M, Gullberg D. Fibroblast alpha11beta1 Integrin Regulates Tensional Homeostasis in Fibroblast/A549 Carcinoma Heterospheroids. PloS one. 2014; 9(7):e103173. doi: 10.1371/journal.pone.0103173 PMID: 25076207.

19. Thompson TC, Timme TL, Kadmon D, Park SH, Egawa S, Yoshida K. Genetic predisposition and mesenchymal-epithelial interactions in ras+myc-induced carcinogenesis in reconstituted mouse prostate. Mol Carcinog. 1993; 7(3):165–79. Epub 1993/01/01. PMID: 8489712.

20. Popova SN, Barczyk M, Tiger CF, Beertsen W, Zigrino P, Aszodi A, et al. Alpha11 beta1 integrin-dependent regulation of periodontal ligament function in the erupting mouse incisor. Mol Cell Biol. 2007; 27(12):4306–16. Epub 2007/04/11. doi: 10.1128/mcb.00041-07 PMID: 17420280; PubMed Central PMCID: PMCPMC1900066.

21. Wiig H, Reed RK, Aukland K. Measurement of interstitial fluid pressure: comparison of methods. Ann Biomed Eng. 1986; 14(2):139–51. Epub 1986/01/01. PMID: 3740566.

22. Velling T, Kusche-Gullberg M, Sejersen T, Gullberg D. cDNA cloning and chromosomal localization of human alpha(11) integrin. A collagen-binding, I domain-containing, beta(1)-associated integrin alpha-chain present in muscle tissues. J Biol Chem. 1999; 274(36):25735–42. Epub 1999/08/28. PMID: 10464311.

23. Heppner GH, Miller FR, Shekhar PM. Nontransgenic models of breast cancer. Breast cancer research: BCR. 2000; 2(5):331–4. Epub 2001/03/16. PMID: 11250725; PubMed Central PMCID: PMC138654.

24. Wang KK, Liu N, Radulovich N, Wigle DA, Johnston MR, Shepherd FA, et al. Novel candidate tumor marker genes for lung adenocarcinoma. Oncogene. 2002; 21(49):7598–604. Epub 2002/10/19. doi: 10.1038/sj.onc.1205953 PMID: 12386823.

25. Schulz JN, Zeltz C, Sorensen IW, Barczyk M, Carracedo S, Hallinger R, et al. Reduced Granulation Tissue and Wound Strength in the Absence of alpha11beta1 Integrin. The Journal of investigative dermatology. 2015. Epub 2015/01/31. doi: 10.1038/jid.2015.24 PMID: 25634355.

26. Dvorak HF. Tumors: wounds that do not heal. Similarities between tumor stroma generation and wound healing. The New England journal of medicine. 1986; 315(26):1650–9. Epub 1986/12/25. doi: 10.1056/nejm198612253152606 PMID: 3537791.

27. Ishii G, Ochiai A, Neri S. Phenotypic and functional heterogeneity of cancer-associated fibroblast within the tumor microenvironment. Adv Drug Deliv Rev. 2015. Epub 2015/08/19. doi: 10.1016/j.addr.2015.07.007 PMID: 26278673.

28. Kharaishvili G, Simkova D, Bouchalova K, Gachechiladze M, Narsia N, Bouchal J. The role of cancer-associated fibroblasts, solid stress and other microenvironmental factors in tumor progression and therapy resistance. Cancer cell international. 2014; 14:41. Epub 2014/06/03. doi: 10.1186/1475-2867-14-41 PMID: 24883045; PubMed Central PMCID: PMCPmc4038849.

29. Carracedo S, Lu N, Popova SN, Jonsson R, Eckes B, Gullberg D. The fibroblast integrin alpha11beta1 is induced in a mechanosensitive manner involving activin A and regulates myofibroblast differentiation. J Biol Chem. 2010; 285(14):10434–45. Epub 2010/02/05. doi: 10.1074/jbc.M109.078766 PMID: 20129924; PubMed Central PMCID: PMCPMC2856250.

30. Talior-Volodarsky I, Connelly KA, Arora PD, Gullberg D, McCulloch CA. alpha11 integrin stimulates myofibroblast differentiation in diabetic cardiomyopathy. Cardiovascular research. 2012; 96(2):265–75. Epub 2012/08/08. doi: 10.1093/cvr/cvs259 PMID: 22869616.

31. Tong RT, Boucher Y, Kozin SV, Winkler F, Hicklin DJ, Jain RK. Vascular normalization by vascular endothelial growth factor receptor 2 blockade induces a pressure gradient across the vasculature and improves drug penetration in tumors. Cancer research. 2004; 64(11):3731–6. Epub 2004/06/03. doi: 10.1158/0008-5472.can-04-0074 PMID: 15172975.

32. Heldin CH, Rubin K, Pietras K, Ostman A. High interstitial fluid pressure—an obstacle in cancer therapy. Nature reviews Cancer. 2004; 4(10):806–13. doi: 10.1038/nrc1456 PMID: 15510161.

33. Friman T, Gustafsson R, Stuhr LB, Chidiac J, Heldin NE, Reed RK, et al. Increased Fibrosis and Interstitial Fluid Pressure in Two Different Types of Syngeneic Murine Carcinoma Grown in Integrin beta3-Subunit Deficient Mice. PloS one. 2012; 7(3):e34082. Epub 2012/04/06. doi: 10.1371/journal.pone.0034082 PONE-D-11-22052 [pii]. PMID: 22479530; PubMed Central PMCID: PMC3316610.

34. Oldberg A, Kalamajski S, Salnikov AV, Stuhr L, Morgelin M, Reed RK, et al. Collagen-binding proteoglycan fibromodulin can determine stroma matrix structure and fluid balance in experimental carcinoma. Proceedings of the National Academy of Sciences of the United States of America. 2007; 104 (35):13966–71. Epub 2007/08/24. doi: 10.1073/pnas.0702014104 PMID: 17715296; PubMed Central PMCID: PMCPMC1955775.

35. Westcott JM, Prechtl AM, Maine EA, Dang TT, Esparza MA, Sun H, et al. An epigenetically distinct breast cancer cell subpopulation promotes collective invasion. The Journal of clinical investigation. 2015; 125(5):1927–43. Epub 2015/04/07. doi: 10.1172/jci77767 PMID: 25844900; PubMed Central PMCID: PMCPMC4463195.

36. Ke XS, Qu Y, Goldfinger N, Rostad K, Hovland R, Akslen LA, et al. Epithelial to mesenchymal transition of a primary prostate cell line with switches of cell adhesion modules but without malignant transformation. PloS one. 2008; 3(10):e3368. Epub 2008/10/15. doi: 10.1371/journal.pone.0003368 PMID: 18852876; PubMed Central PMCID: PMCPmc2557125.

37. Fernando RI, Litzinger M, Trono P, Hamilton DH, Schlom J, Palena C. The T-box transcription factor Brachyury promotes epithelial-mesenchymal transition in human tumor cells. The Journal of clinical investigation. 2010; 120(2):533–44. Epub 2010/01/15. doi: 10.1172/jci38379 PMID: 20071775; PubMed Central PMCID: PMCPMC2810072.

BMC Cancer

Stromal integrin α11-deficiency reduces interstitial fluid pressure and perturbs collagen structure in triple-negative breast xenograft tumors

Hilde Ytre-Hauge Smeland[1,2]* , Ning Lu[1,2], Tine V. Karlsen[1], Gerd Salvesen[1], Rolf K. Reed[1,2] and Linda Stuhr[1,2]

Abstract

Background: Cancer progression is influenced by a pro-tumorigenic microenvironment. The aberrant tumor stroma with increased collagen deposition, contractile fibroblasts and dysfunctional vessels has a major impact on the interstitial fluid pressure (PIF) in most solid tumors. An increased tumor PIF is a barrier to the transport of interstitial fluid into and within the tumor. Therefore, understanding the mechanisms that regulate pressure homeostasis can lead to new insight into breast tumor progression, invasion and response to therapy. The collagen binding integrin α11β1 is upregulated during myofibroblast differentiation and expressed on fibroblasts in the tumor stroma. As a collagen organizer and a probable link between contractile fibroblasts and the complex collagen network in tumors, integrin α11β1 could be a potential regulator of tumor PIF.

Methods: We investigated the effect of stromal integrin α11-deficiency on pressure homeostasis, collagen organization and tumor growth using orthotopic and ectopic triple-negative breast cancer xenografts (MDA-MB-231 and MDA-MB-468) in wild type and integrin α11-deficient mice. PIF was measured by the wick-in-needle technique, collagen by Picrosirius Red staining and electron microscopy, and uptake of radioactively labeled 5FU by microdialysis. Further, PIF in heterospheroids composed of MDA-MB-231 cells and wild type or integrin α11-deficient fibroblasts was measured by micropuncture.

Results: Stromal integrin α11-deficiency decreased PIF in both the orthotopic breast cancer models. A concomitant perturbed collagen structure was seen, with fewer aligned and thinner fibrils. Integrin α11-deficiency also impeded MDA-MB-231 breast tumor growth, but no effect was observed on drug uptake. No effects were seen in the ectopic model. By investigating the isolated effect of integrin α11-positive fibroblasts on MDA-MB-231 cells in vitro, we provide evidence that PIF regulation was mediated by integrin α11-positive fibroblasts.

Conclusion: We hereby show the importance of integrin α11β1 in pressure homeostasis in triple-negative breast tumors, indicating a new role for integrin α11β1 in the tumor microenvironment. Our data suggest that integrin α11β1 has a pro-tumorigenic effect on triple-negative breast cancer growth in vivo. The significance of the local microenvironment is shown by the different effects of integrin α11β1 in the orthotopic and ectopic models, underlining the importance of choosing an appropriate preclinical model.

Keywords: Integrin α11β1, Interstitial fluid pressure, Cancer associated fibroblasts, Collagen organization, Triple-negative breast cancer

* Correspondence: hilde.smeland@uib.no
[1]Department of Biomedicine, University of Bergen, P.O. Box 7804, 5020 Bergen, Norway
[2]Centre of Cancer Biomarkers, Norwegian Centre of Excellence, University of Bergen, P.O. Box 7804, 5020 Bergen, Norway

Smeland *et al. BMC Cancer* (2019) 19:234

Page 2 of 13

Background

Triple-negative breast cancer (TNBC) is defined by the absence of estrogen receptors, progesterone receptors and HER-2 amplification and represents an aggressive breast cancer subtype. Despite significant advancements in the treatment of other breast cancer subtypes, there is still no licensed targeted therapy available for the treatment of TNBC, and therefore little improvement in survival has been observed for this patient population over the last years [1, 2]. This highlights the need for better understanding of TNBC and identification of mechanisms involved in disease progression and treatment response.

It is now well recognized that breast cancer progression can be influenced by a pro-tumorigenic microenvironment surrounding the malignant epithelial cells. This environment consists of a heterogeneous mixture of stromal cells, including a diversity of cancer associated fibroblasts (CAFs), a biological active network comprising the extracellular matrix (ECM), in addition to the interstitial fluid and its solutes [3, 4]. New knowledge about the components of the microenvironment and how they interact with tumor cells can hopefully identify new biomarkers or potential targets in TNBC.

The aberrant stroma affects the physiological forces within the tumor. Indeed, the hydrostatic pressure in the tumor interstitium, known as interstitial fluid pressure (PIF), is considerably increased in the majority of solid tumors [5], including human breast cancer [6, 7], and this poses a major physiological barrier to transport of soluble factors within the tumor [8].

Increased PIF has been shown to predict poor prognosis in some solid tumors [9, 10], and can also hinder effective delivery of drugs into the tumor [11–13]. Finding ways to lower tumor PIF may therefore increase efficiency of cancer therapy.

Fibroblasts can actively modify PIF and transcapillary fluid exchange (reviewed in [8, 14, 15]) and the molecular mechanisms are outlined by collagen contraction assays [16, 17] and heterospheroids [18–20], as well as parallel in vivo experiments [21–23]. Dysfunctional blood and lymph vessels will lead to fluid accumulation in the tumor interstitium, and swelling of hyaluronan and proteoglycans would in normal conditions hinder an increase in PIF [8, 24]. Tension exerted by fibroblasts and collagen network can probably counteract this swelling, resulting in a persistent increased PIF [14]. However, although fibroblast-mediated contraction has previous been shown to be dependent on β1-integrins [21], fibroblast-mediated PIF influence is still not fully understood.

Integrin α11β1 is a collagen binding integrin expressed during differentiation of myofibroblasts [25–27] and is involved in collagen organization [17, 28] and tumor stiffness [28]. As a collagen organizer and a link between contractile fibroblasts and the complex collagen network, integrin

α11β1 could be a regulator of tumor PIF. Although a few studies indicate that it has a physiological role in the regulation of PIF in dermis [29, 30], its influence on PIF in tumors remains to be demonstrated. A better understanding of the mechanisms that regulate pressure homeostasis within a tumor, can probably lead to a new insight into breast carcinogenesis, and we therefore investigated the effect of stromal integrin α11-deficiency on pressure homeostasis, ECM organization and tumor growth using two human TNBC xenograft models.

Methods

Cell lines

MDA-MB-231 (ATCC® HTB-26™) was provided by Professor James Lorens (University of Bergen, Bergen, Norway), and MDA-MB-468 (ATCC® HTB-132™) was obtained from the American Type Culture Collection (Manassas, VA., USA). The MDA-MB-231 cells were fingerprinted before use and matched with the cell line MDA-MB-231 (ATCC® HTB-26™) in the ATCC database. MDA-MB-231 was used at passage number five to nine, while the MDA-MB-468 cells were used at passage number two to five. These TNBC cell lines have high tumor take in SCID mice and slowly forming tumors, which may be more stromal dependent than more rapidly growing xenografts. Wild type (WT) and integrin α11-deficient (α11-KO) mouse embryonic fibroblasts (MEFs) were obtained from mouse embryos of embryonic day 14.5 as described previously [31]. In order to obtain immortalized MEFs, primary MEF cultures were infected with recombinant retrovirus-transducing simian virus 40 (SV40) [32]. All cell lines were grown in Nutrient Mixture F-12 Ham (Sigma-Aldrich, Steinheim, Germany) supplemented with 10% Foetal Bovine Serum, 100 units/ml penicillin, 100 μg/ml streptomycin, and 1–2% L-glutamine (all from Sigma-Aldrich). The cells were grown as single monolayers in a humidified incubator at 37 °C in 5% CO_2 and in all experiments used at log phase. All cell lines tested negative for mycoplasma contamination.

Xenograft models

The integrin α11-deficient heterozygous SCID mouse strain was generated as previously described [28]. PCR-genotyping was performed on DNA extracted from ear biopsies [32]. The animals were kept in individually ventilated cages, cared for regularly and efforts were made to age- and weight match the animals. All animal experiments were approved by the Norwegian Food Safety Authority (Permit Number 20168751) which is the competent body responsible for authorizing research projects in animals in Norway. This is in accordance with the EU directive 2010/63 article 36.

A total of 5×10^5 MDA-MB-231 or 1.5×10^5 MDA-MB-468 tumor cells in 0.15 ml PBS were injected into the fourth mammary fat pad (orthotopic), and for the

Smeland *et al. BMC Cancer*   (2019) 19:234

Page 3 of 13

MDA-MB-231 also subcutaneously on the mouse flank (ectopic). Tumor size was measured using a caliper. The tumor volume was calculated using the formula; *tumor volume* $(mm^3) = (\pi/6) \times a^2 \times b$, where a represents the shortest diameter and b represents the longest diameter of the tumor. All animals were anesthetized using Isofluran (Isoba®vet. 100%, Schering-Plough A/S, Farum, Denmark) and eventually sacrificed by cervical dislocation under deep anesthesia. For investigation of the primary tumor, all the MDA-MB-231 injected mice were sacrificed day 57 post injection. For the MDA-MB-468 injected mice, some of the tumors showed tendency to ulcerate the skin, and these mice were sacrificed immediately. To make the groups comparable, one mouse from the opposite group and with similar tumor load was sacrificed on the same day.

To evaluate metastatic spread to the lungs, they were processed and fixed as previously described [33] ($n = 5$ WT and 5 α11-KO and $n = 5$ WT and 4 α11-KO for the MDA-MB-231 and MDA-MB-468 injected mice, respectively).

All measurements and analysis in this study were performed blinded to genotype.

Measurement of interstitial fluid pressure
The wick-in-needle technique was used to measure the tumor PIF [34]. Briefly, a standard 23-gauge needle with a side hole filled with nylon floss and saline was connected to a PE-50 catheter, a pressure transducer and a computer for pressure registrations, using the software Powerlab chart (version 5, PowerLab/ssp. AD instruments, Dunedin, New Zealand). The needle was inserted into the central part of the tumor after calibration. After a period of stable pressure measurements, the fluid communication was tested by clamping the catheter which shall cause a transient rise and then return to pressure prior to clamping. Measurements were accepted if the pre- to post-clamping value was within ±1 mmHg.

PIF in heterospheroids was measured with the micropuncture technique described previously [18]. Briefly, the spheroids were collected and transferred to 10-cm Lysine-coated cell culture dishes (Nunc, Thermo Fisher, Waltham, MA., USA) and left to attach for 2 h at 37 °C. PIF was measured using sharpened glass capillaries (tip diameter 3–5 μm) connected to a servo-controlled counter pressure system. The glass capillaries were filled with hypertonic saline (0.5 M) colored with Evans blue dye and inserted into the central parts of the spheroid with the help of a stereomicroscope (Wild M5, Heerbrugg, Switzerland). PIF in the cell culture medium directly outside the spheroid was defined as the zero reference pressure.

Electron microscopy of collagen fibrils in the tumor
Tumor samples were taken from the tumor periphery and were fixed and processed as previously described [33]. A JEM-1230 Transmission Electron Microscope (TEM) (Jeol, Tokyo, Japan) was used to measure the diameter and organization of the collagen fibrils, and images from four to six different areas of the tissue were analyzed. Pictures were captured at × 100,000 magnification and analyzed using Image J 1.46 (National Institute of Health, Bethesda, MD., USA) to measure the fibril diameter. To investigate the organization of the collagen fibrils, pictures were captured at × 30,000 magnification and scored from one to four considering collagen fibril organization and alignment within the collagen fibers.

A JSM-7400F Scanning Electron microscope (Jeol) was used to study the tumor collagen fibril scaffold architecture. Five images from different areas of the tumor were captured from each tumor at × 10,000 magnification.

Immunostaining and Picrosirius-red staining
Histological analysis was performed on both paraffin embedded sections and cryosections. For paraffin embedded sections, 5 μm thick sections were deparaffinizated and rehydrated, followed by heat induced antigen retrieval at pH 6 (#S1699, Dako, Agilent, Santa Clara, CA., USA) for Ki67 (100 °C, 20 min) and αSMA (100 °C, 25 min), pH 9 (#2367, Dako) for Coll III (100 °C, 25 min) or pH 10 (#T6455, Sigma Aldrich) for PDGFRβ (110 °C, 5 min). After antigen retrieval, the sections were incubated with peroxidase block (#K006, Dako) and then primary antibody. Envision+ System-HRP (#K4006 or #K4010, Dako) was used as secondary antibody, in addition to rabbit anti-goat for collagen III (1:1000, #6164–01, Southern Biotech, Birmingham, AL., USA), and DAB was used as chromogen, except for αSMA staining, where a FITC-conjugated antibody was used. Analysis of immunohistochemistry was performed using Leica DN 2000 Led (Leica Microsystems, Wetzlar, Germany). The following primary antibodies were used on paraffin sections: rabbit anti-mouse PDGFRβ mAb (1:100, #3169, Cell Signaling Technology, Danvers, MA., USA), goat anti-mouse Type III Collagen pAb (1:100, #1330–08, Southern Biotech), anti-mouse αSMA mAb (F3777, dilution 1:200, Sigma Aldrich) and mouse anti-human Ki67 mAb (1:100, #M7240, Dako).

Cryosections with a thickness of 6 μm were fixed in ice-cold methanol (− 20 °C, 8 min) and rehydrated with PBS, followed by blocking with 10% goat serum. Afterwards, the following primary antibodies were supplied: rabbit anti-mouse integrin α11 pAb (1:200, custom-made, Innovagen AB, Lund, Sweden, [31]), mouse anti-human cytokerain AE1/AE3 mAb (1:200, #M3515, Dako) and mouse anti αSMA mAb (1:200, #A5228, Sigma Aldrich). Goat anti-rabbit Alexa 594 (1:400, #111–585-144, Jackson ImmunoResearch, Ink., West Grove, PA., USA) and goat anti-mouse Alexa 488 (1:400, #315–545-045, Jackson ImmunoResearch) were used as secondary antibodies. Mounting was done with

ProLong Gold Antifade Mountant with DAPI (#P36934, ThermoFisher). The staining results were evaluated under an Axioscope fluorescence microscope and micrographs were acquired using a digital AxioCam MRm camera (Zeiss, Oberkochen, Germany).

Picrosirius-red stain (Polysciences inc, Warrington, FL., USA) was used for a semi-quantitative measurement of collagen type I and III as previously described [33].

Evaluation of the staining

For Picrosirius-red, collagen III, PDGFRβ and αSMA, a total of four to six pictures were captured from each tumor with × 100 magnification. Images were taken in the tumor periphery in order to avoid the necrotic central area. The software Image J 1.46 (National Institute of Health, Bethesda, MD., USA) was used to identify the amount of positive pixels.

For Ki67, the tumors were examined using light microscopy with an eye-piece grid at × 630 magnification. A total of 500 tumor cells from the tumor periphery were evaluated, and distinct nuclear staining regardless of intensity was registered as positive. Areas with necrosis, bleeding or inflammation were avoided.

Microdialysis

Microdialysis was performed as previously described [35] on the MDA-MB-231 mammary fat pad tumors. Briefly, after anesthesia with Ketalar (Pfizer Inc., NY., USA) and Dormitor (Orin Pharma AS, Espoo, Finland), one microdialysis probe was placed in the MDA-MB-231 mammary fat pad tumor (CMA12 Elite Microdialysis probe, ref.nr 8,010,434) and one in the jugular vein (CMA12 Elite Metal free, ref.nr 80,111,204). The probes were connected to a PE-50 catheter, perfused by a pump (CMA100 Microinjection pump, ref.nr 8,210,040) at a rate of 1 μl/min and left to stabilize for 30 min. After intravenous injection of 0.15 ml 0.65 MBq ^{3}H-5FU (Nycomed Amersham, Buckinghamshire, UK), dialysate was sampled and pooled every 10 min for a total of 90 min. Scintillation counting solution (Optiphase Hisafe 3, PerkinElmer, Inc., Waltham, MA., USA) was added, and the radioactivity measured using a liquid scintillation analyzer (Tri-Carb 2900TR, PerkinElmer, Inc.). The probes and pump were delivered by CMA Microdialysis AB, Kista, Sweden.

The area under the curve (AUC) for the plasma and tumor was calculated with Graph Pad Prism 7 (GraphPad Software Inc., La Jolla, CA., USA) as the total radioactivity collected, i.e. as the product of radioactivity (counts per minute) and time. Finally, transport of ^{3}H-5FU was expressed as AUC tumor divided by AUC plasma.

After each experiment, the probes were tested in saline with a known amount of ^{3}H-5FU, and experiments with probes that differed more than 15% in permeability were excluded.

Heterospheroids

Heterospheroids containing a mixture of SV40-immortalized MEFs and MDA-MB-231 cells were prepared using the hanging drop method as described previously [19]. Briefly, sub-confluent cells were trypsinized and suspended in culture medium to a concentration of 1×10^6/ ml. The MEFs (WT or integrin α11-KO MEFs) and MDA-MB-231 cell suspensions were then mixed at a ratio of 4:1 to make WT MEFs + MDA-MB-231 and α11-KO MEFs + MDA-MB-231 spheroids. Approximately 40 drops (25 μl/ drop, 2.5×10^4 cells/drop) were dispensed onto a lid of a cell culture dish. The lid was then inverted and placed over a cell culture dish containing medium for humidity, and cultured in a humidified incubator at 37 °C in 5% CO_2 for 5 days.

Statistical analysis

Sigmaplot 13.0 (Systat Software Inc., Chicago, IL., USA) and Graph Pad Prism 7 (GraphPad Software) were used for statistical analysis. Either the unpaired two-tailed t-test or the Mann- Whitney U test, was used to analyze statistical differences between the two groups. Results were accepted as statistically different when $p < 0.05$. Data are given as mean ± SD, and number of measurements (n) refers to number of tumors or heterospheroids unless otherwise specified.

Results

Effect of stromal integrin α11β1 on breast tumor growth

MDA-MB-231 and MDA-MB-468 tumor cells were injected into WT and α11-KO mice. As expected, we found that integrin α11 was expressed in the tumor stroma in WT mice, but not in α11-KO mice (Fig. 1d). Furthermore, the immunofluorescent staining of integrin α11 (Fig. 1d) did not show differences in the amount of integrin α11 expression between the MDA-MB-231 orthotropic and subcutaneous model ($n = 3$–5). The tumor volumes in MDA-MB-231 mammary fat pad tumors were significantly reduced ($p < 0.01$) in α11-KO mice compared to tumors grown in WT mice during their 57 days growth period (Fig. 1a). A clear tendency towards reduced MDA-MB-468 mammary fat pad tumor growth was also seen, but this did not reach statistical significance ($p = 0.059$) (Fig. 1b). Of note, there was no difference in MDA-MB-231 tumor growth when the cells were injected subcutaneously on the back (Fig. 1c).

In the MDA-MB-231 mammary fat pad tumors, there was a slight, but statistically significant difference in the number of proliferating tumor cells, indicated by positive Ki67 staining (Fig. 2a and d). However, in the two other tumor models, there were no significant differences in number of proliferating tumor cells (Fig. 2b-d).

Smeland *et al. BMC Cancer* (2019) 19:234

Page 5 of 13
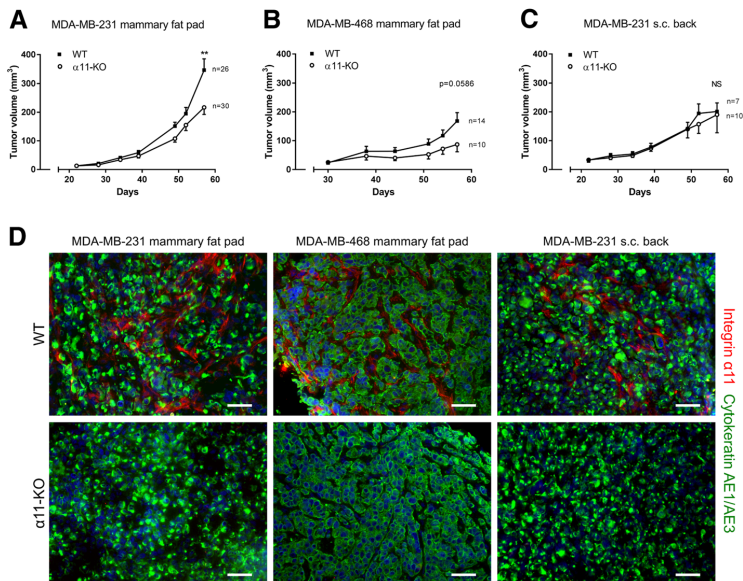
Fig. 1 Tumor growth. The growth of MDA-MB-231 and MDA-MB-468 xenograft tumors (**a-c**) in WT and α11-KO mice. A total of 5×10^5 MDA-MB-231 and 1.5×10^6 MDA-MB-468 cells were injected into the mammary fat pad, and for MDA-MB-231, also subcutaneously (s.c.) on the back. All MDA-MB-231 injected mice were sacrificed at day 57 post injection. The MDA-MB-468 injected mice were sacrificed at different time points starting with $n = 20$ WT and $n = 16$ α11-KO. Mean ± SEM. ** $p < 0.01$. Immunofluorescence staining of integrin α11 (red), cytokeratin AE1/AE3 (green) and DAPI (blue) in MDA-MB-231 and MDA-MB-468 xenograft tumors (**d**) in WT and α11-KO mice. Scale bars indicate 50 μm

Integrin α11-deficiency reduces tumor interstitial fluid pressure

The tumor PIF was measured by the wick-in-needle method. PIF was significantly reduced in both MDA-MB-231 and MDA-MB-468 mammary fat pad tumors grown in α11-KO mice compared to WT (Fig. 3a-b). No difference in PIF was seen in the MDA-MB-231 subcutaneous tumors (Fig. 3c).

Integrin α11-deficiency perturbs collagen structure

Picrosirius-red and collagen III staining did not demonstrate differences in the amount of collagen in either of the tumor models (Fig. 4a-c and Additional file 1: Figure S1).

Collagen fibril organization and structure in the xenograft tumors were investigated using TEM. As seen in Fig. 5a-b and d, integrin α11-deficiency lead to more disorganized collagen fibril architecture with fewer aligned collagen fibrils in both the MDA-MB-231 and MDA-MB-468 mammary fat pad tumor models. In these tumors, there was also a shift towards thinner collagen fibrils in α11-KO compared to WT mice (Fig. 6a-b and d). No difference was seen in either collagen fibril alignment or collagen fibril diameter in the MDA-MB-231 subcutaneous tumors when comparing α11-KO mice with WT (Figs. 5c and 6c). In addition, SEM did not demonstrate visual differences in

the collagen fibril structure between tumors grown in α11-KO mice versus WT (Fig. 7).

Immunostaining of αSMA and PDGFRβ, common markers of activated fibroblasts and pericytes, was used to quantify the relative amount of activated fibroblasts in the tumor stroma. Although integrin α11 partially co-localized with αSMA in xenograft tumors in WT mice (Fig. 8c), no significant differences in the amount of PDGFRβ or αSMA expression (Fig. 8a-b and Additional file 1: Figure S1) in tumors in α11-KO compared to WT mice were found.

Integrin α11β1 does not affect uptake of ³H-5FU

The reduced tumor PIF found in MDA-MB-231 mammary fat pad tumors in α11-KO mice was not associated with increased uptake of ^{3}H-5FU measured by microdialysis (Fig. 9).

Pressure homeostasis and integrin α11β1 in heterospheroids

Since the in vivo results demonstrate that stromal integrin α11β1 has a role in maintaining pressure homeostasis in triple-negative breast xenograft tumors, we also investigated the isolated effect of integrin α11-positive fibroblasts on tumor PIF in a simplified system. Spheroids composed

Smeland et al. BMC Cancer   (2019) 19:234

Page 6 of 13

Fig. 2 Tumor cell proliferation. The fraction of Ki67-positive tumor cells in MDA-MB-231 and MDA-MB-468 xenograft tumors (**a-c**). Reduced percentage of Ki67-positive tumor cells was only seen in MDA-MB-231 mammary fat pad tumors in α11-KO mice compared to WT ($n = 7$ for MDA-MB-231 and MDA-MB-468 mammary fat pad tumors, and $n = 4$ WT and $n = 5$ α11-KO for MDA-MB-231 subcutaneous tumors). Mean ± SD. * $p < 0.05$. Representative images of Ki67 staining of sections from all xenograft tumors in WT and α11-KO mice (**d**). Scale bars indicate 100 μm

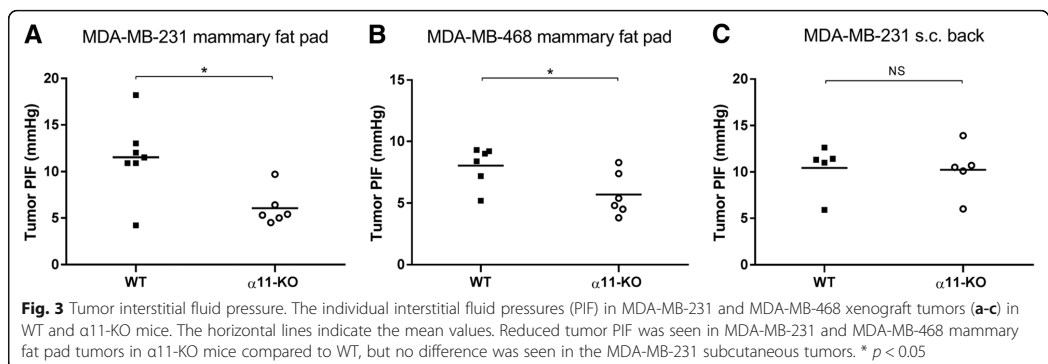of fibroblasts lacking integrin α11 grown together with MDA-MB-231 cells had significantly lower PIF compared to spheroids with MDA-MB-231 cells and WT fibroblasts (Fig. 10a-b). These data indicate that the difference in PIF is, at least in part, due to integrin α11-positive fibroblasts.

Tumor metastases

No lung metastases were seen when investigating coronal HE stained sections from lungs at end stage.

Discussion

Integrins are essential adhesion receptors necessary for intercellular communication, attachment of cells to the ECM and modulation of the tumor microenvironment [36–39]. In this study, we have demonstrated that stromal integrin α11-deficiency markedly decreased PIF in vivo using two orthotopic human triple-negative breast cancer cell lines. A perturbed collagen structure was seen, with fewer aligned and thinner collagen fibrils. Furthermore, integrin α11-deficiency impeded orthotopic breast tumor growth in the MDA-MB-231 model, and the same trend

Fig. 3 Tumor interstitial fluid pressure. The individual interstitial fluid pressures (PIF) in MDA-MB-231 and MDA-MB-468 xenograft tumors (**a-c**) in WT and α11-KO mice. The horizontal lines indicate the mean values. Reduced tumor PIF was seen in MDA-MB-231 and MDA-MB-468 mammary fat pad tumors in α11-KO mice compared to WT, but no difference was seen in the MDA-MB-231 subcutaneous tumors. * $p < 0.05$

Smeland *et al. BMC Cancer* (2019) 19:234

Page 7 of 13

Fig. 4 Collagen amount. The total fraction of Picrosirius-red and collagen III positive staining quantified in MDA-MB-231 (**a**) and MDA-MB-468 mammary fat pad tumors (**b**) in WT and α11-KO mice showed no differences (*n* = 6 in both models). Mean ± SD. Representative images of Picrosirius-red staining of sections from MDA-MB-231 and MDA-MB-468 mammary fat pad tumors in WT and α11-KO mice (**c**). Scale bars indicate 100 μm

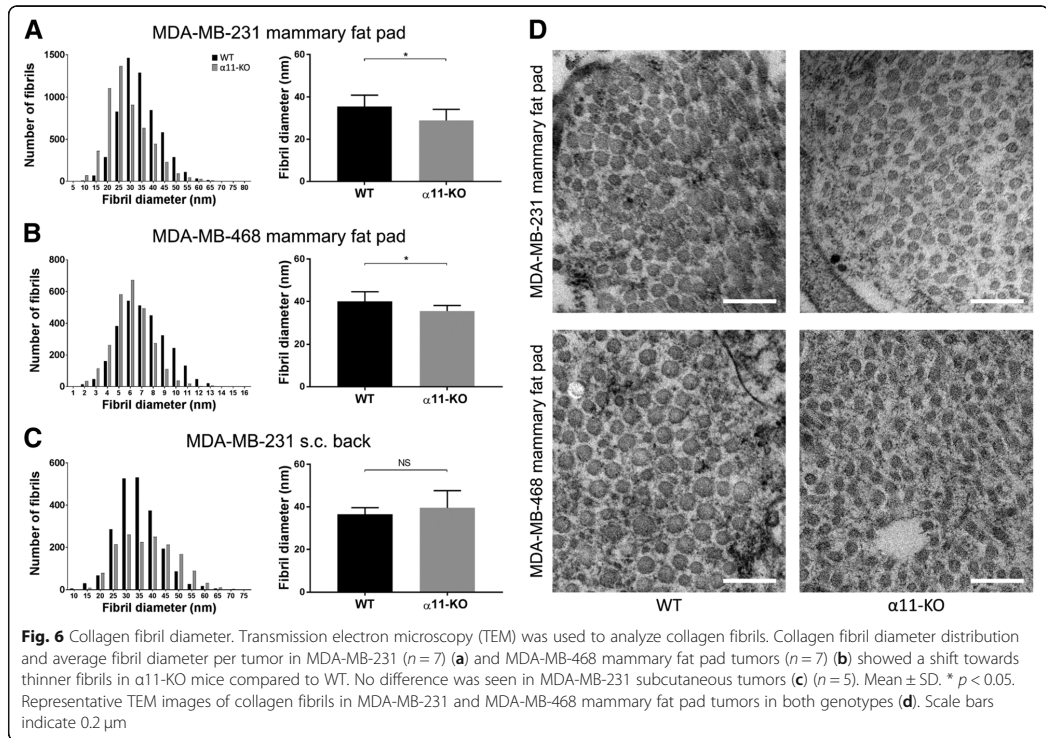was also found in the MDA-MB-468 orthotopic model. By investigating the isolated effect of integrin α11-positive fibroblasts on MDA-MB-231 tumor cells in vitro, we provide here evidence that PIF regulation is, at least partly, mediated by integrin α11-positive fibroblasts.

Integrin α11β1 has arisen as a possible marker of a pro-tumorigenic subset of CAFs in the tumor microenvironment [40, 41]. It has been found to be overexpressed in the stroma of lung cancer and head and neck cancer [40, 42]. Further, it stimulates lung cancer cell

Fig. 5 Collagen fibril organization. Transmission electron microscopy pictures from the xenograft tumors were scored from 1 to 4 according to collagen organization. The average collagen organization score per tumor in MDA-MB-231 (**a**) and MDA-MB-468 mammary fat pad tumors (**b**) were lower in α11-KO mice compared to WT (*n* = 8 WT and *n* = 7 α11-KO mice in both models). No difference was found in the MDA-MB-231 subcutaneous tumors (**c**) (*n* = 5). Mean ± SD. * *p* < 0.05, ** *p* < 0.01. Examples of the different scoring values from MDA-MB-468 tumors are shown in (**d**) (1- highly disorganized, 2-moderately disorganized, 3-moderately organized and 4-highly organized). Scale bars indicate 0.5 μm

Smeland *et al. BMC Cancer*   (2019) 19:234

Page 8 of 13

Fig. 6 Collagen fibril diameter. Transmission electron microscopy (TEM) was used to analyze collagen fibrils. Collagen fibril diameter distribution and average fibril diameter per tumor in MDA-MB-231 ($n = 7$) (**a**) and MDA-MB-468 mammary fat pad tumors ($n = 7$) (**b**) showed a shift towards thinner fibrils in α11-KO mice compared to WT. No difference was seen in MDA-MB-231 subcutaneous tumors (**c**) ($n = 5$). Mean ± SD. * $p < 0.05$. Representative TEM images of collagen fibrils in MDA-MB-231 and MDA-MB-468 mammary fat pad tumors in both genotypes (**d**). Scale bars indicate 0.2 μm
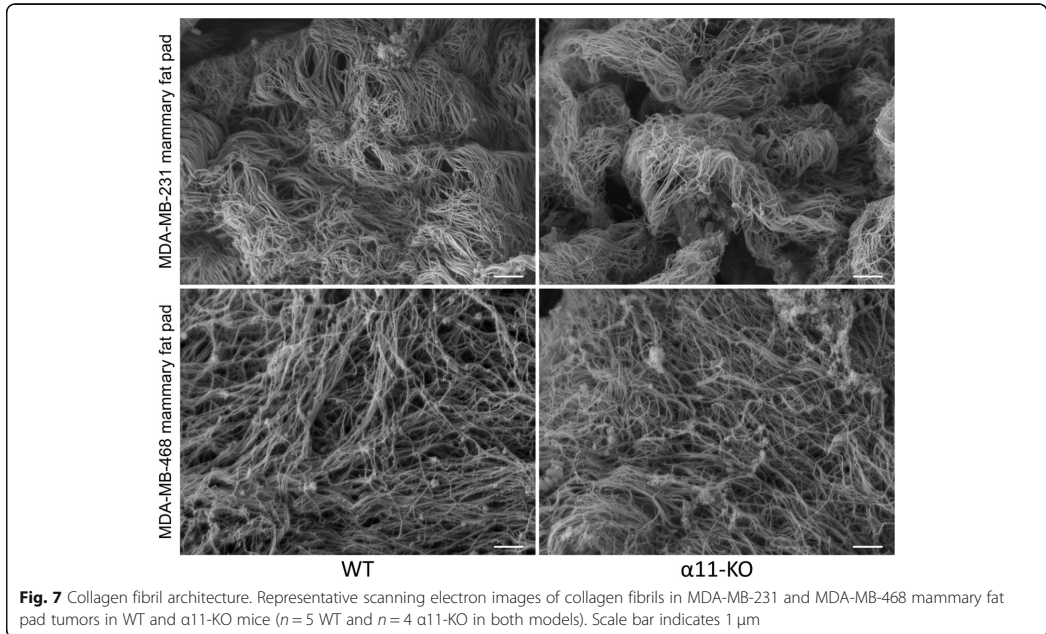
growth in vitro [20], and lung and prostate cancer growth in vivo [28, 33]. However, its role in tumor growth and progression is still not clear, especially in breast tumors where we recently reported that it did not affect the growth of the murine TNBC cell line 4 T1 in vivo [33].

In the present study, we found that stromal integrin α11-deficiency led to reduced tumor PIF in both ortho-topic xenograft models. This demonstrates for the first time that integrin α11β1 has a role in maintaining an elevated PIF in solid tumors. A dense ECM, contractile fibroblasts, leaky blood vessels and dysfunctional lymphatic drainage are possible causes of increased PIF in tumors [8]. PIF can be actively modulated through interactions between contractile fibroblasts and ECM molecules [8, 23], where fibroblasts have been proposed to normally exert a tension on the collagen network through collagen-binding integrins [14]. Furthermore, integrin α11β1 contracts collagen matrices experimen-tally [17], and we therefore suggest that integrin α11β1-mediated PIF modifications can involve a contraction of the interstitial space mediated by direct or indirect binding of integrin α11-positive fibroblasts to collagen.

The involvement of integrin α11-positive fibroblasts in tumor PIF homeostasis is supported by our study of het-erospheroids, where we observed a similar PIF reduction in spheroids composed of MDA-MB-231 cells and integ-rin α11-deficient fibroblasts. This simplified system allows us to investigate how fibroblasts grown together with tumor cells can influence PIF [18–20]. In line with our results, a similar integrin α11β1 function in pressure regulation has previously been shown in fibroblasts/lung cancer heterospheroids [20]. However, although these avascular spheroid studies indicate that the pressure regulatory abilities of integrin α11β1 is, at least in part, mediated by integrin α11-positive fibroblasts, the mech-anisms behind integrin α11-mediated effect on PIF in heterospheroids are not investigated in detail in this study. In addition, we cannot exclude additional factors in the more complex in vivo system, such as influence of the tumor vasculature, which has been shown to have an important impact on tumor PIF [13, 43–45].

Furthermore, integrin α11-deficiency led to less organized and thinner collagen fibrils in the orthotopic models, which could be a contributing factor to reduced tumor PIF. Al-though it has been shown that the collagen-binding proteo-glycan fibromodulin promotes the formation of a dense

Fig. 7 Collagen fibril architecture. Representative scanning electron images of collagen fibrils in MDA-MB-231 and MDA-MB-468 mammary fat pad tumors in WT and α11-KO mice ($n = 5$ WT and $n = 4$ α11-KO in both models). Scale bar indicates 1 μm
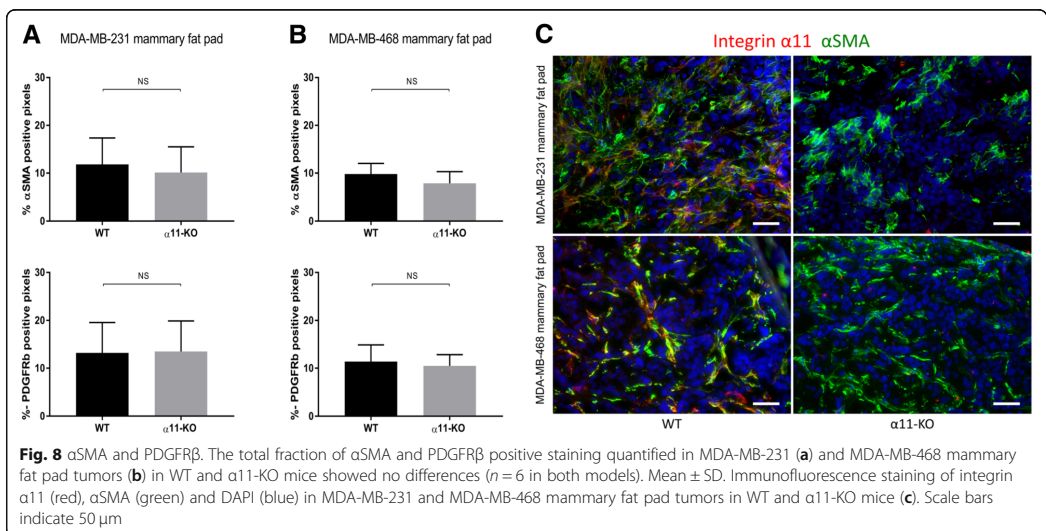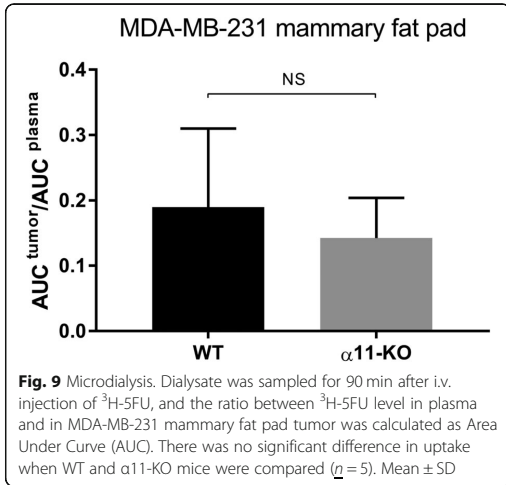
stroma and increased tumor PIF [46], it is nevertheless difficult to predict how different components in the extracellular matrix affect the hydraulic conductivity of tissues and thereby fluid flow and PIF [47].

Although the present study is the first to identify integrin α11β1 as participating in regulation of pressure in solid tumors, it is already known to maintain a homeostatic PIF in dermis [29, 30]. Furthermore, we have previously demonstrated the function of β1-integrins in the regulation of dermal PIF by inhibiting β1-integrins [21].

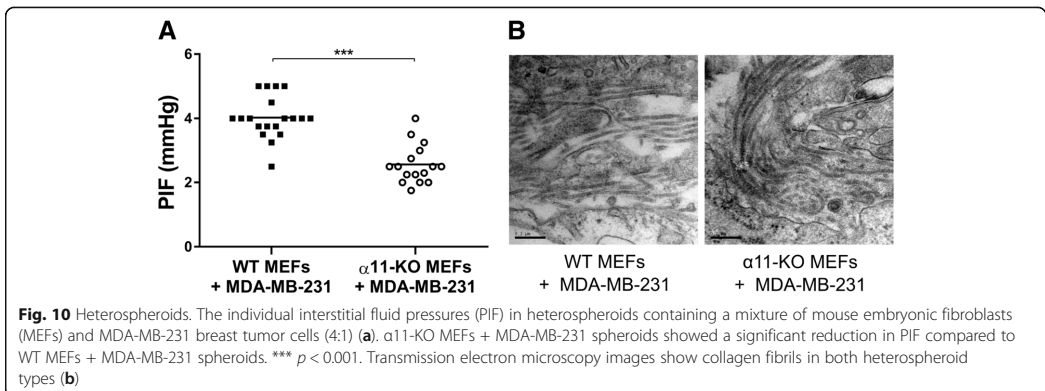Numerous studies have highlighted the role of CAFs in tumor progression, invasion and metastasis, either

Fig. 8 αSMA and PDGFRβ. The total fraction of αSMA and PDGFRβ positive staining quantified in MDA-MB-231 (**a**) and MDA-MB-468 mammary fat pad tumors (**b**) in WT and α11-KO mice showed no differences ($n = 6$ in both models). Mean ± SD. Immunofluorescence staining of integrin α11 (red), αSMA (green) and DAPI (blue) in MDA-MB-231 and MDA-MB-468 mammary fat pad tumors in WT and α11-KO mice (**c**). Scale bars indicate 50 μm

Smeland et al. BMC Cancer (2019) 19:234

Page 10 of 13

Fig. 9 Microdialysis. Dialysate was sampled for 90 min after i.v. injection of ^{3}H-5FU, and the ratio between ^{3}H-5FU level in plasma and in MDA-MB-231 mammary fat pad tumor was calculated as Area Under Curve (AUC). There was no significant difference in uptake when WT and α11-KO mice were compared (_n_ = 5). Mean ± SD

directly by stimulation of tumor cells via production of pro-tumorigenic growth factors or indirectly by for example remodeling the ECM (reviewed in [48]). Here we show that integrin α11β1, known to be expressed during myofibroblast differentiation [25, 26], seems to facilitate breast tumor growth in vivo.

In previous studies, the pro-tumorigenic abilities of integrin α11β1 have been associated with increased matrix stiffness, collagen reorganization and increased levels of IGF-2 [28, 40]. In the present study, changes in pressure homeostasis and collagen organization could both influence tumor growth and invasion. Of interest, increased tumor PIF has been linked to tumor aggressiveness in some human cancers [9, 49], and is an independent poor prognostic factor in cervical cancer [10, 50].

There have been reports suggesting that increased tumor PIF can both facilitate and inhibit tumor progression. First,

major pressure gradients due to increased tumor PIF can enhance interstitial fluid flow at and lymph drainage from the tumor margins, which probably increase the risk of cancer cells leaving the tumor. Increased flow can also facilitate tumor progression indirectly by either mechano-modulation of the tumor stroma or by changing the host immune response and thereby promote immunological tolerance (reviewed in [51, 52]). Further, in vitro elevation of tumor PIF increased proliferation of human osteosarcoma [53] and oral squamous cell carcinoma cells [54]. Similarly, in vivo lowering of tumor PIF, and thereby reduction of mechanical stretch for 24 h, reduced tumor cell proliferation in vulva and lung xenograft tumors [55]. However, contrary to these findings, increased tumor PIF may also limit uptake of nutrition and growth factors into the tumor and thereby inhibit tumor cell progression [8]. In the context of breast cancer, MDA-MB-231 cells have actually been shown to invade towards regions of higher pressure in vitro [56, 57], indicating that the elevated tumor PIF may in fact restrain breast tumor invasion. In summary, these findings demonstrate that maintenance of a high tumor PIF may be a contributing factor to integrin α11β1's pro-tumorigenic effects, but at the same time, it can have opposite effects during tumorigenesis, pinpointing the need for further preclinical investigation.

Although increased tumor PIF can be a major barrier in cancer treatment, lowering of tumor PIF by integrin α11-deficiency did not increase the uptake of the low molecular weight drug ^{3}H-5FU into MDA-MB-231 tumor interstitium. Low molecular weight compounds are transported by both diffusion and bulk flow/convection, and we have previously shown that reducing PIF can increase the uptake of the small molecular weight drugs ^{3}H-5FU [11, 58] and ^{51}Cr-EDTA [12, 59] into the tumor interstitium. However, in parallel with the results in the present study, it is evident that lowering of PIF will not always increase the uptake of low molecular

Fig. 10 Heterospheroids. The individual interstitial fluid pressures (PIF) in heterospheroids containing a mixture of mouse embryonic fibroblasts (MEFs) and MDA-MB-231 breast tumor cells (4:1) (**a**). α11-KO MEFs + MDA-MB-231 spheroids showed a significant reduction in PIF compared to WT MEFs + MDA-MB-231 spheroids. *** *p* < 0.001. Transmission electron microscopy images show collagen fibrils in both heterospheroid types (**b**)

Smeland *et al. BMC Cancer*   (2019) 19:234

Page 11 of 13

weight drugs [35, 60]. Similarly, Flessner et al. showed that decapsulation of ovarian xenografts markedly decreased PIF to zero, but did not increase penetration of the high molecular weight drug trastuzumab into the tumor [61]. In summary, probably other features of the tumor microenvironment can also contribute to the failure of transport within solid tumors [5, 61].

Our data show that integrin α11-deficiency leads to thinner and less organized collagen fibrils in the orthotopic tumor stroma. Changes in collagen composition and organization are already known to influence tumorigenesis and can predict breast cancer behavior [3]. For example, progressive deposition of collagen [62] and increased collagen fiber linearization [63, 64] are associated with breast cancer aggressiveness.

While integrin α11-deficiency influenced tumor growth and reduced PIF with concomitantly more disorganized collagen fibrils in the orthotopic tumors, no effect was seen in the MDA-MB-231 ectopic tumors. Interestingly, there was similar amount of integrin α11β1 expression in both the MDA-MB-231 models. In a previous study, we also observed that while integrin α11-deficiency reduced RM11 tumor growth, but did not affect 4 T1 tumor growth, the integrin α11β1 expression was not higher in RM11 than in 4 T1 tumors [33]. Thus, differences in integrin α11β1-expression cannot explain the contrasting effect seen in these in vivo models.

The different effects seen between the MDA-MB-231 orthotopic and ectopic tumors show that tumor location significantly influences the effect of integrin α11β1 in vivo. The tumor microenvironment displays a significant heterogeneity [65], and the subcutaneous location probably does not always give rise to a representative tissue-specific stromal infiltration [66–68]. Supporting the fact that the organ-specific fibroblasts influence breast tumor growth differently, co-injection of breast fibroblast with breast tumor cells increased tumor growth, whereas no enhancement was seen with the co-injection of skin fibroblasts [69]. The significance of the local microenvironment illustrates the complexity of in vivo studies, and may explain some of the discrepancies seen with different mouse models. This underlines the importance of choosing the appropriate preclinical model, particularly when investigating the tumor microenvironment. If possible, orthotopic models should be preferred rather than ectopic ones.

Conclusion

Our findings indicate an important role for integrin α11β1 in interstitial fluid pressure regulation in the breast tumor microenvironment. Further, since integrin α11β1 seems to impede breast cancer growth, it may be an interesting candidate for stromal targeted therapy.

Additional file

Additional file 1: Figure S1. Collagen and activated fibroblasts in MDA-MB-231 subcutaneous tumors. The total fraction of Picrosirius-red, αSMA and PDGFRβ positive staining demonstrated no differences between MDA-MB-231 subcutaneous tumors in WT and α11-KO mice (n = 3 WT and n = 4 α11-KO). Mean ± SD. (TIF 242 kb)

Smeland *et al. BMC Cancer*   (2019) 19:234

Page 12 of 13

References

1. Alluri P, Newman LA. Basal-like and triple-negative breast cancers: searching for positives among many negatives. Surg Oncol Clin N Am. 2014;23(3):567–77.
2. Lee A, Djamgoz MBA. Triple negative breast cancer: emerging therapeutic modalities and novel combination therapies. Cancer Treat Rev. 2018;62:110–22.
3. Giussani M, Merlino G, Cappelletti V, Tagliabue E, Daidone MG. Tumor-extracellular matrix interactions: identification of tools associated with breast cancer progression. Semin Cancer Biol. 2015;35:3–10.
4. Maman S, Witz IP. A history of exploring cancer in context. Nat Rev Cancer. 2018; 18:359–76.
5. Stylianopoulos T, Munn LL, Jain RK. Reengineering the physical microenvironment of tumors to improve drug delivery and efficacy: from mathematical modeling to bench to bedside. Trends Cancer. 2018;4(4):292–319.
6. Nathanson SD, Nelson L. Interstitial fluid pressure in breast cancer, benign breast conditions, and breast parenchyma. Ann Surg Oncol. 1994;1(4):333–8.
7. Less JR, Posner MC, Boucher Y, Borochovitz D, Wolmark N, Jain RK. Interstitial hypertension in human breast and colorectal tumors. Cancer Res. 1992;52(22):6371–4.
8. Heldin CH, Rubin K, Pietras K, Ostman A. High interstitial fluid pressure - an obstacle in cancer therapy. Nat Rev Cancer. 2004;4(10):806–13.
9. Curti BD, Urba WJ, Alvord WG, Janik JE, Smith JW 2nd, Madara K, Longo DL. Interstitial pressure of subcutaneous nodules in melanoma and lymphoma patients: changes during treatment. Cancer Res. 1993;53(10 Suppl):2204–7.
10. Milosevic M, Fyles A, Hedley D, Pintilie M, Levin W, Manchul L, Hill R. Interstitial fluid pressure predicts survival in patients with cervix cancer independent of clinical prognostic factors and tumor oxygen measurements. Cancer Res. 2001;61(17):6400–5.
11. Salnikov AV, Iversen VV, Koisti M, Sundberg C, Johansson L, Stuhr LB, Sjoquist M, Ahlstrom H, Reed RK, Rubin K. Lowering of tumor interstitial fluid pressure specifically augments efficacy of chemotherapy. FASEB J. 2003;17(12):1756–8.
12. Rubin K, Sjoquist M, Gustafsson AM, Isaksson B, Salvessen G, Reed RK. Lowering of tumoral interstitial fluid pressure by prostaglandin E(1) is paralleled by an increased uptake of (51)Cr-EDTA. Int J Cancer. 2000;86(5):636–43.
13. Eikenes L, Bruland OS, Brekken C, Davies Cde L. Collagenase increases the transcapillary pressure gradient and improves the uptake and distribution of monoclonal antibodies in human osteosarcoma xenografts. Cancer Res. 2004;64(14):4768–73.
14. Reed RK, Rubin K. Transcapillary exchange: role and importance of the interstitial fluid pressure and the extracellular matrix. Cardiovasc Res. 2010; 87(2):211–7.
15. Reed RK, Liden A, Rubin K. Edema and fluid dynamics in connective tissue remodelling. J Mol Cell Cardiol. 2010;48(3):518–23.
16. Berg A, Ekwall AK, Rubin K, Stjernschantz J, Reed RK. Effect of PGE1, PGI2, and PGF2 alpha analogs on collagen gel compaction in vitro and interstitial pressure in vivo. Am J Phys. 1998;274(2 Pt 2):H663–71.
17. Tiger CF, Fougerousse F, Grundstrom G, Velling T, Gullberg D. alpha11beta1 integrin is a receptor for interstitial collagens involved in cell migration and collagen reorganization on mesenchymal nonmuscle cells. Dev Biol. 2001; 237(1):116–29.
18. Stuhr LE, Reith A, Lepsoe S, Myklebust R, Wiig H, Reed RK. Fluid pressure in human dermal fibroblast aggregates measured with micropipettes. Am J Physiol Cell Physiol. 2003;285(5):C1101–8.
19. Osterholm C, Lu N, Liden A, Karlsen TV, Gullberg D, Reed RK, Kusche-Gullberg M. Fibroblast EXT1-levels influence tumor cell proliferation and migration in composite spheroids. PLoS One. 2012;7(7):e41334.
20. Lu N, Karlsen TV, Reed RK, Kusche-Gullberg M, Gullberg D. Fibroblast alpha11beta1 integrin regulates tensional homeostasis in fibroblast/A549 carcinoma Heterospheroids. PLoS One. 2014;9(7):e103173.
21. Reed RK, Rubin K, Wiig H, Rodt SA. Blockade of beta 1-integrins in skin causes edema through lowering of interstitial fluid pressure. Circ Res. 1992;71(4):978–83.
22. Rodt SA, Ahlen K, Berg A, Rubin K, Reed RK. A novel physiological function for platelet-derived growth factor-BB in rat dermis. J Physiol. 1996;495 (Pt 1):193–200.
23. Reed RK, Berg A, Gjerde EA, Rubin K. Control of interstitial fluid pressure: role of beta1-integrins. Semin Nephrol. 2001;21(3):222–30.
24. Meyer FA. Macromolecular basis of globular protein exclusion and of swelling pressure in loose connective tissue (umbilical cord). Biochim Biophys Acta. 1983;755(3):388–99.
25. Carracedo S, Lu N, Popova SN, Jonsson R, Eckes B, Gullberg D. The fibroblast integrin alpha11beta1 is induced in a mechanosensitive manner involving activin a and regulates myofibroblast differentiation. J Biol Chem. 2010;285(14): 10434–45.
26. Talior-Volodarsky I, Connelly KA, Arora PD, Gullberg D, McCulloch CA. alpha11 integrin stimulates myofibroblast differentiation in diabetic cardiomyopathy. Cardiovasc Res. 2012;96(2):265–75.
27. Schulz JN, Plomann M, Sengle G, Gullberg D, Krieg T, Eckes B. New developments on skin fibrosis - essential signals emanating from the extracellular matrix for the control of myofibroblasts. Matrix Biol. 2018;68-69:522–32.
28. Navab R, Strumpf D, To C, Pasko E, Kim KS, Park CJ, Hai J, Liu J, Jonkman J, Barczyk M, et al. Integrin alpha11beta1 regulates cancer stromal stiffness and promotes tumorigenicity and metastasis in non-small cell lung cancer. Oncogene. 2015;35:1899–908.
29. Svendsen OS, Barczyk MM, Popova SN, Liden A, Gullberg D, Wiig H. The alpha11beta1 integrin has a mechanistic role in control of interstitial fluid pressure and edema formation in inflammation. Arterioscler Thromb Vasc Biol. 2009;29(11):1864–70.
30. Liden A, Karlsen TV, Guss B, Reed RK, Rubin K. Integrin alphaV beta3 can substitute for collagen-binding beta1 -integrins in vivo to maintain a homeostatic interstitial fluid pressure. Exp Physiol. 2018;103:629–34.
31. Popova SN, Rodriguez-Sanchez B, Liden A, Betsholtz C, Van Den Bos T, Gullberg D. The mesenchymal alpha11beta1 integrin attenuates PDGF-BB-stimulated chemotaxis of embryonic fibroblasts on collagens. Dev Biol. 2004;270(2):427–42.
32. Popova SN, Barczyk M, Tiger CF, Beertsen W, Zigrino P, Aszodi A, Miosge N, Forsberg E, Gullberg D. Alpha11 beta1 integrin-dependent regulation of periodontal ligament function in the erupting mouse incisor. Mol Cell Biol. 2007;27(12):4306–16.
33. Reigstad I, Smeland HY, Skogstrand T, Sortland K, Schmid MC, Reed RK, Stuhr L. Stromal integrin alpha11beta1 affects RM11 prostate and 4T1 breast xenograft tumors differently. PLoS One. 2016;11(3):e0151663.
34. Wiig H, Reed RK, Aukland K. Measurement of interstitial fluid pressure: comparison of methods. Ann Biomed Eng. 1986;14(2):139–51.
35. Moen I, Tronstad KJ, Kolmannskog O, Salvesen GS, Reed RK, Stuhr LE. Hyperoxia increases the uptake of 5-fluorouracil in mammary tumors independently of changes in interstitial fluid pressure and tumor stroma. BMC Cancer. 2009;9:446.
36. Barczyk M, Carracedo S, Gullberg D. Integrins. Cell Tissue Res. 2010;339(1):269–80.
37. Desgrosellier JS, Cheresh DA. Integrins in cancer: biological implications and therapeutic opportunities. Nat Rev Cancer. 2010;10(1):9–22.
38. Zeltz C, Gullberg D. The integrin-collagen connection--a glue for tissue repair? J Cell Sci. 2016;129(4):653–64.
39. Hamidi H, Ivaska J. Every step of the way: integrins in cancer progression and metastasis. Nat Rev Cancer. 2018;18(9):532–47.
40. Zhu CQ, Popova SN, Brown ER, Barsyte-Lovejoy D, Navab R, Shih W, Li M, Lu M, Jurisica I, Penn LZ, et al. Integrin alpha 11 regulates IGF2 expression in fibroblasts to enhance tumorigenicity of human non-small-cell lung cancer cells. Proc Natl Acad Sci U S A. 2007;104(28):11754–9.
41. Navab R, Strumpf D, Bandarchi B, Zhu CQ, Pintilie M, Ramnarine VR, Ibrahimov E, Radulovich N, Leung L, Barczyk M, et al. Prognostic gene-expression signature of carcinoma-associated fibroblasts in non-small cell lung cancer. Proc Natl Acad Sci U S A. 2011;108(17):7160–5.
42. Parajuli H, Teh MT, Abrahamsen S, Christoffersen I, Neppelberg E, Lybak S, Osman T, Johannessen AC, Gullberg D, Skarstein K, et al. Integrin alpha11 is overexpressed by tumour stroma of head and neck squamous cell carcinoma and correlates positively with alpha smooth muscle actin expression. J Oral Pathol Med. 2017;46(4):267–75.
43. Stylianopoulos T, Martin JD, Chauhan VP, Jain SR, Diop-Frimpong B, Bardeesy N, Smith BL, Ferrone CR, Hornicek FJ, Boucher Y, et al. Causes, consequences, and remedies for growth-induced solid stress in murine and human tumors. Proc Natl Acad Sci U S A. 2012;109(38):15101–8.
44. Stapleton S, Dunne M, Milosevic M, Tran CW, Gold MJ, Vedadi A, McKee TD, Ohashi PS, Allen C, Jaffray DA. Radiation and heat improve the delivery and efficacy of Nanotherapeutics by modulating Intratumoral fluid dynamics. ACS Nano. 2018;12(8):7583–600.
45. Boucher Y, Jain RK. Microvascular pressure is the principal driving force for interstitial hypertension in solid tumors: implications for vascular collapse. Cancer Res. 1992;52(18):5110–4.
46. Oldberg A, Kalamajski S, Salnikov AV, Stuhr L, Morgelin M, Reed RK, Heldin NE, Rubin K. Collagen-binding proteoglycan fibromodulin can determine

Smeland *et al. BMC Cancer*   (2019) 19:234

Page 13 of 13

stroma matrix structure and fluid balance in experimental carcinoma. Proc Natl Acad Sci U S A. 2007;104(35):13966–71.

47. Levick JR. Flow through interstitium and other fibrous matrices. Q J Exp Physiol. 1987;72(4):409–37.

48. LeBleu VS, Kalluri R. A peek into cancer-associated fibroblasts: origins, functions and translational impact. Dis Model Mech. 2018;11(4). https://doi.org/10.1242/dmm.029447.

49. Mori T, Koga T, Shibata H, Ikeda K, Shiraishi K, Suzuki M, Iyama K. Interstitial fluid pressure correlates Clinicopathological factors of lung Cancer. Ann Thorac Cardiovasc Surg. 2015;21(3):201–8.

50. Yeo SG, Kim JS, Cho MJ, Kim KH, Kim JS. Interstitial fluid pressure as a prognostic factor in cervical cancer following radiation therapy. Clin Cancer Res. 2009;15(19):6201–7.

51. Swartz MA, Lund AW. Lymphatic and interstitial flow in the tumour microenvironment: linking mechanobiology with immunity. Nat Rev Cancer. 2012;12(3):210–9.

52. Shieh AC, Swartz MA. Regulation of tumor invasion by interstitial fluid flow. Phys Biol. 2011;8(1):015012.

53. Nathan SS, DiResta GR, Casas-Ganem JE, Hoang BH, Sowers R, Yang R, Huvos AG, Gorlick R, Healey JH. Elevated physiologic tumor pressure promotes proliferation and chemosensitivity in human osteosarcoma. Clin Cancer Res. 2005;11(6):2389–97.

54. Yu T, Liu K, Wu Y, Fan J, Chen J, Li C, Zhu G, Wang Z, Li L. High interstitial fluid pressure promotes tumor cell proliferation and invasion in oral squamous cell carcinoma. Int J Mol Med. 2013;32(5):1093–100.

55. Hofmann M, Guschel M, Bernd A, Bereiter-Hahn J, Kaufmann R, Tandi C, Wiig H, Kippenberger S. Lowering of tumor interstitial fluid pressure reduces tumor cell proliferation in a xenograft tumor model. Neoplasia. 2006;8(2):89–95.

56. Tien J, Truslow JG, Nelson CM. Modulation of invasive phenotype by interstitial pressure-driven convection in aggregates of human breast cancer cells. PLoS One. 2012;7(9):e45191.

57. Piotrowski-Daspit AS, Tien J, Nelson CM. Interstitial fluid pressure regulates collective invasion in engineered human breast tumors via snail, vimentin, and E-cadherin. Integr Biol. 2016;8(3):319–31.

58. Stuhr LE, Salnikov AV, Iversen VV, Salvesen G, Rubin K, Reed RK. High-dose, short-term, anti-inflammatory treatment with dexamethasone reduces growth and augments the effects of 5-fluorouracil on dimethyl-alpha-benzanthracene-induced mammary tumors in rats. Scand J Clin Lab Invest. 2006;66(6):477–86.

59. Pietras K, Ostman A, Sjoquist M, Buchdunger E, Reed RK, Heldin CH, Rubin K. Inhibition of platelet-derived growth factor receptors reduces interstitial hypertension and increases transcapillary transport in tumors. Cancer Res. 2001;61(7):2929–34.

60. Jevne C, Moen I, Salvesen G, Reed RK, Stuhr L. A reduction in the interstitial fluid pressure per se, does not enhance the uptake of the small molecule weigh compound 5-fluoruracil into 4T1 mammary tumors. Drugs Ther Stud. 2011;1:e5.

61. Flessner MF, Choi J, Credit K, Deverkadra R, Henderson K. Resistance of tumor interstitial pressure to the penetration of intraperitoneally delivered antibodies into metastatic ovarian tumors. Clin Cancer Res. 2005;11(8):3117–25.

62. Provenzano PP, Inman DR, Eliceiri KW, Knittel JG, Yan L, Rueden CT, White JG, Keely PJ. Collagen density promotes mammary tumor initiation and progression. BMC Med. 2008;6:11.

63. Conklin MW, Eickhoff JC, Riching KM, Pehlke CA, Eliceiri KW, Provenzano PP, Friedl A, Keely PJ. Aligned collagen is a prognostic signature for survival in human breast carcinoma. Am J Pathol. 2011;178(3):1221–32.

64. Acerbi I, Cassereau L, Dean I, Shi Q, Au A, Park C, Chen YY, Liphardt J, Hwang ES, Weaver VM. Human breast cancer invasion and aggression correlates with ECM stiffening and immune cell infiltration. Integr Biol. 2015; 7(10):1120–34.

65. Junttila MR, de Sauvage FJ. Influence of tumour micro-environment heterogeneity on therapeutic response. Nature. 2013;501(7467):346–54.

66. Gould SE, Junttila MR, de Sauvage FJ. Translational value of mouse models in oncology drug development. Nat Med. 2015;21(5):431–9.

67. Ruggeri BA, Camp F, Miknyoczki S. Animal models of disease: pre-clinical animal models of cancer and their applications and utility in drug discovery. Biochem Pharmacol. 2014;87(1):150–61.

68. Zhao X, Li L, Starr TK, Subramanian S. Tumor location impacts immune response in mouse models of colon cancer. Oncotarget. 2017;8(33):54775–87.

69. Yashiro M, Ikeda K, Tendo M, Ishikawa T, Hirakawa K. Effect of organ-specific fibroblasts on proliferation and differentiation of breast cancer cells. Breast Cancer Res Treat. 2005;90(3):307–13.

Supplementary material.

Fig S1. Collagen and activated fibroblasts in MDA-MB-231 subcutaneous tumors. The total fraction of Picrosirius-red, αSMA and PDGFRβ positive staining demonstrated no differences between MDA-MB-231 subcutaneous tumors in WT and α11-KO mice (n=3 WT and n=4 α11-KO). Mean ± SD.

Fig S1.

ORIGINAL ARTICLE
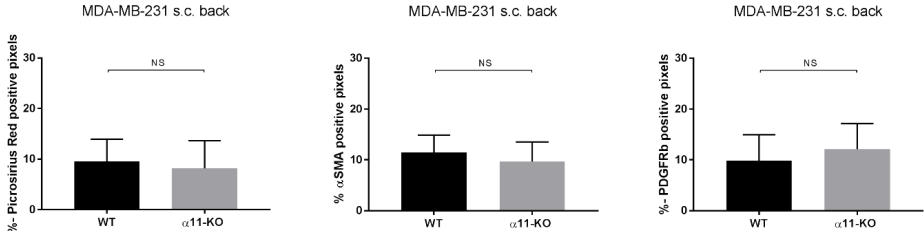
Integrin α11β1 is expressed in breast cancer stroma and associates with aggressive tumor phenotypes

Hilde Ytre-Hauge Smeland[1,2] (ORCID), Cecilie Askeland[1,3], Elisabeth Wik[1,3], Gøril Knutsvik[1,3], Anders Molven[3,4], Reidunn J Edelmann[1], Rolf K Reed[2], David J Warren[5], Donald Gullberg[2], Linda Stuhr[2] and Lars A Akslen[1,3]*

[1]Centre for Cancer Biomarkers CCBIO, Department of Clinical Medicine, University of Bergen, Bergen, Norway
[2]Centre for Cancer Biomarkers CCBIO, Department of Biomedicine, University of Bergen, Bergen, Norway
[3]Department of Pathology, Haukeland University Hospital, Bergen, Norway
[4]Gade Laboratory for Pathology, Department of Clinical Medicine, University of Bergen, Bergen, Norway
[5]Department of Medical Biochemistry, Oslo University Hospital, Oslo, Norway

*Correspondence: Lars A Akslen, Centre for Cancer Biomarkers CCBIO, Department of Clinical Medicine, Section for Pathology, University of Bergen, Haukeland University Hospital, N-5021 Bergen, Norway. E-mail: lars.akslen@uib.no

Abstract

Cancer-associated fibroblasts are essential modifiers of the tumor microenvironment. The collagen-binding integrin α11β1 has been proposed to be upregulated in a pro-tumorigenic subtype of cancer-associated fibroblasts. Here, we analyzed the expression and clinical relevance of integrin α11β1 in a large breast cancer series using a novel antibody against the human integrin α11 chain. Several novel monoclonal antibodies against the integrin α11 sub-unit were tested for use on formalin-fixed paraffin-embedded tissues, and Ab 210F4B6A4 was eventually selected to investigate the immunohistochemical expression in 392 breast cancers using whole sections. mRNA data from METABRIC and co-expression patterns of integrin α11 in relation to αSMA and cytokeratin-14 were also investigated. Integrin α11 was expressed to varying degrees in spindle-shaped cells in the stroma of 99% of invasive breast carcinomas. Integrin α11 co-localized with αSMA in stromal cells, and with αSMA and cytokeratin-14 in breast myoepithelium. High stromal integrin α11 expression (66% of cases) was associated with aggressive breast cancer features such as high histologic grade, increased tumor cell proliferation, ER negativity, HER2 positivity, and triple-negative phenotype, but was not associated with breast cancer specific survival at protein or mRNA levels. In conclusion, high stromal integrin α11 expression was associated with aggressive breast cancer phenotypes.

Keywords: integrin α11β1; monoclonal antibody; breast cancer; cancer associated fibroblasts; myoepithelial cells; clinico-pathologic features

Introduction

Breast cancer is a heterogeneous disease developed from genetically altered mammary epithelial cells, and there is a complex interplay between tumor cells and the surrounding tumor microenvironment (TME). The TME consists of various stromal cells, the extracellular matrix (ECM) scaffold, and the interstitial fluid, and both cellular and noncellular components have been shown to play an active role in tumor development, progression and metastasis [1]. Features of the TME contribute to clinically relevant variations in breast cancer phenotypes and have also been shown to predict patient outcome [2,3].

Integrins are transmembrane cell-surface receptors crucial for bidirectional communication between cells and the surrounding ECM [4]. The collagen receptor integrin α11β1 has emerged as a potentially important marker which is upregulated in fibroblasts during their differentiation into an activated phenotype [5–7]. Activated fibroblasts in the TME, termed cancer-associated fibroblasts (CAFs), constitute an abundant stromal cell type, especially in tumors with high stromal content such as pancreatic and breast carcinomas [1,8].

Accumulating data suggest the existence of diverse CAF subtypes, which differ in their biological functions, source of origin and expression of various markers [9–14]. Different fibroblasts may vary in their proliferative, secretory and contractile abilities and, most importantly, their influence on tumor growth and progression [9–14].

Integrin α11β1 contributes to fibroblast function in wound healing, fibrosis and in different tumor models (reviewed in Zeltz and Gullberg [5]), binds to fibrillar collagen [15], and has been linked to collagen reorganization [5,15] and tumor interstitial fluid pressure [16,17]. *In vivo*, stromal integrin α11-deficiency reduced the growth of triple-negative breast cancer [16] and prostate cancer xenografts [18], and reduced primary tumor growth [19,20] and metastasis [20] in lung cancer xenografts models. Thus, integrin α11β1 could potentially represent a novel marker for a tumor-supportive subtype of CAFs and thereby play an important role in breast cancer progression.

The lack of reliable anti-human integrin α11 antibodies has limited the investigation of integrin α11 in retrospective studies using formalin-fixed and paraffin-embedded (FFPE) tumor material. We here present for the first time a study of integrin α11 expression in a large human breast cancer cohort with long-term follow-up, using a new in-house antibody specific for the human integrin α11 chain, aiming to investigate the expression of integrin α11 in human breast cancer, associations with aggressive phenotypes, as well as potential prognostic impact.

Materials and methods

Anti-human integrin α11 antibodies

Mouse monoclonal antibodies reactive to the extracellular domain of the integrin α11 subunit were generated by NanoTools (Teningen, Germany) for CCBIO (Centre of Cancer Biomarkers, University of Bergen, Bergen, Norway) as described in [21] and conducted in accordance with the German Animal Welfare Act and approved by the local German Authorities (RP Freiburg, AZ35/9185.82/I-13/03). In brief, mice were immunized with soluble human integrin α11β1. Primary hybridoma screening was performed as described in [21]. In brief, selected hybridomas were reactive to C2C12-α11 cells, but not to C2C12, C2C12-α2 cells or A431 (expressing integrin β1 and a variety of integrin α chains such as α2, α3, and α5, but not integrin α11 [22]). Secondary hybridoma screening was performed with flow cytometry and

western blotting as described elsewhere [23]. Anti-integrin α11 antibodies were then tested on FFPE tissue.

Mouse monoclonal antibodies reactive to the cytoplasmic domain of integrin α11 subunit were generated using the peptide H-CRREPGLDPTPKVLE-OH by Oslo University Hospital (Oslo, Norway). The peptide was custom-synthesized and conjugated to keyhole limpet hemocyanin (KLH) (Mimotopes, Clayton, Australia). BALB/c mice were immunized with the peptide-KLH conjugate and hybridomas constructed by fusion of splenocytes with the NS0 myeloma cell line (approved by the Norwegian Food Safety Authority with permit number 7903). Primary hybridoma screening was performed using antibody capture assays with biotinylated peptide (Biotin-SGSGRREP GLDPTPKVLE-OH) presented on streptavidin-coated 96-well microplates (Wallac Oy, Turku, Finland). Secondary screening was undertaken by western blotting and immunostaining of integrin α11-positive and -negative cell lines and also frozen sections of pancreatic ductal adenocarcinoma (PDAC). D120.4 was then selected for use on FFPE tissue.

Monoclonal antibodies were purified from hybridoma culture supernatants by protein-A chromatography.

Cell culture

The integrin α11- or α2- overexpressing C2C12 cell lines, C2C12-α11, or C2C12-α2, were prepared as described previously [15], while U2OS and HEK293 were purchased from the American Type Culture Collection (ATCC, Manassas, VA, USA). All cells were cultured in DMEM with Glutamax (Gibco, Gaithersburg, MD, USA) supplemented with 10% fetal bovine serum, 100 units/ml of penicillin and 0.1 mg/ml of streptomycin (all from GE Healthcare, Chicago, IL, USA) under standard culture conditions (5% CO_2, 37 °C).

Western blotting and RT-qPCR

The cells were cultured to subconfluence and washed with PBS, lysed and collected in RIPA buffer (150 mM NaCl, 50 mM Tris base, 0.1% sodium dodecyl sulfate, 12 mM deoxycholate, 1% Nonidet-P40, 1% Triton X-100, pH 8) and supplemented with protease inhibitors (Roche Diagnostics, Basel, Switzerland). Protein concentration was determined by BCA assay (Bio-Rad, Hercules, CA, USA) after centrifugation. Of cleared lysates, 20 μg were analyzed by SDS-PAGE and blotted onto PVDF membranes (Millipore, Burlington, MA, USA). The antibodies used were as

follows: mouse anti-human monoclonal integrin α11 antibody 210F4B6A4 (custom-made by NanoTools for CCBIO) (2.9 µg/ml), mouse anti-human monoclonal integrin α11 antibody D120.4 (custom-made by Oslo University Hospital) (2.8 µg/ml), rabbit anti-human polyclonal integrin α11 antibody [24] (1,9 µg/ml), anti-β-actin (Sigma–Aldrich, Steinheim, Germany) (1:5000), in addition to goat anti-rabbit and goat anti-mouse HRP-conjugated antibodies (Santa Cruz Biotechnology, Dallas, TX, USA) (1:5000). Chemiluminescence signals were developed using the ECL Western-blotting systems kit (GE Healthcare) and photographed using the ChemiDoc XRS device and the Quantity One 1-D Analysis Software (Bio-Rad).

RT-qPCR was performed as previously described [6]. In brief, total RNA was prepared from the cells using RNeasy Mini Kit (Qiagen, Hilden, Germany), and 1 µg RNA was used for reverse transcription to cDNA using iScript Reverse Transcription Supermix (Bio-Rad). qPCR mixtures were prepared with 20 ng of reverse-transcribed cDNA as a template, along with 0.5 µM of each primer, in a 10 µl qPCR using iQ SYBR Green Supermix (Bio-Rad). The qPCR was performed in a LightCycler 480 Instrument II (Roche Diagnostics). The reactions were prepared in triplicate for individual cDNA sample along with the negative controls where no cDNA was added for each primer pair. The experiment was repeated three times. The primers used were for target gene *ITGA11* and two references genes 18S rRNA and β-actin, and their sequences are shown in Table 1.

FFPE cell pellets

The cell lines were collected at subconfluence, centrifuged and washed with PBS. Plasma (Octaplas, Haukeland University Hospital, Bergen, Norway) and thrombin (Merck, Darmstadt, Germany) were added sequentially, and the pellets were fixed in 4% formaldehyde for 24 h and transferred to ethanol/xylene prior to embedding in paraffin wax.

Pancreatic ductal adenocarcinomas

Expression of the integrin α11 chain was investigated in corresponding cryosections and FFPE sections from five different PDACs from a research biobank (Regional Ethical Committee approval 2013/1772) collected at Haukeland University Hospital [25].

Breast cancer series

Integrin α11 expression was investigated in a population-based cohort of 534 women diagnosed with primary invasive breast carcinoma (aged 50–69 at diagnosis) during 1996–2003 who resided in Hordaland County in Norway, as described previously [26]; treatment was given according to standard national guidelines at the time. Patients with distant metastatic disease at diagnosis were not included. Also, 14 cases were not included because of insufficient tissue in remaining blocks, leaving 520 cases for initial inclusion. Follow-up data were provided by the Norwegian Cause of Death Registry. Median follow-up time of survivors was 216 months (range 166–256), and last follow-up date was 30 June 2017. The study was approved by the Regional Committee for Medical and Health Sciences Research Ethics (REK #2014/1984), and was performed in accordance with the Declaration of Helsinki. In accordance with national ethics guidelines and procedures for such retrospective studies, all participants were contacted with written information on the study and asked to respond if they objected.

Immunohistochemistry

Cryosections of PDACs (4–5 µm) were fixed in acetone, rehydrated with PBS, and endogenous peroxidase activity was blocked with peroxidase block (Dako, K4007, Agilent, Santa Clara, CA, USA). Anti-integrin α11 210F4B6A4 (0.39 µg/ml) was incubated in a humidity chamber overnight (4 °C), followed by HRP-labeled anti-mouse antibody (Dako, K4001) (30 min), diaminobenzidine (DAB) (5 min) and hematoxylin (Dako, S2020) (3 min). A polyclonal antibody [24] and the new monoclonal antibody 203E3, recently demonstrated to be suitable for immunostaining of cryosections [21], were used as controls.

Immunohistochemical staining of FFPE tumor tissue was done on whole tissue sections (4–5 µm) mounted on poly-lysine coated glasses. The sections were baked

Table 1. Primer sequences for qPCR

Gene symbol	Forward primer	Reverse primer	Amplicon size (bp)
ITGA11	5′-CACGACATCAGTGGCAATAAG	5′-GACCCTTCCCAGGTTGAGTT	132
18S rRNA	5′-GCAATTATTCCCCATGAACG	5′-GGGACTTAATCAACGCAAGC	68
ACTB	5′-GTGTGATGGTGGGAATGGGT	5′-TCTGGGTCATCATTTCACGGTTGG	240

at 56 °C for 48 h followed by cooling to room temperature (RT) (20 min), dewaxed with xylene/ethanol, and antigen retrieval was performed in Target Retrieval Solution pH 9 (Dako, K8010) (120 °C, 10 min) in a pressure cooker (Decloaking Chamber Plus, Biocare Medical, Pacheco, CA, USA). Staining was performed using a Dako autostainer Plus (Dako) with EnVision FLEX+ kit (Dako, K801021-2). Peroxidase Block was applied for 8 min, followed by incubation with anti-integrin α11 210F4B6A4 (0.29 μg/ml) (1 h RT), FLEX+ Mouse Linker (Dako, K8022) (15 min), FLEX+ HRP (20 min), DAB (5 min) and hematoxylin (3 min). Integrin α11-positive and integrin α11-negative FFPE cell pellets in addition to serial sections from one invasive breast carcinoma were used as biological controls. An anti-human IgG2b antibody was used as isotype control. Positive and negative controls were included in each run. Efforts were made to reduce the loss of tissue, such as baking prior to the IHC protocol, and using freshly cut sections and poly-lysine coated glasses.

For double and triple immunohistochemical staining, deparaffinization/rehydration and antigen retrieval were done as described above. Triple staining with antibodies against integrin α11, αSMA and factor VIII (FVIII) was done on 20 FFPE invasive breast carcinomas with Ventana autostainer (Discovery Ultra, Ventana Medical systems, Tuscon, AZ, USA). After peroxidase block (Roche Diagnostics, 760–4840) (8 min), the sections were incubated with anti-integrin α11 210F4B6A4 (0.29 μg/ml) (1 h RT), Omnimap anti-mouse HRP (Roche Diagnostics, 760–4310) (16 min) and amplification with Amp HQ kit (Roche Diagnostics, 760–052) (20 min) and anti-HQ HRP (Roche Diagnostics, 760–4602) (16 min) following visualization with teal (Roche Diagnostics, 760–247) (32 + 16 min). The sections were denatured in CC2 (Ventana, 950–243) (8 min 100 °C), and incubated with anti-αSMA (Dako, M0851) (1:100, 36 °C 32 min), Ultramap-anti mouse AP (Roche Diagnostics, 760–4312) (16 min) and visualized with yellow (Roche Diagnostics, 760–239) (44 min). After another denaturation with reaction buffer (Ventana, 95–300) (95 °C 20 min), the sections were incubated with anti-FVIII (Dako, A0088) (1:1600, 1 h RT), Ultramap anti-rabbit HRP (Roche Diagnostics, 760–4315) (12 min) and then purple (Roche Diagnostics, 760–229) (20 min).

Double immunofluorescent staining with antibodies against integrin α11 and cytokeratin-14 (CK14) was done on 15 FFPE invasive breast carcinomas. After antigen retrieval, the sections were incubated with PBS/1% BSA/0.1% TritonX-100, followed by anti-human integrin α11 210F4B6A4 (1.5 μg/ml) in combination with anti-CK14 (Abcam, Cambridge, United Kingdom, 119695) (1:700) (1 h RT), and then Alexa Fluor® 594 goat anti-mouse IgG (AffiniPure, Jackson ImmunoResearch, West Grove, PA, USA, 115-585-062) (1:700) and Alexa Fluor® 488 goat anti-rabbit IgG (AffiniPure, 111-545-045) (1:700) (1 h RT). Mounting was done with ProLong™ Gold Antifade Mountant with DAPI (ThermoFisher, Waltham, MA, USA, P36931) and results recorded using a Zeiss Axioscope microscope equipped with Colibri 7 light source, AxioCam 503 mono camera and Axiovision software.

Evaluation of staining

Breast cancer sections were examined blinded for patient characteristics and outcome by a senior breast cancer pathologist, LAA, and HYHS. Of 520 stained sections, 128 tumors were excluded from evaluation because of inadequate tissue remaining after the antigen retrieval procedure. Altogether 392 cases were evaluated for integrin α11-positive staining by a staining index (SI) score (0–9) which was obtained by multiplying the score for intensity of staining (0 = absent, 1 = weak, 2 = moderate, or 3 = strong) by the score for percentage of fibrous stroma stained (<10% = 1, 10–50% = 2, >50% = 3) [27]. Only positive staining in the tumor stroma was scored, and areas with hemorrhage and necrosis were avoided. Intratumor heterogeneity of stromal integrin α11 expression was also noted.

As there is no pre-established cut-off value for integrin α11, the distribution and frequency histograms for SI were evaluated. As seen in supplementary material, Figure S1, there was a clear binary distribution, and the breast cancer cases were therefore separated into integrin α11-low expression (SI 0–3 = 34%) and integrin α11-high expression (SI 4–9 = 66%) by this distribution, corresponding to a cut-off value at the lower tertile.

Gene expression data sets

Gene expression microarray data generated by the Molecular Taxonomy of Breast Cancer International Consortium (METABRIC) were included for analyses of *ITGA11* mRNA expression across breast cancer molecular subtypes and its relation to survival (discovery and validation cohorts) [28]. Cases of the normal-like molecular subtype were excluded, leaving $n = 939$ and $n = 843$ for analyses in the two cohorts. Two *ITGA11* probes were present in the METABRIC data. The max probe expression value was selected for

analyses [29]. Lower tertile was applied as cut-off, corresponding to the cut-off level of the protein staining.

Statistical analyses

Associations between categorical data were estimated using the Pearson's chi-square test and OR were computed. Differences in integrin α11 protein and mRNA expression across molecular subgroups were tested by Kruskal–Wallis test. Results were accepted as statistically significant when $p < 0.05$ (two-sided). Univariate survival data were analyzed by the Kaplan–Meier method, with death from breast cancer as end-point (time in months from diagnosis until death from breast cancer), and the significance determined by the log-rank test. Statistical analyses were performed using the IBM SPSS Statistics for Windows, Version 25.0 (IBM Corp, Armonk, NY, USA).

Results

Antibody specificity

As lack of reliable anti-human integrin α11 antibodies has limited the investigation of integrin α11 on FFPE tumor material, several novel monoclonal antibodies specific for human integrin α11 chain were generated and tested on FFPE tissues before use on the breast cancer cohort. Hybridoma screening and antibody characterization are demonstrated in [21,23], respectively. In brief, clones specific to integrin α11 chain, but not to other integrin subunits, such as integrin β1 and α2, were chosen. Furthermore, the specificity of both 210F4B6A4 and D120.4 was validated by western blotting of cell lysates, and a polyclonal antibody was used as control [24]. Both clone 210F4B6A4 and D120.4 verified high expression of integrin α11 in C2C12-α11 cells and no expression in C2C12-α2 cells (Figure 1A). The human osteosarcoma cell line, U2OS, showed low integrin α11 expression while the human embryonic kidney cell line, HEK293, was negative for integrin α11 (Figure 1A). RT-qPCR confirmed the expression levels of integrin α11 in these cell lines (Figure 1B).

The clones were tested on FFPE material, and it became evident that high temperature was crucial to unmask the antigen. Extensive testing of different protocols was done to find the most gentle antigen retrieval protocol with high sensitivity. Several antibodies showed distinct staining on FFPE tissue, including 210F4B6A4 and D120.4. As 210F4B6A4

showed markedly strongest staining on FFPE tissue, this antibody was used for further analyses. Staining of FFPE cell pellets shows the validity of 210F4B6A4 on FFPE material (Figure 1C). Since other anti-integrin α11 antibodies have been shown to lack specificity on FFPE tissue, a positive reagent control was not applicable. Integrin α11 has recently been shown to be highly upregulated in PDAC [21], and corresponding cryo- and FFPE sections from the same PDACs were used in the calibration of the IHC protocol, where the polyclonal integrin α11 antibody and 203E3 [21] were used as a control for the cryosections. After optimizing the antigen retrieval protocol on FFPE sections from cell pellets, PDACs and invasive breast carcinomas, similar intensity and expression pattern were seen in corresponding cryo- and FFPE sections from five different PDACs (one representative of five different tumors is shown in Figure 1D). These sections were then used as biological controls. To exclude run-to-run variability, serial sections from five FFPE invasive breast carcinomas were stained.

Integrin α11 is expressed in fibroblast-like cells in breast cancer stroma

Positive staining was mainly seen as a fibrillar staining pattern in the breast cancer stroma (Figure 2A–I and see supplementary material, Figure S2A–I). Of note, cells positive for integrin α11 were mainly spindle-shaped, fibroblast-like cells, and the staining was often markedly accentuated in direct proximity to the cancer cells, indicating a 'border' between the epithelial component and the ECM (Figure 2B,D,E,G–I and see supplementary material, Figure S2A,B and D–F). In addition to this fibrillar stromal positivity, membrane staining of some of the breast myoepithelial cells was also seen (Figure 3A–I).

Integrin α11 was expressed in spindle-shaped stromal cells in 389 of 392 cases that were included for evaluation (99%). The stromal staining was markedly heterogeneous in 62% of the cases with an uneven distribution of integrin α11 expression (see supplementary material, Figure S3). Most of these heterogeneous cases showed highest integrin α11 expression in the central parts of the tumor with gradual loss of expression towards the invasive front (see supplementary material, Figure S3). Integrin α11 expression was most often weak in areas showing immune cell infiltration (see supplementary material, Figure S2B), and fibrotic, ECM-rich tissue was often positive for integrin α11 (see supplementary material, Figure S2C). No convincing staining of tumor cells was observed, not even
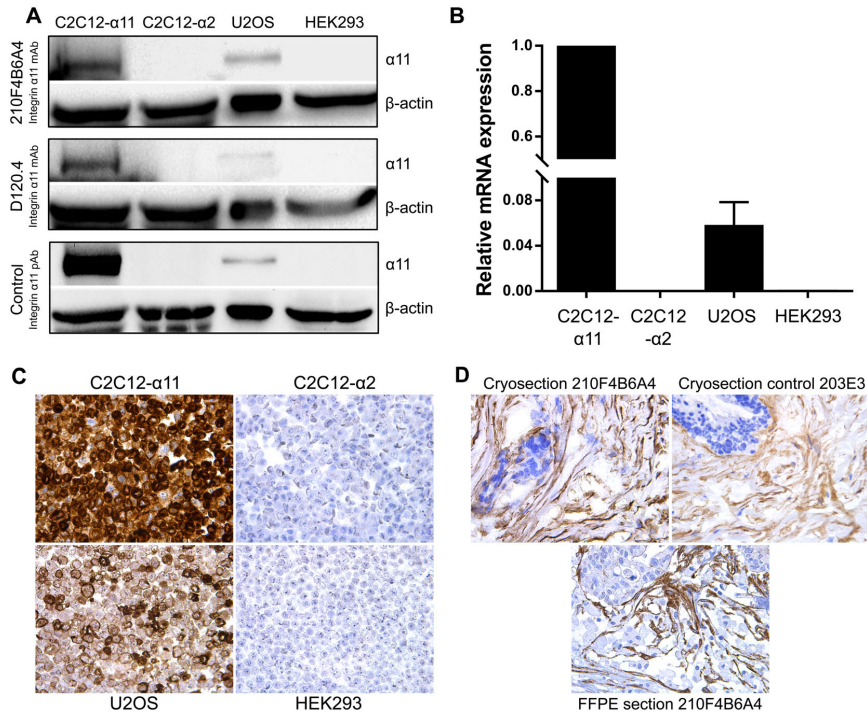
Figure 1. Validation of monoclonal antibodies against the integrin α11 subunit. Integrin α11-positive cell lines (C2C12-α11 and U2OS) and integrin α11-negative cell lines (C2C12-α2 and HEK293) were used to validate the monoclonal antibodies. Western blots show only expression of integrin α11 in cell lysates from integrin α11-positive cells using the monoclonal antibodies (mAbs) 210F4B6A4 and D120.4 where a polyclonal antibody (pAb) was used as control (A). Comparison of mRNA expression of integrin α11 by RT-qPCR (B). *ITGA11* expression level is presented as the fold change in each cell line relative to C2C12-α11. Each column represents the average fold change from three experiments, and error bar indicates standard deviation. Staining with 210F4B6A4 of FFPE cell pellets confirmed the validity on FFPE material (C). Cases of pancreatic ductal adenocarcinoma stained with 210F4B6A4 showed similar stromal expression pattern in corresponding cryosections and FFPE sections; images from one representative tumor are shown in (D). 203E3 was used as control for the cryosections. Magnification: ×400.

in invasive breast carcinomas with basal-like features (see supplementary material, Figure S2G–I).

Integrin α11 co-localizes with αSMA in fibroblast-like cells and with αSMA and cytokeratin-14 in breast myoepithelium

To further characterize the expression of integrin α11, we investigated its expression in relation to αSMA, CK14, and FVIII in invasive breast carcinomas. Integrin α11 and αSMA expression showed a clear co-localization in stromal spindle-shaped cells (Figure 2D–F), but spindle-shaped cells only positive for one of the markers were also observed (Figure 2F).

αSMA-positive, integrin α11-negative fibroblasts were more prevalent than integrin α11-positive, αSMA-negative fibroblasts. A minority of the vessels showed weak integrin α11 expression.

Furthermore, integrin α11 expression was observed in breast myoepithelial cells associated with ductal carcinoma *in situ* (DCIS), where it co-localized with αSMA (Figure 3E–F) and CK14 (Figure 3G–I). Integrin α11-positive myoepithelial cells were more frequent and with higher intensity in DCIS (Figure 3B–C,E–F, and G–I) compared to benign-looking breast tissues where integrin α11 was mostly negative (Figure 3D). Nevertheless, positive integrin α11 staining was also observed in a small minority of
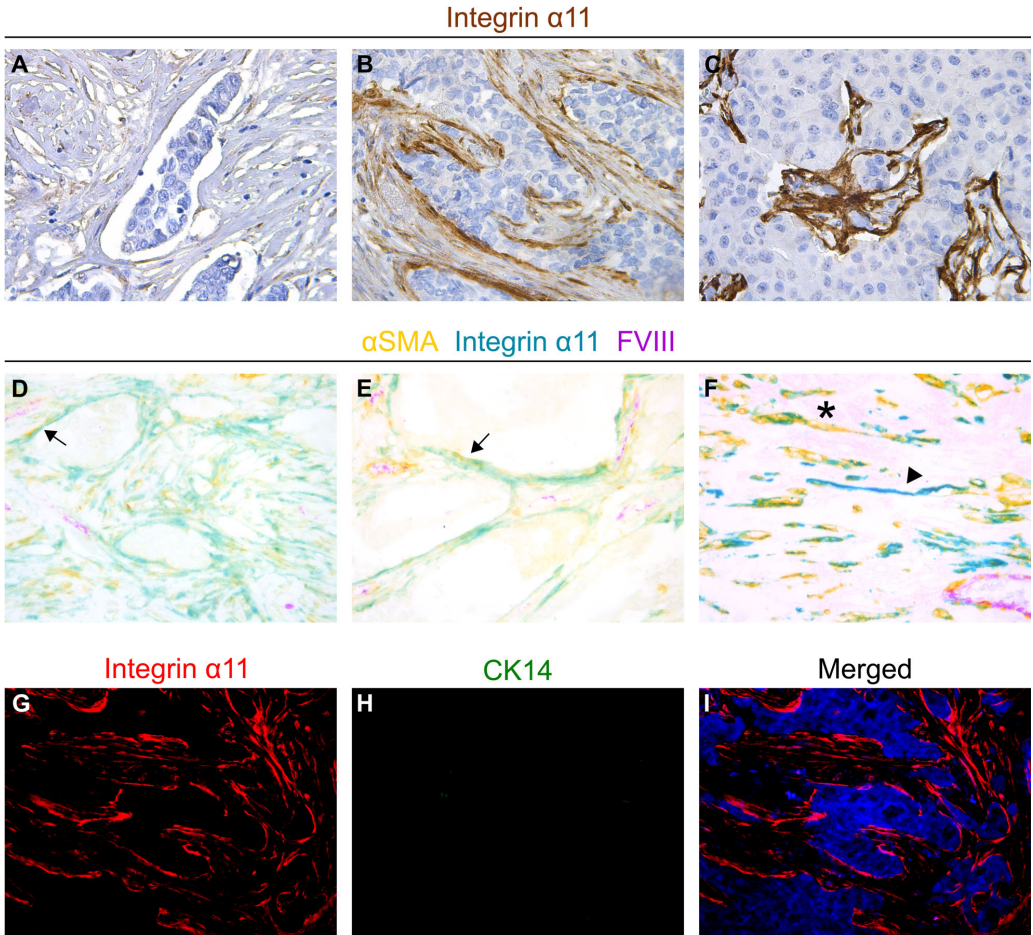
Figure 2. Integrin α11 is expressed in fibroblast-like cells in breast cancer stroma. Integrin α11 expression in spindle-shaped cells in the stroma of different invasive human breast carcinomas by IHC with 210F4B6A4. Different levels of integrin α11 expression are shown in (A–C) (A; low intensity, B; medium strong intensity and C; strong intensity). (D–F) show triple staining of αSMA (yellow), integrin α11 (teal), and FVIII (purple) where co-localization of αSMA and integrin α11 appears green. Note that both integrin α11 and αSMA are expressed in spindle-shaped stromal cells, but do not completely co-localize. Examples of double-positive spindle-shaped cells are marked with arrows, while one integrin α11-positive/αSMA-negative cell is marked with an arrowhead and one integrin α11-negative/αSMA-positive cell marked with an asterisk. (G–I) show immunofluorescent double staining of integrin α11 (red), CK14 (green) and DAPI (blue) of one invasive breast carcinoma. Note the strong integrin α11 expression in direct proximity to the tumor cells seen in (B), (D), (E), and (J–L), and that this border is negative for CK14, indicating that this is not flattened integrin α11-positive breast myoepithelium. Magnification: ×400 and ×200.

histologically benign ducts (Figure 3A). Interestingly, Figure 2G–I and see supplementary material, Figure S2D–F, demonstrate that the accentuated integrin α11 expression in spindle-shaped cells near tumor cells noted above probably represents tightly associated fibroblasts, and not myoepithelial cells, as these cells are negative for the myoepithelial marker CK14.

Integrin α11

αSMA   Integrin α11   FVIII

Integrin α11   CK14   Merged
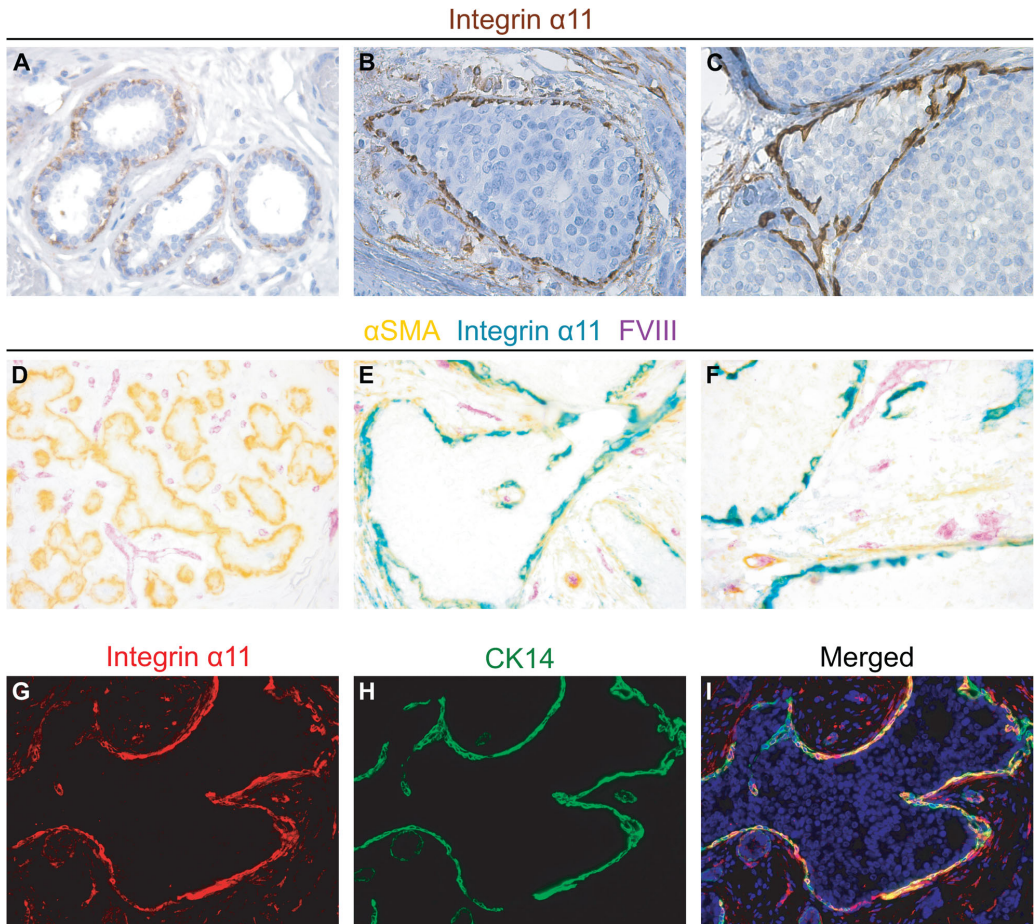
Figure 3. Integrin α11 is expressed in a subgroup of breast myoepithelial cells. (A–C) show single staining of integrin α11 with weak myoepithelial integrin α11 expression in benign-appearing ducts (A) and high myoepithelial integrin α11 expression in DCIS lesions (B and C). (D–F) show triple staining of αSMA (yellow), integrin α11 (teal), and FVIII (purple) where co-localization of αSMA and integrin α11 appears green; (D) shows terminal ducts and lobular units outside an invasive breast carcinoma with αSMA-positive, integrin α11-negative myoepithelial cells, while (E–F) show co-localization of myoepithelial integrin α11 and αSMA in DCIS lesions. (G–I) shows immunofluorescent double staining of integrin α11 (red), CK14 (green) and DAPI (blue) of one DCIS lesion with co-localization of integrin α11 and CK14 in myoepithelial cells. IHC with 210F4B6A4. Magnification: ×400 and ×200.

High integrin α11 expression is associated with features of aggressive breast cancer

Integrin α11 protein expression in stromal, spindle-shaped cells was quantified by SI score (0–9), obtained by multiplying the score for intensity of staining by the score for percentage of fibrous stroma stained. In total, 258 cases (66%) showed high integrin α11 protein expression (SI 4–9), whereas 134 cases (34%) showed low expression (SI 0–3). While invasive carcinoma of no special type, previously named invasive ductal carcinoma, was associated with high integrin α11 protein expression, invasive lobular carcinoma was associated with low integrin α11 protein expression (Table 2).

Table 2. Associations between integrin α11 protein expression and clinico-pathological variables

	α11 low (n = 134)	α11 high (n = 258)		
Variables	n (%)	n (%)	OR (95% CI)	P value*
Ductal carcinoma				<0.001
No	37 (58)	27 (42)	1	
Yes	97 (30)	231 (70)	3.3 (1.9–5.7)	
Lobular carcinoma				<0.001
Yes	27 (67)	13 (33)	1	
No	107 (30)	245 (70)	4.8 (2.4–9.6)	
Histologic grade				<0.001
Grade 1–2	125 (40)	190 (60)	1	
Grade 3	9 (12)	68 (88)	5.0 (2.4–10.3)	
Tumor diameter				0.96
≤2 cm	98 (34)	188 (66)	1	
>2 cm	36 (34)	70 (66)	1.0 (0.6–1.6)	
Mitotic count[†,‡]				<0.001
Low count (≤5.5/mm^2)	117 (43)	158 (57)	1	
High count (>5.5/mm^2)	16 (14)	98 (86)	4.5 (2.5–8.1)	
Lymph node status				0.11
Negative	101 (37)	175 (63.4)	1	
Positive	32 (28)	82 (72)	1.5 (0.9–2.4)	
ER				0.001
Positive (≥10%)	121 (38)	197 (62)	1	
Negative (<10%)	13 (18)	61 (82)	2.9 (1.5–5.5)	
PR				0.53
Positive (≥10%)	91 (35)	167 (65)	1	
Negative (<10%)	43 (32)	91 (68)	1.2 (0.7–1.8)	
HER2[§]				0.004
Negative	123 (37)	209 (63)	1	
Positive	10 (18)	47 (82)	2.7 (1.3–5.7)	
Ki67[†]				<0.001
Low count (≤31.5%)	111 (41)	163 (59)	1	
High count (>31.5%)	22 (19)	93 (81)	2.9 (1.7–4.9)	
Triple-negative				0.022
No	126 (36)	223 (64)	1	
Yes	8 (19)	35 (81)	2.5 (1.1–5.5)	
CK 5/6				0.001
Negative (SI = 0)	124 (38)	207 (62)	1	
Positive (SI > 0)	9 (16)	49 (84)	3.3 (1.5–6.9)	

n, number of patients; ER, estrogen receptor; PR, progesterone receptor; HER2, human epidermal growth factor receptor 2; CK 5/6, cytokeratin 5/6; SI: staining index.
*Pearson chi-square.
[†]Cut-off value by upper quartile.
[‡]Mitotic count: number of mitoses per mm^2.
[§]HER2-positive cases: HER2 IHC3+ and HER2 IHC2+ cases with a HER2/Chr17 ratio by silver *in situ* hybridization ≥ 2.0.

Furthermore, the expression of integrin α11 was significantly higher in the aggressive HER2-positive breast cancer subgroup both at protein and mRNA level (Figures 4A and 5A,C).

Using the lower tertile as cut-off value (SI 0–3 = 34% versus SI 4–9 = 66%), high integrin α11 protein expression was significantly associated with high histologic grade (OR 5.0), estrogen receptor (ER) negativity (OR 2.9), HER2 positivity (OR 2.7), triple-negative phenotype (OR 2.5) and high tumor cell proliferation by Ki-67 (OR 2.9) and mitotic count (OR 4.5) (Table 2). Furthermore, high integrin α11 protein expression was associated with the basal cell marker CK5/6 (OR 3.3), but not with tumor diameter or lymph node metastasis (Table 2).

In univariate survival analyses, neither integrin α11 protein expression nor integrin α11 mRNA expression were significantly associated with breast cancer specific survival (Figures 4B and 5B,D). No significant associations between integrin α11 expression and breast cancer specific survival were found across different molecular breast cancer subgroups (see supplementary material, Figures S4–S6), except that high integrin α11 mRNA expression was found to be associated with reduced survival in the Luminal B subgroup in the METABRIC discovery cohort (see
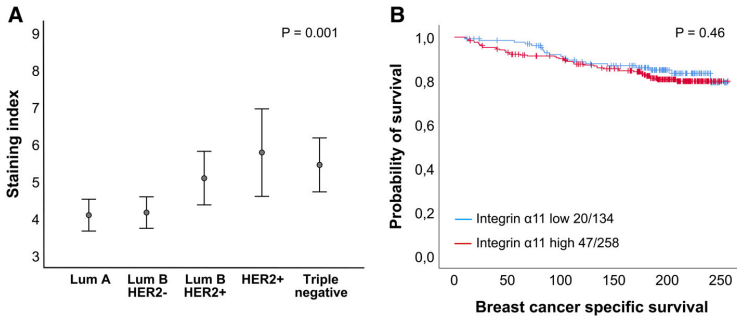
Figure 4. Integrin α11 protein expression in human breast cancer. Integrin α11 protein expression across molecular subtypes of breast cancer; data are presented as error-bars with 95% confidence interval of the mean, and P values by the Kruskal–Wallis test (A). Survival curve by the Kaplan–Meier method for stromal integrin α11 expression; breast cancer specific survival in months, and P value by log-rank test (B). For each category, the number of breast cancer deaths is given, followed by the total number of cases in each category.
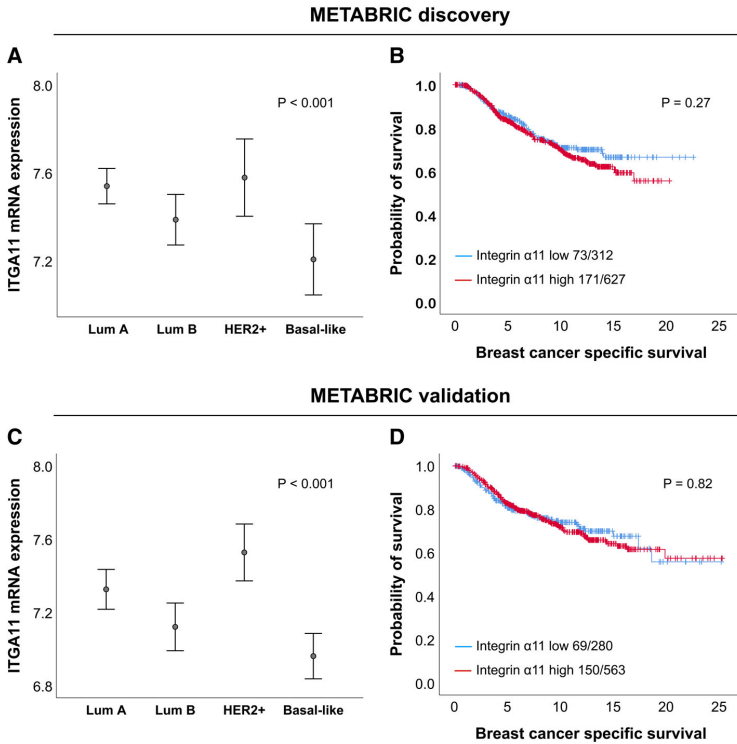
Figure 5. Integrin α11 mRNA expression in human breast cancer in the METABRIC discovery and validation datasets. Integrin α11 mRNA expression across molecular subtypes of breast cancer; data are presented as error-bars with 95% confidence interval of the mean, and P values by the Kruskal–Wallis test (A,C). Survival curves by the Kaplan–Meier method for integrin α11 mRNA expression; breast cancer specific survival in years, and P value by log rank test (B,D). For each category, the number of breast cancer deaths is given, followed by the total number of cases in each category.

supplementary material, Figure S5B), but this was not validated at the protein level or in the METABRIC validation cohort (see supplementary material, Figures S4B,C and S6B).

Discussion

Integrin α11β1 has been shown experimentally to stimulate tumor growth and progression [16,17,19,20], and to be essential for fibroblast-matrix interactions [5,30]. Here, we present two new monoclonal mouse anti-human integrin α11 antibodies, 210F4B6A4 and D120.4, which bind to extracellular and intracellular epitopes of the integrin α11 subunit, respectively. We have established conditions for specific and reproducible integrin α11 staining of human FFPE tumor material with 210F4B6A4. In a large breast cancer cohort with long and complete follow-up, integrin α11 was found to be expressed to varying degrees in the stroma of 99% of the cases. In agreement with a tumor-supportive effect of integrin α11β1, high integrin α11 expression was associated with more aggressive breast cancer phenotypes, even though integrin α11 expression was not significantly correlated to breast cancer specific survival.

Since existing anti-integrin α11 antibodies have been shown to lack specificity on FFPE material in our laboratory, we carefully developed and characterized novel antibodies. Since integrin α2 is one of the most similar integrin chains [24], and is also found expressed on fibroblasts [5], extra efforts were made to exclude cross-reactivity against this integrin subunit. The new monoclonal antibody 210F4B6A4 described herein binds specifically to the integrin α11-chain under several conditions, including western blotting and immunostaining of FFPE material.

Although experimental studies have indicated a tumor-stimulating effect of integrin α11β1 in different preclinical models [16,17,19,20], and integrin α11β1 therefore has been suggested as a potential marker of a pro-tumorigenic CAF subset, few investigations have been performed on human tumor tissue due to lack of a reliable antibody for use on FFPE material. In the present study, investigating a breast cancer cohort of 392 patients, high integrin α11 expression in stromal spindle-shaped cells was significantly associated with high histologic grade, HER2 positivity, ER negativity, triple-negative phenotype and expression of the basal cell marker CK5/6, as well as high tumor cell proliferation by Ki-67 expression and mitotic count - all markers of aggressive breast cancer phenotypes.

Notably, integrin α11 was expressed at higher protein and mRNA levels in the aggressive HER2-positive subtype of breast cancer. In addition to existing preclinical data, these findings may indicate that integrin α11-positive fibroblasts represent a subset of tumor-supportive breast CAFs. However, high integrin α11 protein and mRNA expression was not associated with survival. Similarly, Parajuli et al [31] did not find correlations between stromal integrin α11 expression and patient outcome in a series of head and neck cancers using cryosections from the tumor center.

The cellular expression of different integrins is not only subtype-specific, but is also dependent on tissue type and context [4,32,33]. In the case of integrin α11β1, the expression appears to be restricted to a subgroup of fibroblasts and mesenchymal stem cells [5], but the characterization of expression in human tissue is so far limited. As there is a need to better characterize CAF heterogeneity and to identify markers that can help distinguish between tumor-supportive and tumor-suppressive CAFs, several IHC-based studies have used different markers to identify tumor-supportive breast CAFs, such as αSMA [34,35] and PDGFRβ [36,37]. In the present study, we found that the integrin α11 subunit was expressed in fibroblast-like cells in the breast tumor stroma, and it predominantly co-localized with αSMA. Similarly, αSMA and integrin α11 have previously been found to co-localize in the tumor stroma of human head and neck cancers [31]. However, stromal spindle-shaped cells with expression of either integrin α11 or αSMA only were also observed in the present study, which may represent different subpopulations of CAFs (α11+/αSMA+, α11+/αSMA−, and α11−/αSMA+) with potential functional differences which should be investigated in future studies.

Normal mammary epithelium consists of an inner luminal and a surrounding myoepithelial cell layer [38]. Interestingly, integrin α11 was also found to be expressed on myoepithelial cells surrounding DCIS lesions, where it was found to co-localize with αSMA and CK14, common markers of breast myoepithelium. While αSMA and CK14 are general myoepithelial markers, integrin α11 myoepithelial expression appears to be more restricted, and was mainly detected in in situ lesions, with absent or very weak expression in benign-appearing lobules and ducts. While the myoepithelium of benign ducts is thought to act as an active tumor suppressor, accumulating data indicate that DCIS-associated myoepithelial cells show genetic, epigenetic and molecular changes compared to myoepithelium in benign tissue, and that their tumor-suppressive

function may be lost with DCIS progression [39,40]. As changes in myoepithelial cells have been suggested to be an important contribution in the transition from preinvasive to invasive cancer, the molecular differences in preinvasive lesions may represent markers for risk stratification or even targets for prevention of invasive breast cancer. Interestingly, upregulation of another integrin, integrin αvβ6, in breast myoepithelium, has been associated with poor patient outcome and shown to promote breast tumor proliferation experimentally [41]. Additional studies should address the role of myoepithelial integrin α11 expression in DCIS cohorts.

We observed fibrillar integrin α11 positivity which was clearly strongest in direct proximity to the tumor cells in the majority of breast cancer samples, and dual staining with CK14 demonstrated that these cells are probably not flattened myoepithelial cells. By the methods used in this study, we cannot exclude that such accentuated integrin α11 staining adjacent to cancer cells may represent a subset of the tumor cell population with a mesenchymal phenotype. Indeed, integrin α11β1 has been suggested to be upregulated during epithelial-to-mesenchymal transition, as it was found to be part of a gene signature for some invading breast cancer cells *in vitro* [42], although this has not been confirmed in other models or at the protein level.

In conclusion, we have shown that the integrin α11 subunit is expressed in fibroblasts-like cells in invasive human breast carcinomas, and in myoepithelial cells in *in situ* lesions. High stromal integrin α11 expression was associated with aggressive breast cancer phenotypes, although integrin α11 mRNA and protein expression did not correlate with breast cancer specific survival. It will be of further interest to examine the expression of integrin α11 in relation to other CAF markers, and to study the functional role of integrin α11-expressing subpopulations of breast CAFs.

Acknowledgements

Author contributions statement

HYHS, RKR, and LAA contributed to the concept and design of the study. HYHS, RJE, and LAA planned and analyzed the IHC data. HYHS performed the experiments. DW produced the D120.4 antibody, and purified anti-integrin α11 antibodies from hybridoma culture supernatants. CA, EW, and GK contributed to collection and assembly of data from the patient materials. AM provided frozen and FFPE tissue sections of pancreatic ductal adenocarcinomas. EW collected and analyzed microarray mRNA data sets. HYHS, CA, and EW conducted statistical analyses. HYHS, RJE, RKR, DW, DG, LS, and LAA contributed to reagents/materials/analyses tools. HYHS and LAA wrote the manuscript with critical input from co-authors. All authors read and approved the final version of the manuscript.

References

1. Maman S, Witz IP. A history of exploring cancer in context. *Nat Rev Cancer* 2018; **18:** 359–376.
2. Nienhuis HH, Gaykema SB, Timmer-Bosscha H, *et al*. Targeting breast cancer through its microenvironment: current status of preclinical and clinical research in finding relevant targets. *Pharmacol Ther* 2015; **147:** 63–79.
3. Finak G, Bertos N, Pepin F, *et al*. Stromal gene expression predicts clinical outcome in breast cancer. *Nat Med* 2008; **14:** 518–527.
4. Barczyk M, Carracedo S, Gullberg D. Integrins. *Cell Tissue Res* 2010; **339:** 269–280.
5. Zeltz C, Gullberg D. The integrin-collagen connection – a glue for tissue repair? *J Cell Sci* 2016; **129:** 653–664.
6. Carracedo S, Lu N, Popova SN, *et al*. The fibroblast integrin alpha11beta1 is induced in a mechanosensitive manner involving activin A and regulates myofibroblast differentiation. *J Biol Chem* 2010; **285:** 10434–10445.
7. Talior-Volodarsky I, Connelly KA, Arora PD, *et al*. alpha11 integrin stimulates myofibroblast differentiation in diabetic cardiomyopathy. *Cardiovasc Res* 2012; **96:** 265–275.
8. Bussard KM, Mutkus L, Stumpf K, *et al*. Tumor-associated stromal cells as key contributors to the tumor microenvironment. *Breast Cancer Res* 2016; **18:** 84.
9. Ohlund D, Handly-Santana A, Biffi G, *et al*. Distinct populations of inflammatory fibroblasts and myofibroblasts in pancreatic cancer. *J Exp Med* 2017; **214:** 579–596.
10. Ozdemir BC, Pentcheva-Hoang T, Carstens JL, *et al*. Depletion of carcinoma-associated fibroblasts and fibrosis induces immunosuppression and accelerates pancreas cancer with reduced survival. *Cancer Cell* 2014; **25:** 719–734.
11. Rhim AD, Oberstein PE, Thomas DH, *et al*. Stromal elements act to restrain, rather than support, pancreatic ductal adenocarcinoma. *Cancer Cell* 2014; **25:** 735–747.

12. Costa A, Kieffer Y, Scholer-Dahirel A, *et al*. Fibroblast heterogeneity and immunosuppressive environment in human breast cancer. *Cancer Cell* 2018; **33:** 463–479.e410.

13. Barbazan J, Vignjevic DM. Cancer associated fibroblasts: is the force the path to the dark side? *Curr Opin Cell Biol* 2019; **56:** 71–79.

14. Kwa MQ, Herum KM, Brakebusch C. Cancer-associated fibroblasts: how do they contribute to metastasis? *Clin Exp Metastasis* 2019; **36:** 71–86.

15. Tiger CF, Fougerousse F, Grundstrom G, *et al*. alpha11beta1 integrin is a receptor for interstitial collagens involved in cell migration and collagen reorganization on mesenchymal nonmuscle cells. *Dev Biol* 2001; **237:** 116–129.

16. Smeland HY, Lu N, Karlsen TV, *et al*. Stromal integrin alpha11-deficiency reduces interstitial fluid pressure and perturbs collagen structure in triple-negative breast xenograft tumors. *BMC Cancer* 2019; **19:** 234.

17. Lu N, Karlsen TV, Reed RK, *et al*. Fibroblast alpha11beta1 integrin regulates tensional homeostasis in fibroblast/A549 carcinoma heterospheroids. *PLoS One* 2014; **9:** e103173.

18. Reigstad I, Smeland HY, Skogstrand T, *et al*. Stromal integrin alpha11beta1 affects RM11 prostate and 4T1 breast Xenograft tumors differently. *PLoS One* 2016; **11:** e0151663.

19. Zhu CQ, Popova SN, Brown ER, *et al*. Integrin alpha 11 regulates IGF2 expression in fibroblasts to enhance tumorigenicity of human non-small-cell lung cancer cells. *Proc Natl Acad Sci U S A* 2007; **104:** 11754–11759.

20. Navab R, Strumpf D, To C, *et al*. Integrin alpha11beta1 regulates cancer stromal stiffness and promotes tumorigenicity and metastasis in non-small cell lung cancer. *Oncogene* 2016; **35:** 1899–1908.

21. Zeltz C, Alam J, Liu H, *et al*. alpha11beta1 integrin is induced in a subset of cancer-associated fibroblasts in desmoplastic tumor stroma and mediates in vitro cell migration. *Cancers (Basel)* 2019; **11:** p.ii: E765.

22. Pidgeon GP, Tang K, Cai YL, *et al*. Overexpression of platelet-type 12-lipoxygenase promotes tumor cell survival by enhancing alpha(v)beta(3) and alpha(v)beta(5) integrin expression. *Cancer Res* 2003; **63:** 4258–4267.

23. Erusappan P, Alam J, Lu N, *et al*. Integrin α11 cytoplasmic tail is required for FAK activation to initiate 3D cell invasion and ERK-mediated cell proliferation. *Sci Rep* 2019; **9:** 15283.

24. Velling T, Kusche-Gullberg M, Sejersen T, *et al*. cDNA cloning and chromosomal localization of human alpha(11) integrin. A collagen-binding, I domain-containing, beta(1)-associated integrin alpha-chain present in muscle tissues. *J Biol Chem* 1999; **274:** 25735–25742.

25. El Jellas K, Hoem D, Hagen KG, *et al*. Associations between ABO blood groups and pancreatic ductal adenocarcinoma: influence on resection status and survival. *Cancer Med* 2017; **6:** 1531–1540.

26. Knutsvik G, Stefansson IM, Aziz S, *et al*. Evaluation of Ki67 expression across distinct categories of breast cancer specimens: a population-based study of matched surgical specimens, Core needle biopsies and tissue microarrays. *PLoS One* 2014; **9:** e112121.

27. Straume O, Akslen LA. Alterations and prognostic significance of p16 and p53 protein expression in subgroups of cutaneous melanoma. *Int J Cancer* 1997; **74:** 535–539.

28. Curtis C, Shah SP, Chin SF, *et al*. The genomic and transcriptomic architecture of 2,000 breast tumours reveals novel subgroups. *Nature* 2012; **486:** 346–352.

29. Subramanian A, Tamayo P, Mootha VK, *et al*. Gene set enrichment analysis: a knowledge-based approach for interpreting genome-wide expression profiles. *Proc Natl Acad Sci U S A* 2005; **102:** 15545–15550.

30. Schulz JN, Plomann M, Sengle G, *et al*. New developments on skin fibrosis – essential signals emanating from the extracellular matrix for the control of myofibroblasts. *Matrix Biol* 2018; **68-69:** 522–532.

31. Parajuli H, Teh MT, Abrahamsen S, *et al*. Integrin alpha11 is overexpressed by tumour stroma of head and neck squamous cell carcinoma and correlates positively with alpha smooth muscle actin expression. *J Oral Pathol Med* 2017; **46:** 267–275.

32. Hamidi H, Ivaska J. Every step of the way: integrins in cancer progression and metastasis. *Nat Rev Cancer* 2018; **18:** 532–547.

33. Hamidi H, Pietila M, Ivaska J. The complexity of integrins in cancer and new scopes for therapeutic targeting. *Br J Cancer* 2016; **115:** 1017–1023.

34. Surowiak P, Murawa D, Materna V, *et al*. Occurrence of stromal myofibroblasts in the invasive ductal breast cancer tissue is an unfavourable prognostic factor. *Anticancer Res* 2007; **27:** 2917–2924.

35. Amornsupak K, Jamjuntra P, Warnnissorn M, *et al*. High ASMA (+) fibroblasts and low cytoplasmic HMGB1(+) breast cancer cells predict poor prognosis. *Clin Breast Cancer* 2017; **17:** 441–452.e442.

36. Paulsson J, Ryden L, Strell C, *et al*. High expression of stromal PDGFRbeta is associated with reduced benefit of tamoxifen in breast cancer. *J Pathol Clin Res* 2017; **3:** 38–43.

37. Paulsson J, Sjoblom T, Micke P, *et al*. Prognostic significance of stromal platelet-derived growth factor beta-receptor expression in human breast cancer. *Am J Pathol* 2009; **175:** 334–341.

38. Sirka OK, Shamir ER, Ewald AJ. Myoepithelial cells are a dynamic barrier to epithelial dissemination. *J Cell Biol* 2018; **217:** 3368–3381.

39. Rakha EA, Miligy IM, Gorringe KL, *et al*. Invasion in breast lesions: the role of the epithelial-stroma barrier. *Histopathology* 2018; **72:** 1075–1083.

40. Allen MD, Marshall JF, Jones JL. alphavbeta6 expression in myoepithelial cells: a novel marker for predicting DCIS progression with therapeutic potential. *Cancer Res* 2014; **74:** 5942–5947.

41. Allen MD, Thomas GJ, Clark S, *et al*. Altered microenvironment promotes progression of preinvasive breast cancer: myoepithelial expression of alphavbeta6 integrin in DCIS identifies high-risk patients and predicts recurrence. *Clin Cancer Res* 2014; **20:** 344–357.

42. Westcott JM, Prechtl AM, Maine EA, *et al*. An epigenetically distinct breast cancer cell subpopulation promotes collective invasion. *J Clin Invest* 2015; **125:** 1927–1943.

SUPPLEMENTARY MATERIAL ONLINE

Supplementary figure legends

Figure S1. Frequency histogram for the integrin α11 staining index

Figure S2. Integrin α11 expression in spindle-shaped cells in the stroma of invasive human breast carcinomas by IHC

Figure S3. Intratumor heterogeneity of stromal integrin α11 expression in human invasive breast cancer

**Figure S4.** Survival curves across molecular subtypes according to stromal integrin α11 protein expression

Figure S5. Survival curves across molecular subtypes according to integrin α11 mRNA expression in the METABRIC discovery dataset

Figure S6. Survival curves across molecular subtypes according to integrin α11 mRNA expression in the METABRIC validation dataset

Integrin α11β1 is expressed in breast cancer stroma and associates with aggressive tumor phenotypes

**Supplementary Material.**
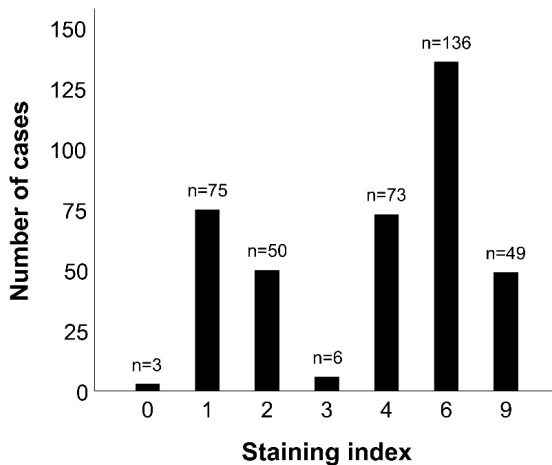
Figure S1. Frequency histogram for the integrin α11 staining index. Integrin α11 expression in spindle-shaped stromal cells was quantified by staining index score (0-9) which was obtained by multiplying the score for intensity of staining (0=absent, 1=weak, 2=moderate, or 3=strong) by the score for percentage of fibrous stroma stained (<10% = 1, 10–50% = 2, >50% = 3).
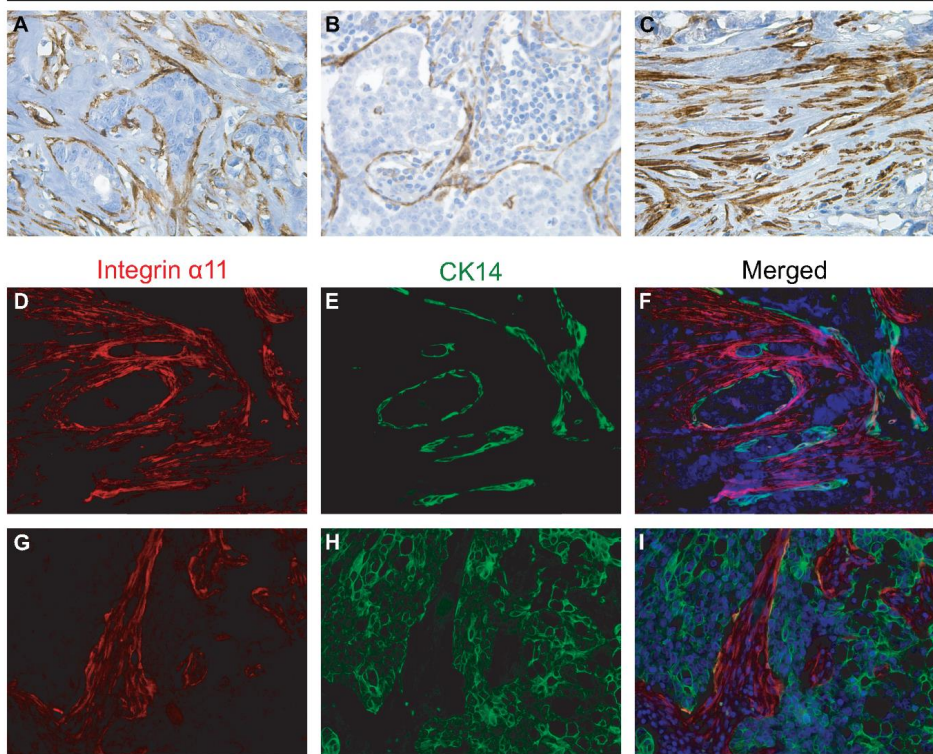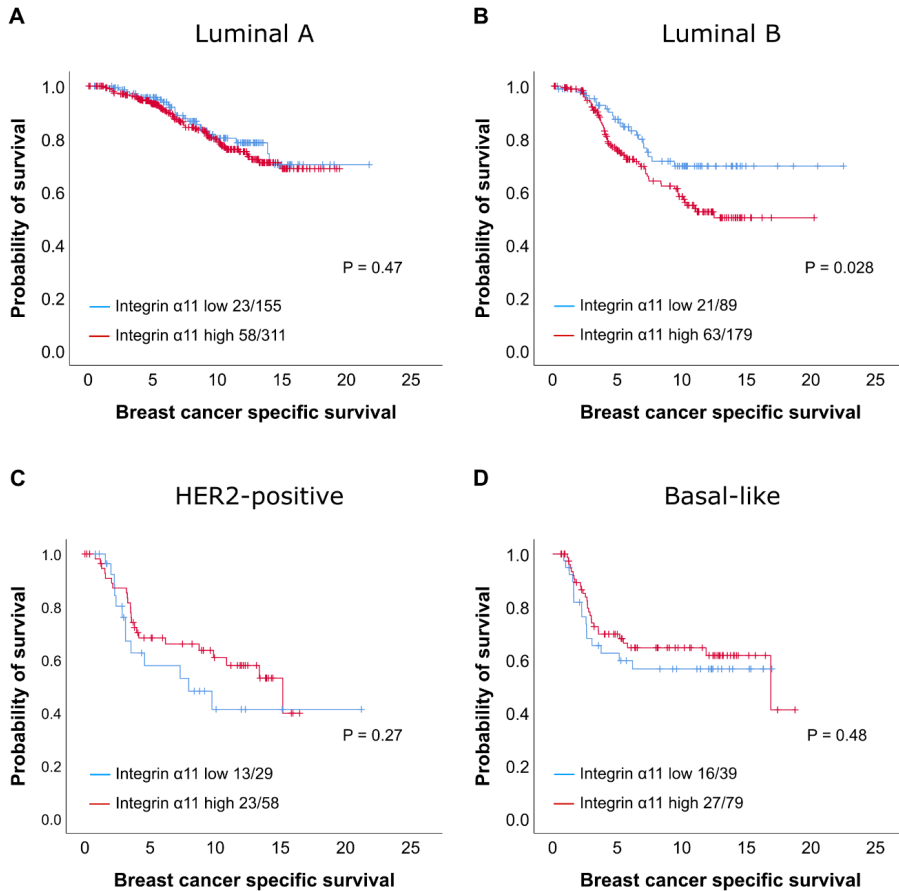
Figure S2. Integrin α11 expression in spindle-shaped cells in the stroma of invasive human breast carcinomas by IHC. **A-C** demonstrate single staining of integrin α11 (brown) while **D-I** shows immunofluorescent double staining of integrin α11 (red), CK14 (green) and DAPI (blue). Note the strong integrin α11 expression in direct proximity to the tumor cells seen in **A**, **B** and **D-F**. Areas with immune cell infiltration showed most often low integrin α11 expression (**B**), while fibrotic, extracellular matrix-rich tissue was mostly integrin α11-positive (**C**). In **D-F**, fibroblast-like cells positive for integrin α11 surrounding integrin α11-negative breast myoepithelium are seen. No convincing staining of breast tumor cells was seen - not even in tumors with basal-like features, as demonstrated by the breast carcinoma seen in **G-I** (tumor cells positive for CK14). IHC with 210F4B6A4. 400x and 200x.
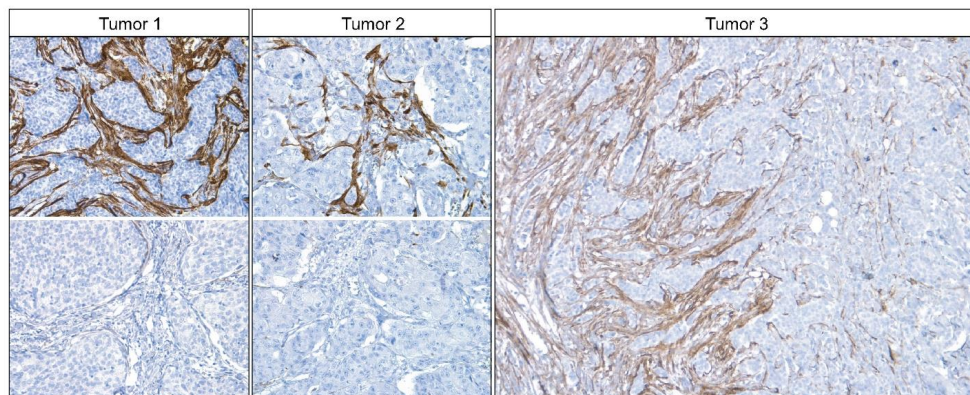
Figure S3. Intratumor heterogeneity of stromal integrin α11 expression in human invasive breast cancer. Images from three invasive human breast carcinomas demonstrate intratumor heterogenity of the expression of integrin α11 by IHC with 210F4B6A4. Note the gradient of integrin α11 expression with weaker expression towards the tumor periphery seen in tumor 3 (tumor periphery right part of the image). 200x and 100x.
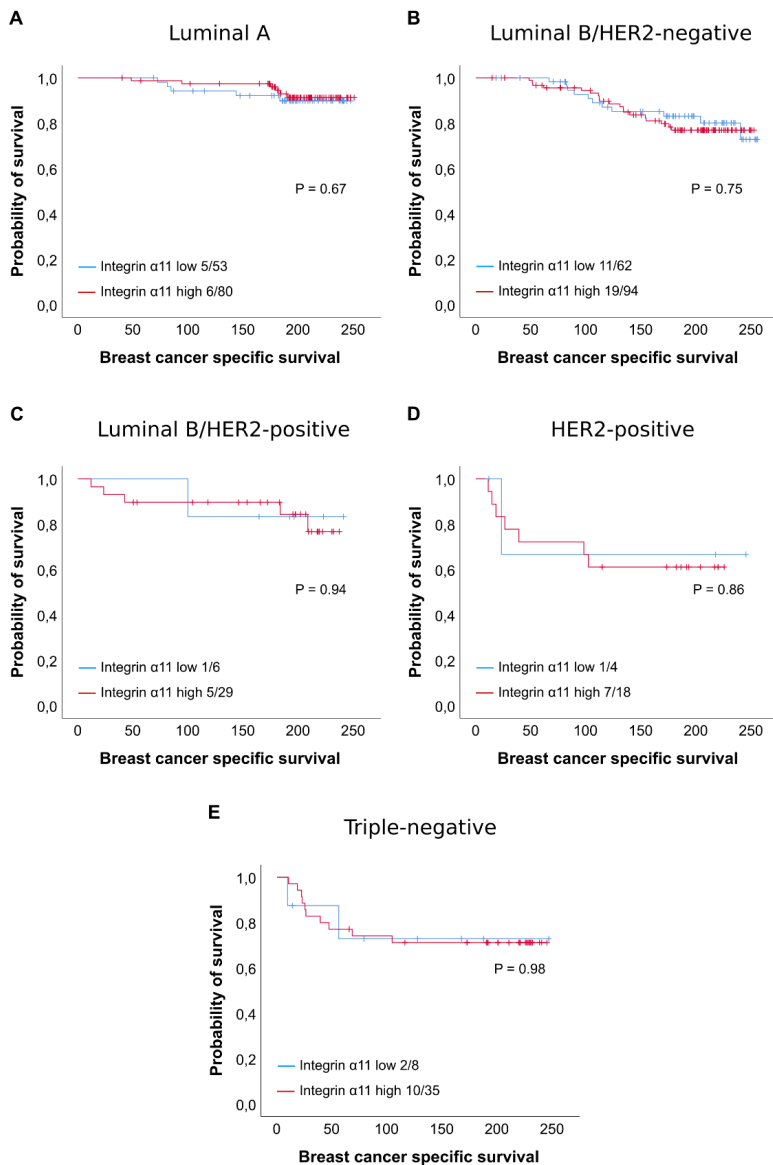
Figure S4. Survival curves across molecular subtypes according to stromal integrin α11 protein expression. Kaplan-Meier method, breast cancer specific survival in months, and p-values by log rank test. For each category, the number of breast cancer deaths is given, followed by the total number of cases in each category.

A Luminal A

P = 0.47

Integrin α11 low 23/155
Integrin α11 high 58/311

B Luminal B

P = 0.028

Integrin α11 low 21/89
Integrin α11 high 63/179

C HER2-positive

P = 0.27

Integrin α11 low 13/29
Integrin α11 high 23/58

D Basal-like

P = 0.48

Integrin α11 low 16/39
Integrin α11 high 27/79

Figure S5. Survival curves across molecular subtypes according to integrin α11 mRNA expression in the METABRIC discovery dataset. Kaplan-Meier method, breast cancer specific survival in years, and p-values by log rank test. For each category, the number of breast cancer deaths is given, followed by the total number of cases in each category.
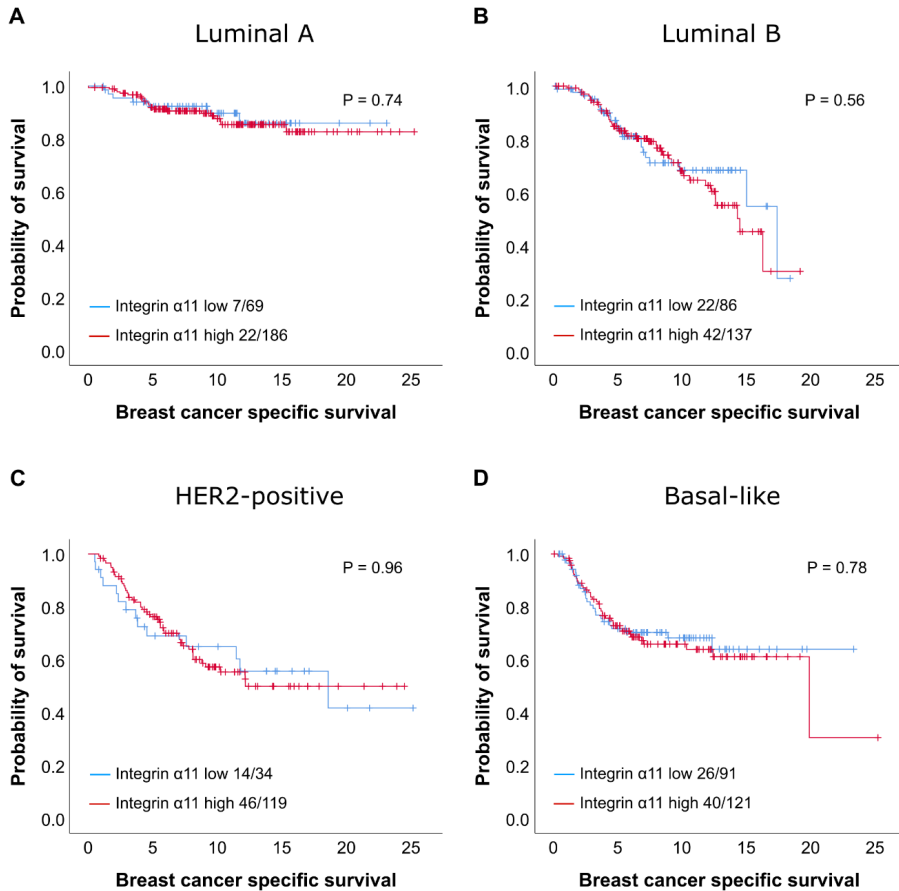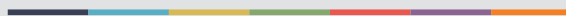
Figure S6. Survival curves across molecular subtypes according to integrin α11 mRNA expression in the METABRIC validation dataset. Kaplan-Meier method, breast cancer specific survival in years, and p-values by log rank test. For each category, the number of breast cancer deaths is given, followed by the total number of cases in each category.

uib.no